DIPLOMARBEIT

Titel der Diplomarbeit

New methods for detection and quantification of DNA in hair and their implementation in forensic medicine

angestrebter akademischer Grad

Magistra der Naturwissenschaften (Mag. rer.nat.)

Verfasserin / Verfasser:	Sandra Szabó
Matrikel-Nummer:	0400589
Studienrichtung /Studienzweig (lt. Studienblatt):	Molekulare Biologie A490
Betreuerin / Betreuer:	Ao.Univ.-Prof. DI Dr. Marcela Hermann Priv.-Doz. DDr. Leopold Eckhart

Wien, am 05.09.2010

This thesis was performed at the Medical University of Vienna, Research Division of Skin Biology and Pathobiology, under the supervision of Priv.-Doz. DDr. Leopold Eckhart. The project was supported by the Austrian Science Fund (FWF): P21312.

ACKNOWLEDGEMENT

First of all, I would like to convey my deepest appreciation to Priv.-Doz. DDr. Leopold Eckhart for allowing me to perform my diploma thesis under his supervision as well as for his kind leadership, patience and critical advice throughout all phases of our collaboration.
Further thanks go out to Dr. Heinz Fischer who has guided me in all kinds of practical work and beyond. His help was additionally responsible for the success of this study.

It is a pleasure to acknowledge the inestimable help I have received from the external supervisor of my thesis, Ao.Univ.-Prof DI Dr. Marcela Hermann, who has supported me whenever possible.

I want to sincerely thank Univ.-Prof. Dr. Erwin Tschachler and all colleagues from the Research Division of Skin Biology and Pathobiology, MUW, for providing a friendly and inspiring work atmosphere and for accepting me as a full member of the team right from the start. Special thanks go to Caroline Stremnitzer who has not only shared ups and downs of (laboratory) life with me, but has also been both a strong motivating force and a great friend whenever I needed one.

I am grateful to all my friends and colleagues who have not only accompanied me throughout all the exciting days of studying at the university, but have also helped me to make it an unforgettable time in many different ways. I would especially like to thank Sophie Windisch for being my best friend for many years and for always accepting me the way I am.

Finally, I want to express my heartfelt gratitude to my family for believing in me in an unwavering and unconditional way. Special thanks go to Matthias for being the greatest brother a little sister could wish for and to my parents for enabling me to pursue an academic career and for patiently supporting every single one of my plans, however unconventional they might have been. Without their steady encouragement nothing I have accomplished during the last few years would have been possible.

ABSTRACT

Hairs and nails are skin appendages that consist of cornified keratinocytes. Nuclear DNA is largely degraded during cornification, however the mechanism of this process has remained elusive. Moreover, forensic investigations have indicated that DNA can be extracted and typed from hair of some individuals but not from others. The biological basis for this phenomenon has been unknown.

The aims of this project were (1) to quantify the contribution of the keratinocyte-specific endonuclease DNase1L2 in the degradation of DNA during cornification and (2) to determine the cause of inter-individual differences in the yield of DNA for forensic investigations. Novel protocols for the *in situ* labeling of nuclear DNA in hair and for the quantification of DNA extracted from hair and nails were established. *In situ* labeling involved permeabilization of hair and incubation with DNA-specific fluorescent dyes, whereas DNA quantification was based on real-time PCR amplification.

Comparative investigations of hair and nails from wild-type mice and mice deficient in the endonuclease DNase1L2 showed that DNase1L2 was essential for the breakdown of nuclear DNA in hair and nails as well as for degrading mitochondrial DNA in nails. Screening of human hair samples with *in situ* DNA labeling and DNA quantification by PCR revealed a significant correlation between the number of residual DNA *in situ* and the PCR yield. *In situ* labeling of DNA allowed the prediction of the success rate of short tandem repeat (STR) genotyping of single hairs.

The results of this study suggest that DNase1L2 has a crucial role in the degradation of DNA in hair and nails and help to explain differences in DNA amplification yields from hair. The method of labeling DNA in hair samples may be applied in future forensic investigations.

ZUSAMMENFASSUNG

Haare und Nägel sind Hautanhangsgebilde, bestehend aus verhornten Keratinozyten. Während der Verhornung wird die nukleäre DNA zum überwiegenden Teil abgebaut, der Mechanismus dieses Prozesses ist jedoch weitgehend unbekannt. Darüber hinaus haben forensische Untersuchungen ergeben, dass es möglich ist, DNA aus den Haaren mancher aber nicht aller Individuen aufzureinigen und zu typisieren; die biologische Grundlage für dieses Phänomen ist unklar.

Die Ziele dieses Projekts waren (1) den Beitrag der Keratinozyten-spezifischen Endonuklease DNase1L2 im DNA-Abbau während der Verhornung zu quantifizieren und (2) die Ursache inter-individueller Unterschiede in der DNA-Ausbeute in forensischen Untersuchungen zu bestimmen. Neuartige Protokolle für *in situ*-Färbung von Kern-DNA in Haaren und für die Quantifizierung von aus Haaren und Nägeln extrahierter DNA wurden etabliert. Während die Kernfärbung *in situ* die Permeabilisierung der Haare und anschließende Inkubation mit DNA-spezifischen fluoreszierenden Farbstoffen beinhaltete, basierte die Quantifizierungsmethode auf der Amplifikation von DNA mittels real-time PCR.

Vergleichende Untersuchungen mit Haaren und Nägeln von normalen Mäusen und von Mäusen mit fehlender Endonuclease DNase1L2 zeigten, dass DNase1L2 essentiell für den Abbau nukleärer DNA in Haaren und Nägeln sowie von mitochondrialer DNA in Nägeln ist. Screenings von humanen Haarproben mit *in situ* Kernfärbungen und DNA-Quantifizierung mittels PCR offenbarten eine signifikante Korrelation zwischen der Anzahl von anfärbbaren Zellkernen in Haaren und der extrahierbaren DNA-Menge. Die *in situ* Färbung von Kernresten in einzelnen Haaren ermöglichte eine Voraussage der Erfolgsrate von Genotypisierungen anhand von Short Tandem Repeats (STRs).

Die Ergebnisse dieser Studie legen nahe, dass DNase1L2 eine entscheidende Rolle im DNA-Abbau in Haaren und Nägeln spielt und helfen dabei, Unterschiede in der DNA-Ausbeute von Haaren zu erklären. Die neue Kernfärbemethode für Haare könnte in zukünftigen forensischen Untersuchungen zur Anwendung kommen.

TABLE OF CONTENT

1. INTRODUCTION 11

1.1 THE BIOLOGY OF THE HAIR 11
  1.1.2 Hair anatomy 11
    1.1.2.1 The hair follicle 11
    1.1.2.2 The hair shaft 13
  1.1.3 The hair follicle cycle 14
  1.1.4 Terminal differentiation of hair keratinocytes 15
  1.1.5 Programmed cell death 15
  1.1.6 Desoxyribonucleases 16
    1.1.6.1 DNase1L2 17
1.2 THE HAIR AS FORENSIC SAMPLE 18
  1.2.1 General considerations 18
  1.2.2 Common microscopic analysis 18
  1.2.3 Analysis of mitochondrial DNA 19
  1.2.4 Analysis of nuclear DNA 20
  1.2.5 Biological methods used in forensic analysis of nuDNA 21
    1.2.5.1 DNA quantitation in human crime scene samples 21
      1.2.5.1.1 Quantitative real-time PCR 21
      1.2.5.1.2 Alu-based real-time PCR 22
    1.2.5.2 STR typing 23

2. AIMS OF THE THESIS 25

3. RESULTS 27

3.1 TARGETED GENE DELETION DEMONSTRATES A ROLE OF DNASE 1L2 IN TERMINAL DIFFERENTIATION OF HAIR KERATINOCYTES 27
  3.1.1 Fluorescent labeling of nuclear DNA in murine hair 27
    3.1.1.1 Murine hair deficient in DNase1L2 comprised Hoechst-positive nuclei 27
    3.1.1.2 DNA-labeling in hair from DNase1L2 knockout mice of the pure background of strain 129 29
    3.1.1.3 Lack of Hoechst-positive nuclei in wild-type hair could not be ascribed to differences during hair permeabilization 29
    3.1.1.4 Nuclear DNA was detectable in all hair types of DNase1L2 deficient mice 30
    3.1.1.5 Hoechst-labeling of nuclear DNA in vibrissae 31
  3.1.2 Quantitation of nuclear and mitochondrial DNA by real-time PCR 32
    3.1.2.1 Determination of nuclear and mitochondrial DNA levels in hair and nail extracts from wild-type mice and DNase1L2 deficient mice 32
    3.1.2.2 Quantitation of DNA in the stratum corneum 35
3.2 FUNCTIONAL CHARACTERIZATION OF OTHER DNASES IN THE SKIN 36
  3.2.1 Hair deficient in DNase1 lacked Hoechst-positive nuclei and showed normal DNA content 36
  3.2.2 Hair from DNase1L3 knockout mice comprised no stainable nuclei 37
3.3 DETECTION OF NUCLEAR DNA IN HAIR FROM DIFFERENT WILD-TYPE MOUSE STRAINS 38
  3.3.1 Hoechst-labeling revealed residual nuclear DNA in hair from BalbC, FVB and CH3 mice 38
  3.3.2 Detection of Hoechst-labeled nuclear DNA in vibrissae from BalbC and FVB mice 39
  3.3.3 Degree of DNA fragmentation in BalbC hair was higher than in DNase1L2 deficient hair 40
  3.3.4 Quantitation of nuclear DNA in hair extracts obtained from different wild-type mouse strains and a DNase1L2 knockout mouse 41

3.4 Establishment of a correlation between the number of Hoechst-positive nuclei and the DNA content in human hair samples ... 43
  3.4.1 Fluorescent labeling of DNA in human hair ... 43
    3.4.1.1 Scalp hairs showed high variation in the number of detectable nuclei ... 44
    3.4.1.2 *In situ* labeling of DNA in various types of body hair ... 44
  3.4.2 Staining of DNase1L2 in a cross section of plucked hairs containing follicular tissue revealed single cells showing down-regulated expression of DNase1L2 ... 47
  3.4.3 Quantitation of nuclear and mitochondrial DNA levels in extracts from human keratinic tissue ... 48
    3.4.3.1 qPCR demonstrated strong correlation between the levels of nuclear and mitochondrial DNA detected in extracts from human finger nails ... 49
    3.4.3.2 Quantitative real-time PCR was performed for lysates of pooled hair shafts ... 50
      3.4.3.2.1 The number of Hoechst-positive nuclei correlated with nuclear but not mitochondrial DNA extracted from human hair shafts ... 50
      3.4.3.2.2 Analysis of the impact of excluding outliers ... 52
      3.4.3.2.3 The number of stainable nuclei in human hair is independent from the donor’s hair colour or age ... 54
      3.4.3.2.4 Natural hair pigmentation reduced detectability of nuclei but did not influence PCR efficiency ... 55
      3.4.3.2.5 In vitro dyeing and bleaching of hair affected both detectability and amplification of nuclear DNA ... 57
  3.4.4 Direct quantitation of DNA levels in Hoechst-labeled hair samples ... 58
    3.4.4.1 Hoechst-labeling of nuclei and subsequent quantitation of DNA levels in single hairs from 40 donors ... 59
    3.4.4.2 The success of DNA genotyping in human hair correlated with the number of Hoechst-positive nuclei ... 60

4. DISCUSSION ... 63

4.1 *In situ* labeling and quantitation of DNA in hair ... 63
4.2 Mechanism of DNA degradation in hair and nails ... 64
4.3 Inter-individual differences in DNA degradation in human hair ... 66

5. MATERIALS ... 69

5.1 Buffers ... 69
5.2 Kits ... 69
5.3 Reagents and solutions ... 69
5.4 Primers ... 70
  5.4.1 Primers for amplification of murine nuclear and mitochondrial DNA ... 70
  5.4.2 Primers for amplification of human nuclear and mitochondrial DNA ... 70
  5.4.3 Primers for sequencing of mitochondrial DNA in the pCR®2.1-TOPO® vector ... 70
  5.4.4 Primers for the amplification of STR loci (miniSTR-multiplex PCR) ... 71
5.5 Equipment and Software ... 71

6. METHODS ... 73

6.1 DNase1L2 KO mouse ... 73
6.2 Murine hair samples ... 74
6.3 Human hair samples ... 74
6.4 Fluorescent dye labeling of DNA *in situ* ... 74
6.5 DAPI-staining of pulverized hair ... 74
6.6 Immunohistochemical and immunofluorescent analysis of plucked scalp hairs ... 75
6.7 Microscopy ... 75

6.8 Analysis of single hairs 75
6.9 *In vitro* dyeing and bleaching of hairs 75
6.10 Lysis of hairs and nails 76
6.11 DNA extraction from hairs and nails 77
6.12 Quantitative real-time PCR 77
6.13 Creation of standard curves for quantification of PCR yield 78
  6.13.1 Creation of a standard curve for the quantification of nuclear DNA 78
  6.13.2 Creation of a standard curve with a plasmid DNA template 79
    6.13.2.1 Cloning of PCR products into the pCR2.1 TOPOR vector 79
    6.13.2.2 Agarose gel electrophoresis 79
    6.13.2.3 DNA extraction from agarose gels 80
    6.13.2.4 DNA sequencing 80
    6.13.2.5 Transformation 80
    6.13.2.6 Direct PCR from bacterial colonies 81
    6.13.2.7 Preparation of plasmid-DNA 81
    6.13.2.8 Preparation of a standard curve with plasmids containing mitochondrial DNA 82
6.14 STR typing 82
6.15 Statistical analyses 83

7. REFERENCES 85

8. APPENDIX 89

8.1 List of figures 89
8.2 List of tables 90
8.3 List of abbreviations 91
8.4 Curriculum Vitae 93

1. INTRODUCTION

1.1 The biology of the hair

1.1.1 Function and mechanical properties of hair

Hairs are strong and flexible epidermal appendages (Moll et al., 2008; Omary et al., 2004), creating a protective layer on the epidermis of mammals, shielding it from chemical and physical influences such as thermal exposure, UV rays and injuries (Bolognia et al., 2003). Thus, the hair coat has an important function in providing insulation against sudden heat loss or gain, thereby contributing to the regulation of the body heat (Bolognia et al., 2003). These crucial epidermal structures are established by the permanently regenerating hair follicles (Bolognia et al., 2003), where matrix cells proliferate rapidly and consequently produce the hair shafts (Paus et al., 1999) which consist of terminally differentiated and tightly compacted keratinocytes (Alibardi et al., 2007; Bolognia et al., 2003; Lippens et al., 2009).

The key property of these appendages is their mechanical resilience which is essential for skin protection and necessary to keep hairs projecting from the epidermis. This toughness is determined by several effects, such as hydrophobic and Coulombic interactions, hydrogen bonds and especially disulfide bridges (Popescu et al., 2009). In general, the mechanical stability of hairs is ascribed to longitudinally arranged keratin fibers (Omary et al., 2004), where macrofibrils composed of intermediate filament bundles are heavily cross-linked (Alonso et al., 2006; Bolognia et al., 2003; Moll et al., 2008; Popescu et al., 2009). The intermediate filaments are built up from α-keratin molecules being organized in a sophisticated way, containing two parallel monomers and antiparallel, shifted dimers oriented according to the amino acid composition and sequence (Popescu et al., 2009). The keratin fibers are embedded in an amorphous, mostly sulphor-rich matrix (Omary et al., 2004), which is responsible for additional resistance to physical stress (Bolognia et al., 2003; Popescu et al., 2009).

1.1.2 Hair anatomy

1.1.2.1 The hair follicle

Throughout embryogenesis approximately 5 million hair follicles are produced within the skin all over the human body (Bolognia et al., 2003, Linch et al., 2001; Paus et al., 1999), where

100.000 follicles cover the scalp alone (Bolognia et al., 2003). While no additional follicles are formed after birth and the total number hence remains constant, the size of individual follicles may change during lifetime, resulting in altered growth of the respective hair (Bolognia et al., 2003; Linch et al., 2001; Paus et al., 1999). The hair follicle itself is a constantly renewing organ (Bolognia et al., 2003), composed of numerous cylindric layers of interacting cells that support and preserve the emerging hair (Linch, 2008). At the point from which the hair grows, it is well supplied with minute blood vessels important for nourishing the growing region (Müller et al., 2007).

Inside the hair follicle lies the hair bulb (Fig. 1), a structure containing a highly proliferative cell population, the matrix keratinocytes (Bolognia et al., 2003). These matrix cells continue to divide, thereby producing progeny cells that, as they grow and develop, gradually push the previously formed cells upwards (Bolognia et al., 2003). Finally, they terminally differentiate to form the growing hair that exits the epidermal surface (Alonso et al., 2006). Once the matrix cells leave the hair bulb they cease to divide and take on characteristic roles as either cuticle, medullary or cortical cells of the hair shaft (Bolognia et al., 2003; Linch et al., 2001). The differentiating keratinocytes synthesize defined sets of keratins which are specific for each layer of the hair (Bolognia et al., 2003; Roberts et al., 2007). Melanosomes are transferred from melanocytes to hair keratinocytes and become integrated into the hair shaft (Bolognia et al., 2003; Roberts et al., 2007).

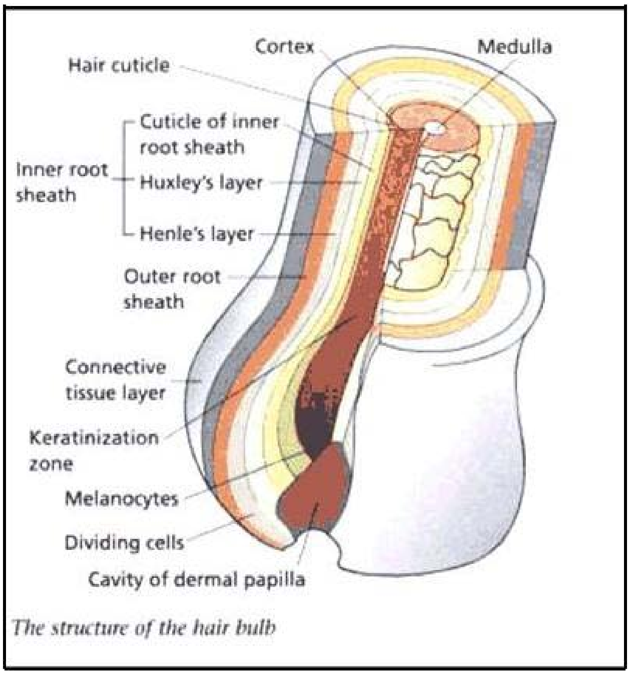
Hair cuticle
Cortex
Medulla
Cuticle of inner root sheath
Inner root sheath
Huxley's layer
Henle's layer
Outer root sheath
Connective tissue layer
Keratinization zone
Melanocytes
Dividing cells
Cavity of dermal papilla
The structure of the hair bulb

Figure 1: **The structure of the hair bulb.** (http://www.texascollaborative.org/hildasustaita/hairstructure.gif)

1.1.2.2 The hair shaft

The pigmented hair shaft is a complex multicellular tissue with astounding tensile strength (Bolognia et al., 2003), constituted of overlapping and interdigitating cells (Omary et al., 2004; Popescu et al., 2009). The dead cells of the mature shaft consist almost completely of tightly packed hair-specific intermediate filaments surrounded by an unstructured matrix of cellular debris and associated proteins (Linch et al., 2001; Omary et al., 2004; Paus et al., 1999). Incorporated into the hair shaft are the natural hair pigments, i.e. the melanins, produced by melanocytes distributed among the matrix cells (Paus et al., 1999). Black or brown hair is characterized by its content of insoluble eumelanin, whereas phaeomelanin, which is soluble in alkaline solutions, is the main pigment of blond and red hair (Müller et al., 2007).

As seen in Fig. 1, the hair follicle consists of six concentric structures (Bolognia et al., 2003): The outermost layer is made up from connective tissue, also called the dermal sheath (Linch, 2008). This composition is followed by the outer root sheath (ORS) which fuses both with the epidermis and the hair bulb (Bolognia et al., 2003). The ORS does not cornify; one of its most important roles is to support and guide the structure for the inner root sheath and the hair shaft (Bolognia et al., 2003). The IRS arises from terminally keratinized matrix cells and cornifies, thereby providing a rigid cylinder which eventually contains the central column of upwards-moving differentiating cells of the hair shaft (Bolognia et al., 2003). The inner root sheath (IRS) itself can be divided into three further layers, namely Henley’s layer, Huxley’s layer, and the IRS’ own cuticle (Bolognia et al., 2003). This structure is followed by the hair cuticle, which in particular is responsible for protection of the shaft from weathering and is also essential for keeping up the integrity of the hair fibres. Cuticle cells are arranged in a roof-tile pattern and consist mainly of proteins with a high number of cysteine residues.

Covered by these cells is the cortex, the main structural component of the hair shaft, which is built up from a dense package of interdigitating keratinocytes (Bolognia et al., 2003). Mature trichocytes are fully keratinized and are tightly attached to each other. The cortex is followed by the innermost structure of the hair shaft, namely the medulla. Medullary cells that have completely disintegrated are loosely packed (Bolognia et al., 2003), thereby providing an open column of large intercellular air spaces in the hair shaft’s centre (Linch et al., 2001); this structure may have a role in thermal insulation (Bolognia et al., 2003). The degree of medullation varies greatly between hair types. Human scalp hairs often lack medullated hairs whereas other types of human hair such as beard hairs contain a medulla (Linch et al., 2001).

Although the basic structure of the hair is conserved, there are significant differences in the fine architecture of hair among mammalian species. For example, in the most important model species, i.e. the mouse, most hair types contain a medulla.

1.1.3 The hair follicle cycle

To ensure persistent growth and replacement of hairs, human hair follicles will go through a life-long, well defined cycle of growth, regression and regeneration phases and are thus steadily transformed and restored in an exceptional process called the hair cycle (Bolognia et al., 2003, Linch et al., 2001). The phase where a hair follicle produces an entire hair shaft by growth of cells in the matrix is called anaphase (Roberts et al., 2007), the duration of which determines the final length of the hair (Alonso et al., 2006). During the anaphase the hair root is constantly supplied with nutrients and matrix keratinocytes are permanently proliferating (Müller et al., 2007), before differentiating into cells of the hair shaft cuticle, the cortex or the medulla (Bolognia et al., 2003). The following keratinisation process involves destruction of all cell organelles, so that only decomposed nuclei can be found in the hair shaft (Müller et al., 2007). This phase of active hair growth may last for 3-7 years (Linch et al., 2001; Müller et al., 2007).

After this period of steady proliferation and growth, the hair is no longer supplied with nutrients and the hair ceases to grow, thereby entering the catagen phase (Linch et al., 2001; Müller et al., 2007). Resulting from termination of mitosis in hair bulb matrix cells, hair shaft differentiation comes to a halt (Linch et al., 2001; Roberts et al., 2007) before the hair bulb is disassembled to a high degree by an apoptosis-driven process (Bolognia et al., 2003; Haake et al., 2007). Then the hair follicle enters the resting telogen phase, where the follicles lie dormant (Alonso et al., 2006), leading to their lowest proliferative and biochemical activities throughout the entire hair cycle (Bolognia et al., 2003).

During the telogen stage the hair shaft matures into a fully keratinized, dead club hair (Paus et al., 1999), while the hair root stem contracts until it is only one third of the original size it had in the anagen phase (Linch et al., 2001; Müller et al., 2007). Follicle stem cells are then stimulated to commence a new cycle of hair growth. A new hair follicle is allowed to form in the old cavity that still accommodates the club hair, which will finally be shed after three to four months (Alonso et al., 2006; Müller et al., 2007), usually during combing or washing (Paus et al., 1999), which is sometimes referred to as the exogen phase (Alonso et al., 2006).

On a normal scalp, 70-150 telogen hairs are usually lost per day, explaining why this hair type is most commonly found at sites of criminal investigations (Müller et al., 2007).

1.1.4 Terminal differentiation of hair keratinocytes

During hair shaft formation in the anagen phase of the hair cycle, keratinocytes undergo terminal differentiation (Alonso et al., 2006), involving events of complete keratinisation and the loss of nuclei and other organelles (Alonso et al., 2006; Haake et al., 2007; Linch, 2009; Müller et al., 2007). During the conversion of living cells to dead corneocytes (Haake et al., 2007), the cells become tightly packed with bundles of cysteine-rich keratins, thereby providing the hair shaft with strength and flexibility (Alonso et al., 2006).

At the point of complete keratinisation, mitochondria, ribosomes and other organelles are believed to disintegrate (Linch et al., 2001). Nuclear material is then degraded by a yet uncharacterized mechanism. It has been suggested that nuclear DNA loses its nucleus rather than the DNA is degraded within the nuclei (Linch, 2009). While at the beginning of gradual cellular cytolysis mitochondria may still protect mitochondrial DNA from degradation, this protection is probably not available to the nuclear genome (Linch et al., 2001), thus leading to a high level of degradation within nuclear DNA molecules. The breakdown of nuclear DNA is one of the hallmarks of programmed cell death (Fischer et al., 2007; Kawane et al., 2008).

1.1.5 Programmed cell death

Eukaryotic cells can undergo different forms of programmed cell death (PCD), where the cell metabolism is terminated due to genetically determined, cell-autonomous processes (Nagata, 2000 and 2005). Classical apoptosis is an efficient mechanism by which either potentially harmful or superfluous cells are removed (Fadeel et al., 1999; Hengartner, 2000; Kerr et al., 1972; Shiokawa et al., 2001). It is also a key mechanism in development and homeostasis (Kerr et al., 1972; Samejima et al., 2005; Wyllie et al., 1980) and is characterized by several morphological and biochemical changes (Kerr et al., 1972; Nagata, 2000; Polakowska et al., 1994; Samejima et al., 2005; Wyllie et al., 1980).

These alterations include the fragmentation of cell membranes, cytoskeletal rearrangements as well as condensation and shrinkage of both the cytoplasm and chromatin (Kerr et al., 1972; Nagata, 2000; Polakowska et al., 1994; Samejima et al., 2005; Wyllie et al., 1980). In general, these processes are accompanied by the formation of apoptotic bodies, the loss of microvilli (Kerr et al., 1972; Samejima et al., 2005; Wyllie et al., 1980) and the extensive degradation of nuclear DNA (Kerr et al., 1972; Nagata, 2000; Samejima et al., 2005; Shiokawa et al., 2001; Wyllie et al., 1980). Cleavage of chromosomal DNA at earlier stages of apoptosis leads to the production of 50-200 kb fragments (Nagata, 2000), whereas later the DNA is degraded into nucleosomal units of approximately 180 bp (Nagata, 2000; Polakowska et al., 1994; Shiokawa et al., 2001). Dying cells are immediately engulfed by neighbouring cells or macrophages, leading to the subsequent destruction of the corpses in lysosomes of the phagocytosing cells (Kerr et al., 1972; Nagata, 2000; Polakowska et al., 1994; Samejima et al., 2005; Shiokawa et al., 2001).

Whereas classical apoptosis and phagocytosis remove damaged cells (Nagata, 2005), other forms of PCD have functions in development and morphogenesis. For instance, many processes during mammalian development are accompanied by programmed cell death. Deficiency in cell death and incomplete DNA degradation can cause severe diseases (Nagata, 2005). In certain cases the dead cell remnants are maintained and even fulfil a physiological function. For instance, cells of the eye lens lose their nucleus to establish a transparent lens (Nishimoto et al, 2003).

Cornification of keratinocytes is another form of PCD. Keratinocytes form the cornified layer of the epidermis, i.e. the stratum corneum, the nail plate, papillae on the surface of the tongue and hair. All these structures consist of dead keratinocytes, also known as corneocytes, and PCD is a key element in all cornification processes. The mechanism of cornification-associated PCD is poorly defined (Kroemer et al., 2009). During terminal differentiation of hair keratinocytes (Candi et al., 2005; Lippens et al., 2005), dead cortical cells retain membraneous outlines that persist in the hair shaft (Linch et al., 2001).

1.1.6 Desoxyribonucleases

Intracellular DNA degradation depends on the action of numerous enzymes (Samejima et al., 2005). Major tasks in initiating the apoptotic machinery are performed by cysteine proteases of the caspase family, usually existing as pro-caspases which have to be activated by proteolytical cleavage (Hengartner, 2000). So called initiatior caspases cleave and thus trigger the pro-caspases which in turn target other caspases (Hengartner, 2000). This caspase cascade is essential for the amplification of apoptotic signals, thereby activating desoxyribonucleases (DNases) for their function in the degradation of chromosomal DNA (Hengartner, 2000). The caspase activated DNase (CAD) is the most prominent representative of endonucleases that cut the DNA into nucleosomal fragments (Nagata et al., 2003).

1.1.6.1 DNase1L2

DNase1L2 is a member of the family of DNase1-type endonucleases that catalyze endonucleolytic cleavage of DNA, thereby creating 3'-OH and 5'-P ends (Shiokawa et al., 2001). All DNase1 family proteins have shown dependence on divalent cations such as Ca^{2+} and Mg^{2+}, reaching highest activity levels under neutral pH conditions (Campbell et al., 1980; Laskowski, 1971; Price, 1975; Shiokawa et al., 2001). Additionally, two conserved histidine side-chains seem to be essential for proper DNase1 activity (Jones et al., 1996; Shiokawa et al., 2001).

Endonucleases of the DNase1 family share yet another characteristic structural feature, namely hydrophobic residues in their amino termini (Shiokawa et al., 2001). These signal peptides indicate that the enzymes are most likely located inside cell organelles such as the Golgi complex and the endoplasmatic reticulum (Shiokawa et al., 2001). What sets DNase1L2 apart from its family members is its optimum activity at the acidic pH of 5.6, whereas other DNase1 family members are active at neutral pH (Shiokawa et al., 2001).

DNase1L2 is expressed specifically in the epidermis, as well as in the cortex of hair follicles, sebaceous glands and nail units, which has been demonstrated on both mRNA and protein levels (Fischer et al., 2007; Jäger et al., 2007). The specific expression of DNase1L2 in epidermal appendages suggested an involvement of this enzyme in the mediation of chromosomal DNA degradation during terminal differentiation of keratinocytes (Fischer et al., 2007). As DNase1L2 lacks a nuclear localization signal (NLS) (Shiokawa et al., 2001), permeabilization of the nuclear membrane might be required prior to the degradation of chromatin-associated DNA by this endonuclease (Fischer et al., 2007).

The hypothesis that the enzyme has a specific role in degradation of nuclear DNA (nuDNA) during cornification of keratinocytes was based on the observation that DNase1L2 was the only DNase being upregulated during the differentiation of epidermal keratinocytes, while mRNA levels of other DNases were not altered or even reduced (Fischer et al., 2007). In several skin diseases showing aberrant retention of chromosomal DNA in the stratum corneum, decreased levels of DNase1L2 mRNA were revealed. Downregulation of this endonuclease was reported in parakeratotic epidermis of psoriasis lesions and in Bowen's disease (Fischer et al., 2007). Furthermore, aberrant retention of the nucleus in corneocytes, also known as parakeratosis, could be induced by knocking down of DNase1L2 in a human skin equivalent model (Fischer et al., 2007). This suggested that the enzyme played an important role during the special form of programmed cell death necessary for the terminal differentiation of keratinocytes (Fischer et al., 2007).

1.2 The hair as forensic sample

1.2.1 General considerations

Forensic identification and association of human hair evidence obtained at crime scenes are of major importance in many criminal inquiries (Birngruber et al., 2009; Miller, 1987). Microscopic analysis of hair samples is a method often found inappropriate for the determination of the origin of hairs with absolute certainty since the characteristics of hairs may vary within the same individual (Linch et al., 2001; Miller, 1987). Another factor influencing the results acquired during microscopic analysis is the examiner’s expertise which, if poor, may be responsible for the incorrect attribution of a hair to an individual (Birngruber et al., 2009; Linch et al., 2001; Miller, 1987).

Forensic casework analysis frequently involves sequencing of mitochondrial DNA which sometimes seems to be the only possible solution even if this approach bears several limits (Hellmann et al., 2001; Opel et al., 2008). Thus, typing of nuclear DNA extracted from human hair samples is in the centre of many forensic investigations. Although the typing of short tandem repeats (STRs) is possible in theory, it has shown a relatively low success rate (Birngruber et al., 2009; Hellmann et al., 2001), resulting from the high level of DNA degradation in telogen hair (Opel et al., 2008), which is the most common kind of hair evidence found during criminal investigations (Birngruber et al., 2009). In addition, hair evidence often suffers from environmental stress or contains PCR inhibitors such as hair pigment melanins, thereby further reducing the chances for obtaining a full DNA profile (Niederstätter et al., 2007; Opel et al., 2008).

1.2.2 Common microscopic analysis

Prior to typing of DNA from hair evidence which is a destructive process, hair samples are usually subject of microscopic analyses, focussing on characterization of common features within the hair cell ultrastructure (Linch et al., 2001; Linch et al., 2009). Among the most palpable variables in hair morphology are the colour, size, distribution and overall pattern of melanosomes, making these pigment granules the key features studied and compared under the microscope (Linch et al., 2001; Linch, 2009; Roberts et al., 2007). In order to get an overview of the general physical condition of the shaft, examiners will not only observe the medulla’s appearance and the hair shaft’s diameter, but will also search for indications of chemical treatment of the hair, usually resulting from hair dyes or perms (Roberts et al., 2007).

What makes attribution of a hair sample to an individual via morphological evaluation difficult, is the intra-individual variation exhibited by scalp hairs, where different hair types of the same individual can have similar characteristics when studied under the microscope but can also differ greatly (Miller, 1987; Roberts et al., 2007). In addition, labial, scrotal, or chest hairs may as well appear to have pubic origin when viewed individually (Linch et al., 2001), which even increases the already substantial natural range of microscopic variation detected in an individual’s total hair, easily leading to false exclusions when compared to the wrong type of an individual’s hair samples (Linch et al., 2001). Although inter-individual differences in microscopic features exceed intra-individual variation, the risk still persists that hair samples from two individuals may be indistinguishable under the microscope (Roberts et al., 2007).

Furthermore, microscopic characteristic may also change with time and thus again lead to incorrect association of an evidence hair to a suspect (Linch et al., 2001). Since the evaluation of the hair’s characteristics lies to a great part with the subjective opinion of the examiner, common microscopic analysis is not recommended to be the sole approach in order to attribute a hair to an individual, but if possible, a microscopic profile should still be obtained prior to the destructive DNA analysis (Linch et al., 2001; Miller, 1987).

1.2.3 Analysis of mitochondrial DNA

Most hairs secured at crime scenes are hairs in the telogen phase of the hair cycle (Birngruber et al., 2009). These hairs usually exhibit high levels of strongly fragmented nuclear DNA (Müller et al., 2007; Opel et al., 2008), which is the reason why in order to evaluate them in routine forensic casework, these samples are frequently reserved for mitochondrial DNA (mtDNA) analysis instead for typing of chromosomal DNA (Opel et al., 2008; Roberts et al., 2007). Telogen hairs are assumed to contain traces of nuclear DNA only, but extracted DNA is still suitable for the analysis of variable regions of mtDNA exploiting sequencing procedures (Hellmann et al., 2001; Opel et al., 2008). The major advantage of this approach lies in the high copy number of the mtDNA genome within a single cell and the large number of mtDNA molecules within each mitochondrion (Linch et al., 2001; Walker et al., 2003). These features make mtDNA a naturally amplified source of genetic variation persisting in the cell to a high extent (Walker et al., 2003).

The inheritance pattern of mtDNA is exclusively maternal (Linch et al., 2001), leading to the same mtDNA haplotype shared by maternally related individuals (Roberts et al., 2007). Hence, the possibility of two unrelated individuals sharing a common sequence of mtDNA cannot be ruled out completely (Roberts et al., 2007). Given the lower power of discrimination resulting from the only little polymorphic characteristics of mtDNA (Roberts et al., 2007), namely haploidy, its small size and the matrilineal inheritance pattern (Opel et al., 2008), typing of mtDNA is much less conclusive than typing of short tandem repeats (STRs) in nuclear DNA (Opel et al., 2008). In addition, the results gained during sequencing of mtDNA cannot be matched with DNA profiles implemented in forensic intelligence databases (Hellmann et al., 2001; Müller et al., 2007). Instead, a comparison of mtDNA sequences is only possible if a certain suspect already exists (Müller et al., 2007).

1.2.4 Analysis of nuclear DNA

The use of DNA profiling, i.e. the analysis of certain nuclear loci, is of major importance in numerous criminal investigations (Walker et al., 2003). Accurate quantitation of the nuclear DNA extracted from a crime scene sample is an essential step prior to the actual typing of STRs, which has often been difficult when using hair samples (Nicklas et al., 2003b; Opel et al., 2008; Walker et al., 2003). Partial profiles may be obtained provided that sufficient nuclear DNA can be extracted from the evidence hair; in rare cases a higher number of loci can be typed correctly due to larger amounts of isolated nuclear DNA (Opel et al., 2008). While usually it is no problem to recover enough DNA from roots of hairs in the anaphase, DNA extraction from telogen hairs has turned out to be a much more complicated issue as in these hairs the amount of amplifiable DNA is much lower than in anagen hairs (Müller et al., 2007). Only minute amounts of nuDNA can be detected in hair shafts, and these DNA molecules, often suffering from additional impairments resulting from chemical or sunlight oxidation processes (Müller et al., 2007), are highly fragmented due to the keratinization process (Opel et al., 2008). Since the resting telogen hair root is mainly composed of keratin it is only a poor source of nuDNA, while soft tissue, such as hair follicle sheaths, follicular tags and growing root stems, can be considered a good supply of chromosomal DNA (Linch et al., 2001). Single hairs have hence only been subjected to DNA profiling if such cells were still attached to the hair, taking into account that STR typing of hairs lacking adhering cells has merely shown little success or has failed completely (Hellmann et al., 2001).

The amount of DNA extracted from hair and thus the ability to obtain a DNA profile varies not only from person to person but also between different hair samples of the same individual (Müller et al., 2007; Opel et al., 2008). These fluctuations in PCR yield have mainly been accredited to different amount of PCR inhibitors present in the hair, such as melanin and substances used for hair dyeing, another factor being considered was the increasing instability of DNA with time (Niederstätter et al., 2007). Taken together, the reduced copy number of chromosomal DNA and the high level of DNA degradation are the key factors responsible for failures in typing nuDNA isolated from hair shafts (Linch et al., 2001). The probability of correct STR profiling is increased significantly by thorough extraction of the trace amounts of nuDNA and careful removal or neutralization of PCR inhibitors (Müller et al., 2007).

1.2.5 Biological methods used in forensic analysis of nuDNA

1.2.5.1 DNA quantitation in human crime scene samples

A step of major importance for successful DNA genotyping is the preceding quantitation of DNA extracted from crime scene samples, such as human evidence hairs (Nicklas et al., 2003b; Opel et al., 2008; Walker et al., 2003). Application of the appropriate amount of template is essential, since using too little or much DNA can be responsible for difficulties during amplification of the STR loci, often requiring repetition of the PCR (Krenke et al., 2002; LaFountain et al., 2001; Moretti et al., 2001; Nicklas et al., 2003b). Out of several methods used to quantify DNA, from basic UV spectrometry through various blotting techniques, PCR has become widely accepted as one of the fastest, least expensive and thus ideal technique for the forensic laboratory (Nicklas et al., 2003a).

1.2.5.1.1 Quantitative real-time PCR

In contrast to traditional polymerase chain reaction (PCR) which is a qualitative approach much rather than a quantitative one, the application of quantitative real-time PCR allows direct and independent evaluation of each sample during the exponential phase of the PCR product's accumulation (Nicklas et al., 2003b; Real-time PCR methods (Roche Applied Science)). The time-consuming analysis step usually performed after PCR is abolished by detection instruments which are much more sensitive than the commonly used gel electrophoresis and ethidium bromide staining (Real-time PCR methods (Roche Applied Science)). If fluorescent dyes are incorporated into DNA products, the increasing concentration of products can be monitored by measuring the levels of fluorescence (Nicklas et al., 2003b; Real-time PCR methods (Roche Applied Science)). Fluorescence is then plotted against the cycle number, subsequently revealing the cycle threshold (Ct), i.e. the point where the amount of PCR product and thus the amplification curve crosses a previously defined fluorescence value (Nicklas et al., 2003b). This Ct value is inversely proportional to the DNA level in the corresponding PCR reaction, delivering the final readout for each sample (Nicklas et al., 2003b).

1.2.5.1.2 Alu-based real-time PCR

Alu sequences are transposable elements (Nicklas et al., 2003a; Walker et al., 2003) that seem to have their origin in 7SL RNA, a cytoplasmic RNA found in large quantity throughout all species (Nicklas et al., 2003a; Ullu et al., 1984). These retrosposons have amplified extensively during primate evolution (Nicklas et al., 2003a; Walker et al., 2003), leading to an estimated number of 1 million copies per human genome (Nicklas et al., 2003b; Walker et al., 2003). Two similar monomers flanking a region with high A-content represent the 280 bp consensus sequence (Nicklas et al., 2003b) which is found exclusively in primate genomes (Nicklas et al., 2003b; Walker et al., 2003).

The expanding Alu elements have generated a wide range of subfamilies that seem to stem from different genetic ages (Walker et al., 2003), such as the J family being the oldest having evolved 80 million years ago or the much younger Y family, having developed only 3-4 million years ago (Nicklas et al., 2003a). In approximately 37 million years after the Sx family's initial emergence, its members have been amplified to such a high extent that nearly half of all human Alu elements are derived from this subfamily (Nicklas et al., 2003a).

The fact that some of the younger Alu families have only emerged in the human genome, Alu-based quantitative real-time PCR assays provide a very specific technique for quantitation and identification of human DNA (Walker et al., 2003). Amplification of the high-copy ALU elements dramatically increases the sensitivity of normal real-time PCR assays, thus resulting in a method especially useful in forensic investigations of legal cases (Walker et al., 2003). Due to the poor detection limit of traditional quantitation procedures, human evidence material often appears to contain no DNA at all, thereby leading to wrong assumptions concerning the chances for successful DNA typing (Walker et al., 2003). With Alu-based quantitation assays followed by modern DNA profiling techniques, essential progress has been made towards accurate and reliable determination of human DNA concentrations in a wide range of complex sources (Nicklas et al., 2003b; Walker et al., 2003).

1.2.5.2 STR typing

Short tandem repeats (STRs), also known as simple sequence repeats (SSRs) or microsatellites (Butler, 2007), are small sequences of DNA usually found in non-coding intron regions of the human genome (Butler, 2005). These oligos, typically in the length of 2-7 nucleotides, are tandemly repeated between approximately 5 and 50 times, the number of repeats being a random variable. This gives rise to polymorphisms resulting from homologous STR loci differing in the exact number of repeats, a phenomenon exploited in genetic fingerprinting (Butler, 2005). Thousands of characteristic STR markers can be found in the human genome, the combination of which is unique and varies from person to person (Butler, 2005 and 2007). In order to allow generation of STR profiles that can be compared on an international basis, a uniform core set of loci have been selected for use in forensic DNA investigations (Butler, 2007).

The whole STR typing procedure starts with extraction and quantitation of DNA from the casework sample (Butler, 2005 and 2007), followed by simultaneous amplification of up to 16 polymorphic regions via PCR (Butler, 2005 and 2007; Grubwieser et al., 2006). Analysis of multiple STR loci, offering excellent discrimination power while consuming only minute amounts of sample, is achieved by use of distinguishable fluorescent dyes, amplicons of different lengths and spatial separation of the loci (Grubwieser et al., 2006). STR typing kits traditionally provide primers for 15 loci, accompanied by a sex-typing assay detecting amelogenin on the Y-chromosome (Butler, 2007). PCR products are then subjected to separation via capillary electrophoresis, revealing each amplicon’s size and thus the number of STRs present in each allele (Butler, 2005 and 2007). This size-based separation is followed by the actual typing step and interpretation of the obtained profile, along with determination of statistical significances of possible matches (Butler, 2005).

In practice, casework samples frequently comprise highly degraded DNA and thus give rise to only partial DNA profiles, leading to random matches given the much lower discrimination power (Grubwieser et al., 2006). In order to successfully amplify such degraded DNA samples, so called miniSTR systems have been developed, using redesigned primers resulting in much smaller amplification products (Butler, 2007; Grubwieser et al., 2006). Amplification of such degradation-sensitive loci could be significantly improved by the use of miniSTR primers, subsequently increasing the success rate for typing of DNA samples suffering from high levels of fragmentation (Grubwieser et al., 2006).

2. AIMS OF THE THESIS

The first aim of this thesis was to quantify the contribution of DNase1L2 to degradation of DNA during cornification of keratinocytes. For this purpose, a DNase1L2 knockout mouse model was investigated. An *in situ* staining protocol for DNA in hair had to be established for detection of nuclei retained in hair, and the results were compared with a quantitative method, namely quantitative real-time PCR.

The second aim was to investigate whether differences in the breakdown of nuclei might explain inter-individual differences in the yield of DNA from human hair, which had been observed in forensic investigations. This aim required the optimization of the *in situ* DNA labeling protocol and linking of this method with DNA extraction from human hair and subsequent short tandem repeat (STR) typing. The ultimate aim was to evaluate the use of *in situ* DNA labeling in hair for potential applications in forensic medicine.

3. RESULTS

3.1 Targeted gene deletion demonstrates a role of DNase 1L2 in terminal differentiation of hair keratinocytes

Since the first aim of the study was to determine the role of DNase1L2 *in vivo*, DNase1L2-deficient mice were generated by Leopold Eckhart and colleagues at the Department of Dermatology, Medical University of Vienna (Fischer et al., manuscript submitted for publication). The DNase1L2 knockout mice were viable, apparently healthy up to an age of two years and macroscopically inconspicuous. Unlike DNase1L2 knockdown in human *in vitro* skin models (Fischer et al., 2007), DNase1L2 knockout in the mouse did not result in parakeratotic stratum corneum. However, nuclear remnants were detected in cross-sections of DNase1L2-deficient hair follicles. This indicated that, in the mouse, DNase1L2 may function in skin appendages rather than in the interfollicular epidermis.

3.1.1 Fluorescent labeling of nuclear DNA in murine hair

In order to test the hypothesis that abrogation of DNase1L2 leads to retention of nuclei in corneocytes of skin appendages, a protocol for fluorescent labeling of DNA in hair was established. Murine hairs were permeabilized with 1% ammonia solution and stained with the DNA-specific dyes Hoechst 33258 or DAPI, resulting in (if present) nuclei fluorescing blue under UV light.

3.1.1.1 Murine hair deficient in DNase1L2 comprised Hoechst-positive nuclei

Hairs from both wild-type and knockout mice of mixed background (C57Bl6 / 129) were stained with Hoechst 33258 and viewed under the microscope. Massive retention of nuclear DNA was detected in the hair from knockout mice (Fig. 2D, H) whereas no nuclei could be stained in hair from control mice (Fig. 2B, F). Inhibition of DNase1L2 expression caused retention of DNA in most corneocytes of these epidermal appendages. Nuclei could be labeled in the medulla, the cortex and the cuticle of DNase1L2 deficient hair, irrespective of body site and stage of the hair cycle. Although a quantitative comparison of hair layers was difficult, it appeared that corneocytes of the cortex and cuticle contained less DNA than those of the medulla.

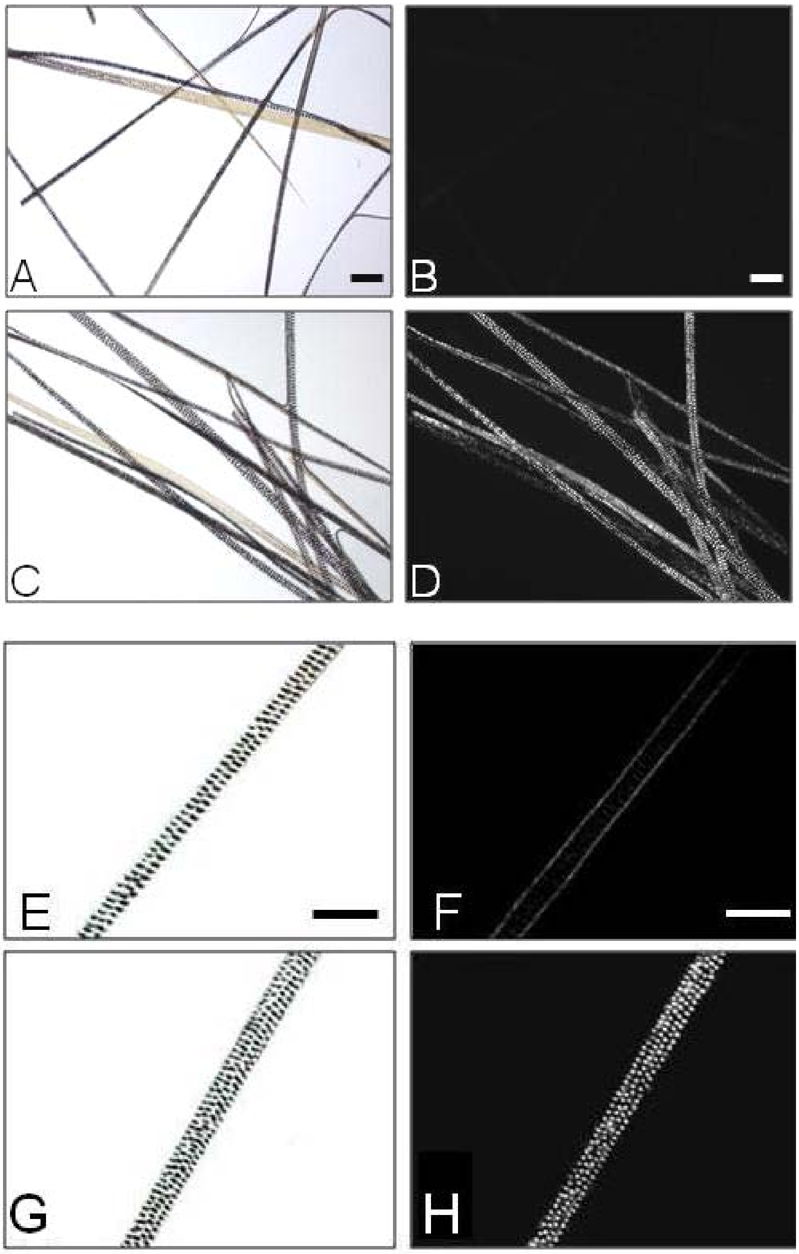

Figure 2: Hoechst staining of nuclear DNA comprised in murine hair. Hairs from back skin of wild-type (A, B, E, F) and DNase1L2 deficient (C, D, G, H) mice were permeabilized with ammonia and stained with Hoechst 33258. Photos under bright field (A, C, E, G) and fluorescence light (B, D, F, H) from the same sites were taken. Bars = 100 µm.

3.1.1.2 DNA-labeling in hair from DNase1L2 knockout mice of the pure background of strain 129

The previous results could be reproduced when staining hair from wild-type and knockout mice with a pure background, namely 129. Again, DNase1L2 deficient hairs comprised nuclear DNA in almost every cell remnant (Fig. 3B and D). This confirmed that the ability to label DNA in hair was not restricted to hair samples obtained from mice with a mixed background.

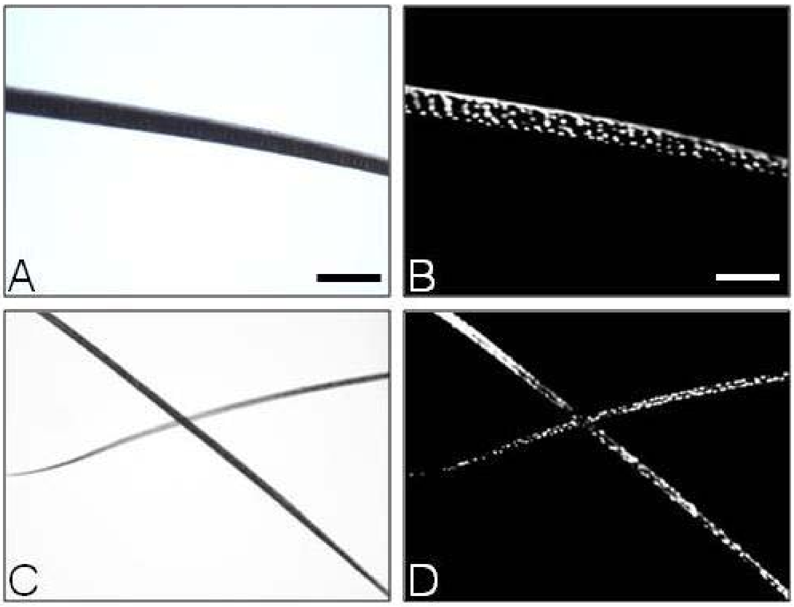

Figure 3: Fluorescent labeling of DNA in hair from strain 129 mice deficient in DNase1L2. (A) and (C) present photos obtained under bright field while (B) and (D) show Hoechst-positive nuclei fluorescing under UV light. Bars = 100 µm.

3.1.1.3 Lack of Hoechst-positive nuclei in wild-type hair could not be ascribed to differences during hair permeabilization

In order to exclude the possibility that the higher number of stainable nuclei in DNase1L2 deficient hair resulted from better accessibility of the fluorescent dye to the nuclei (i.e. better permeabilization) rather than from nuclei being actually retained, hair from both wild-type and DNase1L2 knockout mice were covered with liquid nitrogen and mashed with a mortar to destroy barriers to permeabilization. These hair fragments were then placed next to each other on the same glass slide, followed by embedding in mounting medium containing the DNA-specific dye DAPI. After allowing the fluorescent dye to diffuse into the hair debris, the samples were studied under the microscope.

Whereas the fragments derived from DNase1L2-deficient hair were thoroughly stained with DAPI, thus resembling a fluorescent cloud under UV light (Fig. 4B, right), no DNA-labeling could be observed in debris originating from wild-type hair (Fig. 4B, left). In hair samples from knockout mice, single nuclei were found to be fluorescing brightly, setting themselves apart from the already intense background staining of the entity of hair fragments (Fig. 4B, right). This experiment confirmed that even in the absence of a protective layer on the surface of hair, wild-type hair had little, if any, affinity to DNA-binding dye while DNase1L2-deficient hair was strongly labeled.

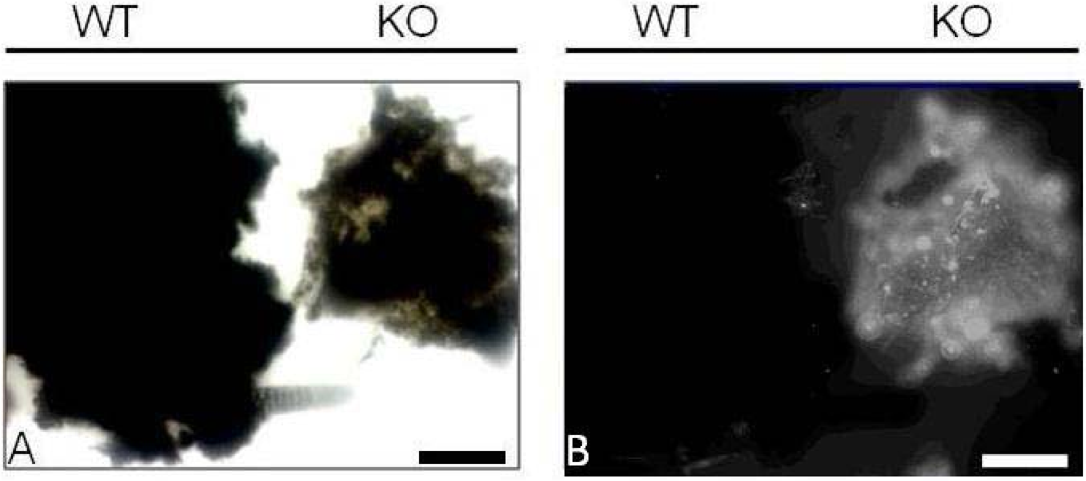

Figure 4: Murine hair debris embedded in mounting medium containing DAPI. Fragmented hairs derived from wild-type (A and B; on the left) and DNase1L2 deficient (A and B; on the right) mice were placed onto the same glass slide and incubated with DAPI; pictures were obtained under bright field (A) and UV light (B). Hoechst-positive nuclei are visible in the thoroughly stained hair debris lacking the endonuclease (B, right). Bars = 100 µm.

3.1.1.4 Nuclear DNA was detectable in all hair types of DNase1L2 deficient mice

The murine fur consists of four different hair types called zigzag, guard, awl and auchene. These hair types differ in length, shape and the number of medullated columns (Schlake, 2007). In order to determine whether DNA was retained to the same extent in all of these hair types, hairs from DNase1L2 deficient mice were separated into these four types under the microscope and stained individually with Hoechst. As seen in Fig. 5, the same levels of nuclear DNA labeling could be detected in all hair types, independent of the number of cell rows in the medulla.

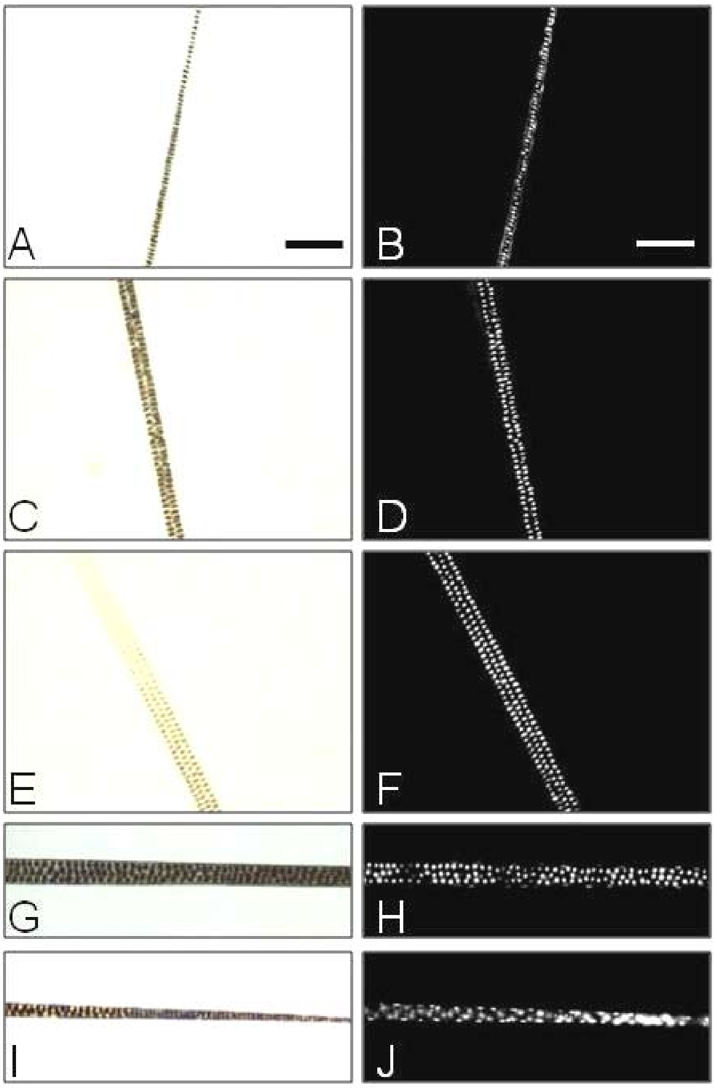

Figure 5: Hoechst-labeling of nuclear DNA in all hair types of the murine fur. Zigzag (A, B), guard (C, D), awl (E, F) and auchene (G-J) hairs were stained for DNA and photographed under bright field (A, C, E, G, I) as well as under UV light (B, D, F, H, J). Bars = 100 µm.

3.1.1.5 Hoechst-labeling of nuclear DNA in vibrissae

After examination of different hair types in the murine fur, we wanted to confirm the presence of retained nuclei in vibrissae, which do not regularily contain a medulla. Vibrissae, also known as whiskers or tactile, sensory and sinus hairs (Davidson et al., 1952) are long stiff hairs with a predominantly sensory function (Danforth nomenclature, 1925). Vibrissae from both wild-type and knockout mice were collected and subsequently stained with Hoechst. Fig. 6B demonstrates that vibrissae obtained from control mice were devoid of nuclear DNA, whereas large numbers of nuclei could be labeled in hair from DNase1L2 deficient mice (Fig. 6D).

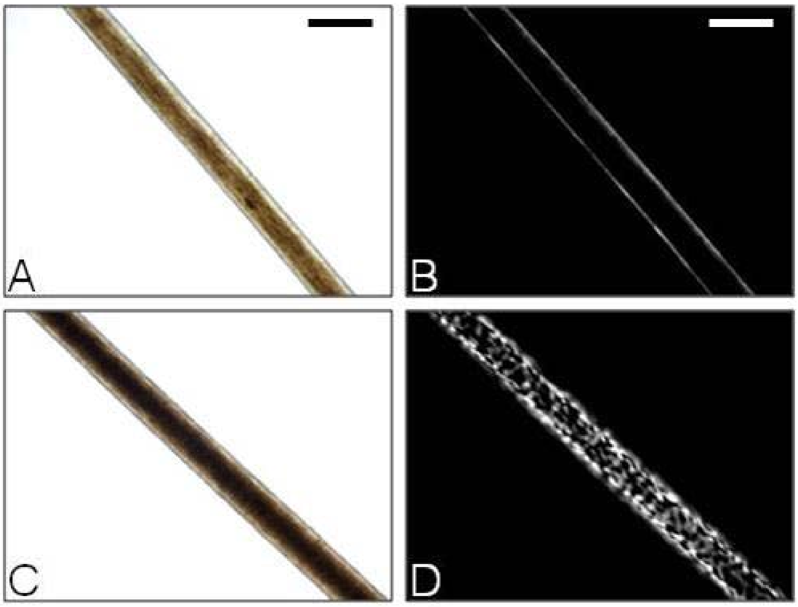

Figure 6: Fluorescent staining of nuclear DNA comprised in vibrissae. Vibrissae from wild-type (A, B) and DNase1L2 knockout mice (C, D) were labeled with Hoechst. Pictures were taken under bright field (A, C) and fluorescent light (B, D). Bars = 100 µm.

3.1.2 Quantitation of nuclear and mitochondrial DNA by real-time PCR

In order to quantitatively determine nuclear DNA in murine hair, a quantitative real-time PCR assay was established. Hair samples were lysed followed by purification and subsequent quantification of the DNA. To achieve maximum sensitivity, the primers were selected to specifically amplify high-copy number transposable elements, namely LINE-1 elements, in the murine genome. Mitochondrial DNA was amplified by primers flanking mitochondrial DNA-specific sequences.

3.1.2.1 Determination of nuclear and mitochondrial DNA levels in hair and nail extracts from wild-type mice and DNase1L2 deficient mice

Two independent experiments were performed in order to quantify the amount of nuclear and mitochondrial DNA in hair from control and DNase1L2 knockout mice. While the first experiment was performed with 5 mg of hair obtained from 5 animals of each genotype (Fig. 7A and B), the second trial used 20 mg of hair derived from 3 mice of each species (Fig. 7C and D). Both experiments produced similar results regarding the relative amounts of DNA extracted from normal and DNase1L2-deficient hair but differed considerably in the total concentrations of amplified DNA. While in the first PCR reaction (i.e. 5 mg of hairs were used) about 55 ng of nuclear DNA per mg hair could be extracted, in the second reaction (i.e. 20 mg were lysed) approximately 285 ng of nuclear DNA per mg of hair could be detected.

As demonstrated in Fig. 7A and C, hair from DNase1L2-deficient mice contained significantly higher levels of nuclear DNA than hair from control mice, irrespective of the amount of input material. After exact ratios between DNA yields obtained from both hair samples were established, differences between the both experiments were observed. When using 20 mg of hair, 180-fold elevated amounts of nuclear DNA were detected in DNase1L2-deficient hair instead of the 470-fold difference found when using only 5 mg of hair sample.

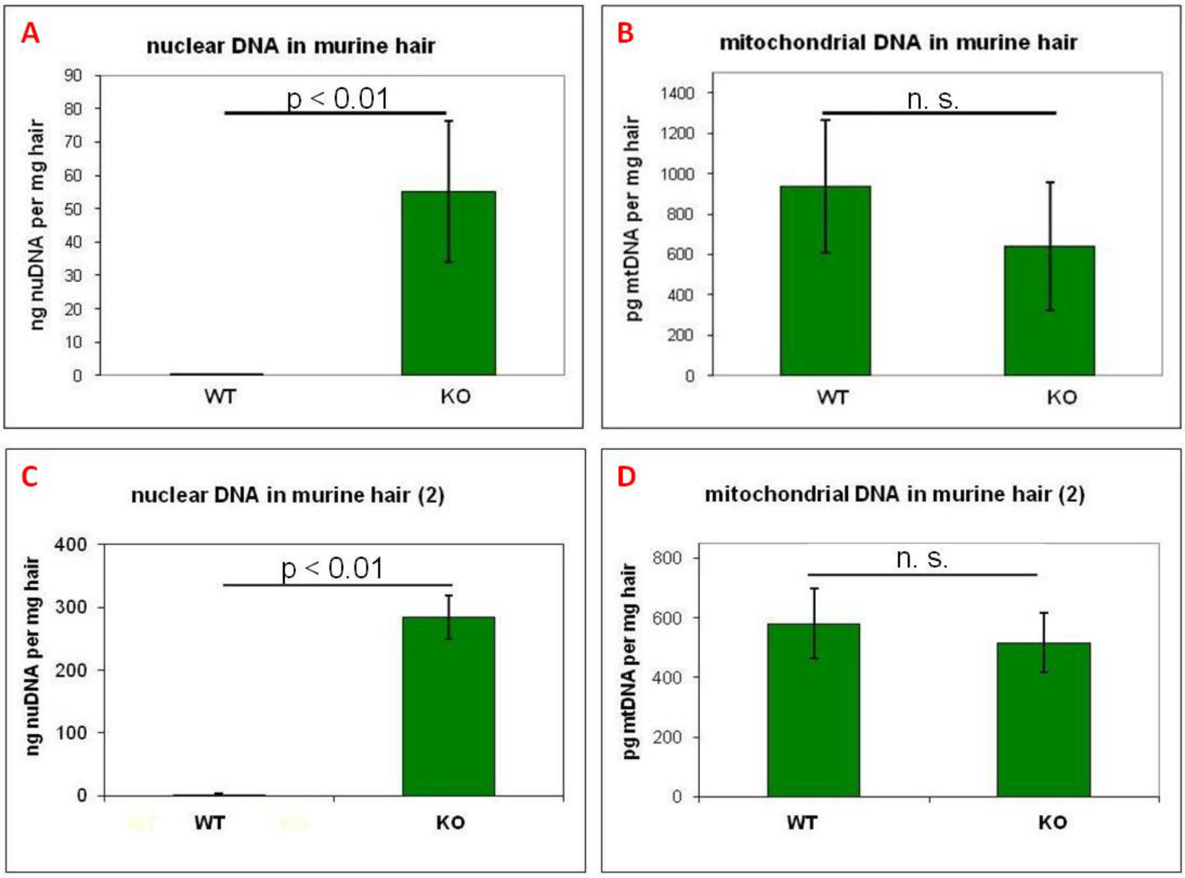

Figure 7: Real-time PCR performed with nuclear and mitochondrial DNA extracted from hair samples obtained from wild-type and DNase1L2-deficient mice. Two independent experiments are shown: (A) and (B) depict analysis of hair samples (5mg) from 5 mice per genotype. (C) and (D) present an experiment using 20 mg of hair from 3 mice per group. P-value of Student’s t-test are shown. WT, wild-type mouse; KO, knockout mouse.

The cause for these differences in total amounts of extractable DNA couldn't be determined since all samples had been processed in a standardized way, although one minor modification during lysis of the hair samples should be mentioned. In order to lyse 5 mg of hair, only 500 µl of lysis buffer were added to the samples instead of 750 µl buffer used for lysis of 20 mg hair. Still, this didn't satisfactorily explain the high deviation of total DNA amounts and suggested that, although the method can be reliably applied for comparative studies, it might need to be further optimized for more accurate quantification of present DNA levels.
Nevertheless, both experiments clearly demonstrate that abrogation of DNase1L2 is responsible for massive retention of nuclear DNA in hair. In contrast, the content of mitochondrial DNA was not significantly different in DNase1L2-deficient and normal hair, which could be shown in both experiments (Fig. 7B and D).

Since nails also consist of cornified cells that express DNase1L2 (Jäger et al., 2007) and lose DNA during terminal differentiation, the impact of the ablation of DNase1L2 on the DNA levels in these hard structures was investigated as well. Again, there was a dramatic difference in amplified nuclear DNA. Nails of DNase1L2-deficient contained about 2000-fold more nuclear DNA (Fig. 8A), and, interestingly, also 30-fold more mitochondrial DNA (Fig. 8B) than control mice. Taken together, these data demonstrated that the breakdown of nuclear DNA in both hair and nail requires DNase1L2. Furthermore, DNase1L2 also seems to participate in the degradation of mitochondrial DNA in nails but not in hair.

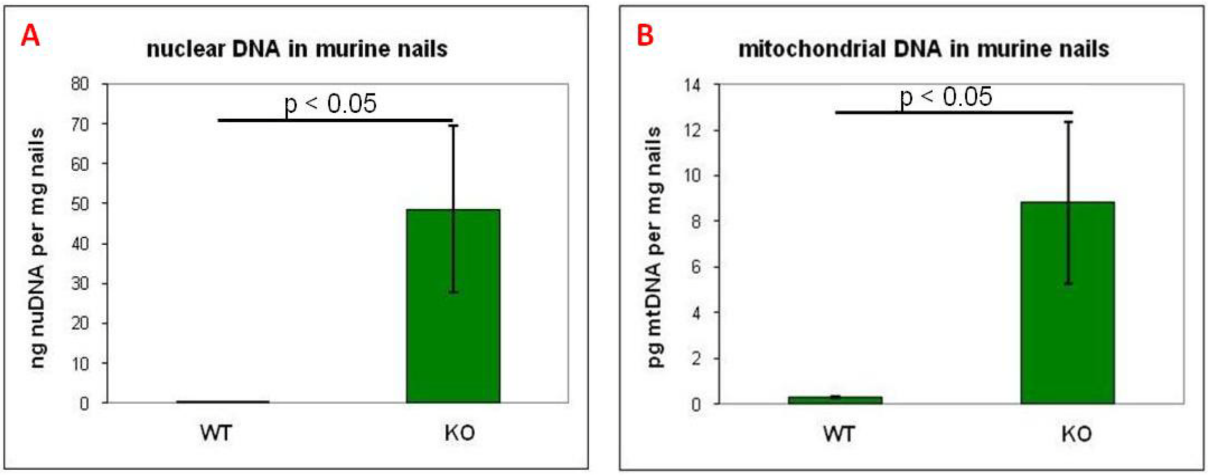

Figure 8: Real-time PCR performed with nuclear and mitochondrial DNA extracted from murine nails. Nail samples from 3 mice per group were analysed. P-value of Student's t-test are shown. WT, wild-type mouse; KO, knockout mouse.

3.1.2.2 Quantitation of DNA in the stratum corneum

In order to study DNA levels in the stratum corneum of DNase1L2-deficient mice, strips of adhesive tape were applied to shaved areas on the backs of both control and knockout mice. The tapestrips and the attached layers of stratum corneum were transferred to small tubes and incubated with extraction buffer. For unknown reasons, negative controls, i.e. tapestrips without adhering stratum corneum, yielded significant background levels of DNA amplification. Furthermore, DNA purification was difficult because the purification columns were frequently blocked with glue from the tapestrips.

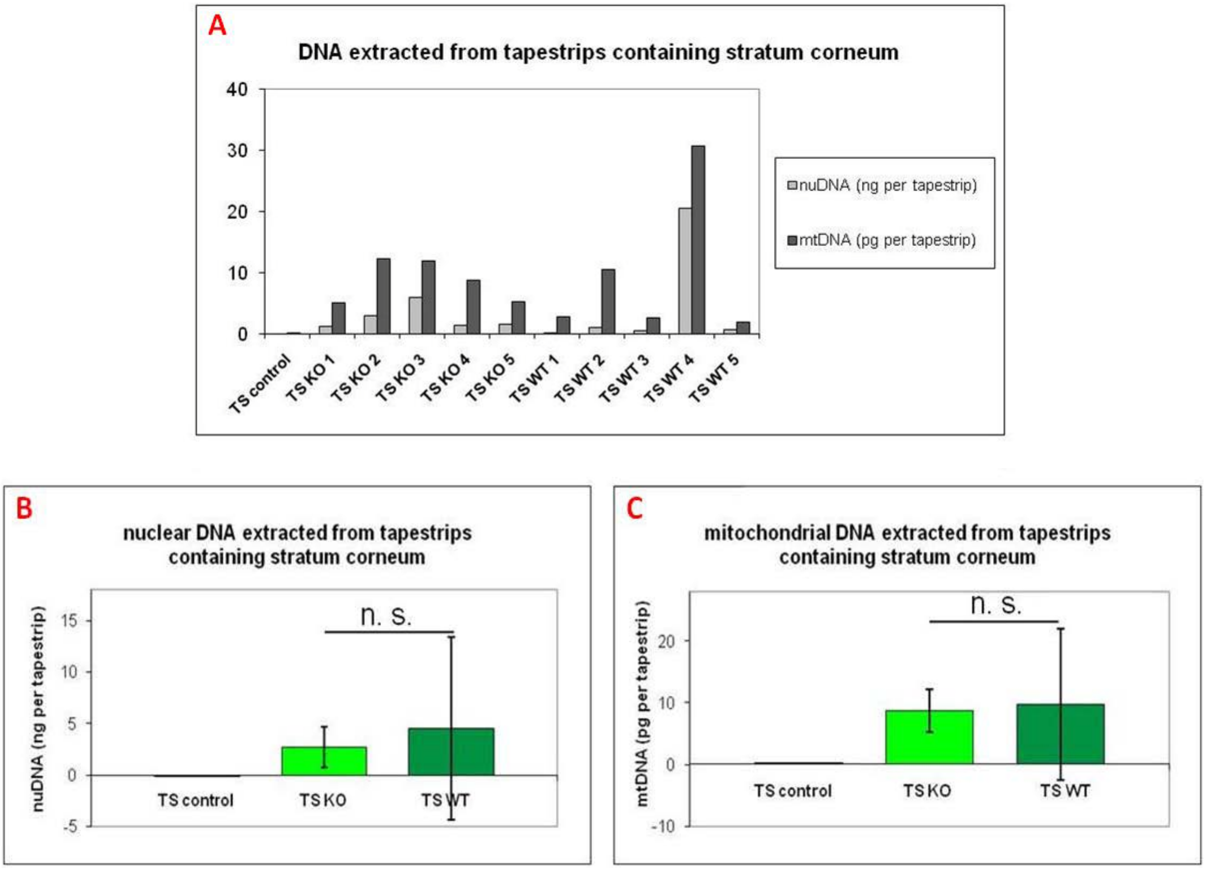

Figure 9: Real-time PCR performed with nuclear and mitochondrial DNA extracted from tapestrips containing murine stratum corneum. A tapestrip (TS) was applied to each of five mice per genotype (DNase1L2 knockout (KO) and wild-type (WT). Nuclear (grey bars; unit = ng) and mitochondrial (black bars; unit = pg) DNA were determined by quantitative PCR for a control tapestrip lacking sample and tapestrips comprising stratum corneum from either DNase1L2 knockout or wild-type mice (A). Direct comparison between the levels of nuclear (B) and mitochondrial (C) DNA detected in control tapestrip and in tapestrips detached from skin is shown. P-values were determined with Student’s t-test.

To test whether the DNA yield was affected or not, equal amounts of a DNA were added to the lysis buffer and the tapestrips, which were then subjected to the purification procedure.

Indeed, there were fluctuations in the PCR yield despite identical concentrations of the input DNA. Another weakness of this method was the lack of a control for the amount of stratum corneum attaching to each tape strip. Although the tapes were of equal diameter and were applied to the skin with approximately equal force, visual inspection of the tapes indicated that the amount of stratum corneum varied considerably between the samples. However, this variance did not appear to be associated with the DNase1L2 genotype.

In spite of methodological problems, the whole procedure of lysis, DNA extraction and quantification was tested with tapestrips containing stratum corneum from 5 mice of both wild-type and knockout species. Because of rather inhomogeneous results within samples having the same origin it was difficult to determine outliers, but altogether no significant difference between the two groups could be observed (Fig. 9).

3.2 Functional characterization of other DNases in the skin

In the course of this project, further DNases of the DNase1 family were investigated for their potential role in DNA breakdown in hair. Mice lacking either the gene of DNase1 or DNase1L3 were obtained from Markus Napirei (University of Bochum, Germany). Hair samples of these mice were subjected to DNA staining with Hoechst, quantitative real-time PCR or both. Since the characterization of these mouse models has not been completed yet, only preliminary results are available.

3.2.1 Hair deficient in DNase1 lacked Hoechst-positive nuclei and showed normal DNA content

In order to investigate whether DNase1 is involved in DNA fragmentation during terminal differentiation of corneocytes, hair from DNase1 knockout mice was treated equally as DNase1L2 deficient hair. Unspecific staining of the cellular structures but no labeling of nuclear DNA was observed. No difference was detected between hair samples from wild-type (Fig. 10B) and DNase1 knockout mice (Fig. 10D). In addition, quantitative real-time PCR was carried out with these hair samples. No differences in DNA levels could be detected when amplifying mitochondrial DNA. Similarly, when using primers specific for murine nuclear DNA, PCR yield was almost equally high in samples from control and knockout mice, the DNA concentration being even slightly lower in extracts obtained from DNase1 deficient mice (data not shown). This suggested that, in contrast to DNase1L2, DNase1has no influence on the degradation of DNA in hair.

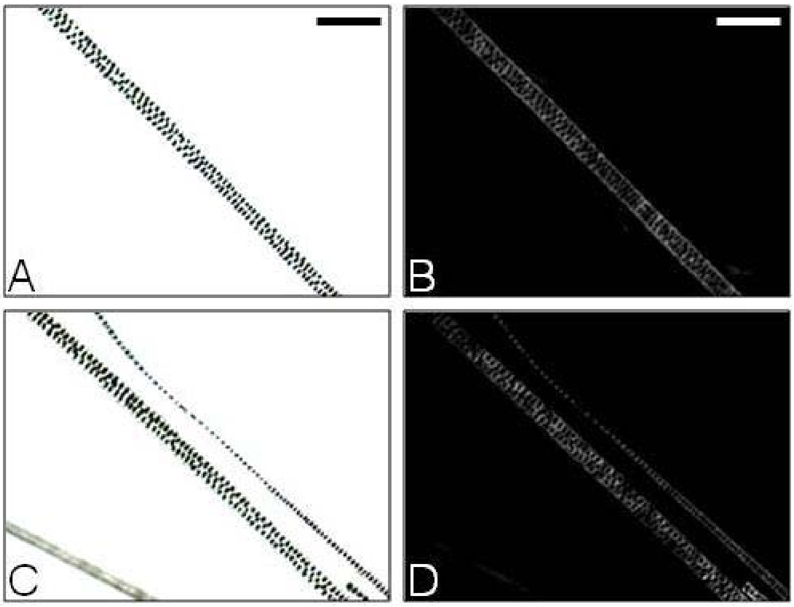

Figure 10: Hoechst-labeling of wild-type and DNase1 deficient hair. Hairs from both wild-type (A, B) and DNase1 deficient mice (C, D) were stained for nuclear DNA. Pictures were taken under bright field (A, C) and fluorescent light (B, D). Note that the fluorescence images were recorded at high sensitivity and that the labeling must be regarded as unspecific binding of the dye to non-DNA structures. Bars = 100 µm.

3.2.2 Hair from DNase1L3 knockout mice comprised no stainable nuclei

Up to now, hair from DNase1L3 deficient mice has only been subjected to DNA-labeling, but quantitative real-time PCR has not been performed yet. Analogically to hair lacking DNase1, when attempting to stain nuclei with Hoechst, a negative result was obtained, i.e. no stainable nuclei could be detected in both DNase1L3 deficient hair (Fig. 11D) and in hair from wild-type control mice (Fig. 11B). Thus, DNase1L3 seems to have a function different from that of DNase1L2.

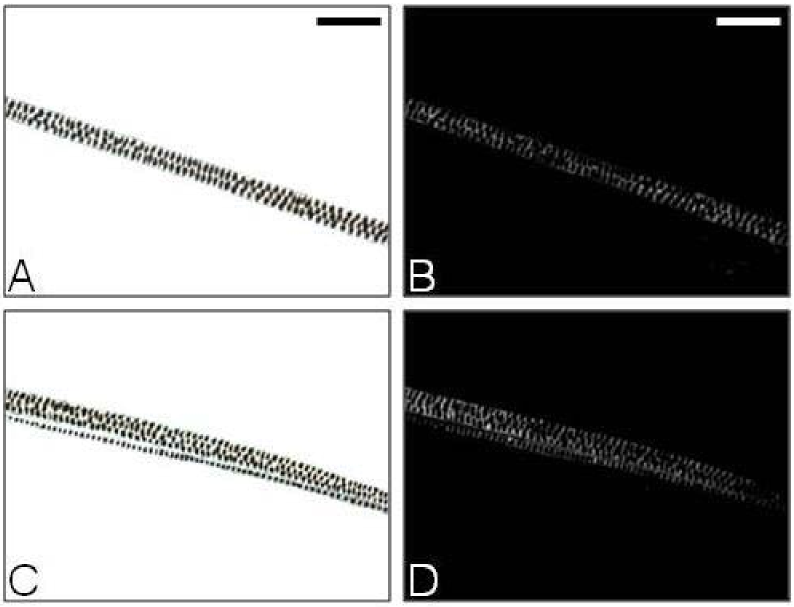

Figure 11: Fluorescent labeling of nuclear DNA in normal and DNase1L3 deficient hair. Hairs from wild-type (A, B) and DNase1L3 knockout mice (C, D) were labeled with Hoechst. Pictures were taken under bright field (A, C) and fluorescent light (B, D). Note that the fluorescence images were recorded at high sensitivity and that the labeling must be regarded as unspecific binding of the dye to non-DNA structures. Bars = 100 µm.

3.3 Detection of nuclear DNA in hair from different wild-type mouse strains

In order to test whether the presence of stainable DNA in hair depended on the genetic background, possibly involving factors different from DNase1L2, hair from several mouse strains was subjected to DNA labeling with Hoechst.

3.3.1 Hoechst-labeling revealed residual nuclear DNA in hair from BalbC, FVB and CH3 mice

Six different wild-type strains were selected and hair samples were obtained. When hairs were labeled with Hoechst, in hair from mice with the background of both 129 and C57Bl6 almost no nuclei were detectable; instead, unspecific staining of the cell remnants was observed (Fig. 12B and F). Similar results were obtained in hair from PWD mice, in which no nuclei at all could be stained (Fig. 12N). By contrast, white hair from BalbC (Fig. 12D) and FVB (Fig. 12L) a high number of nuclei were labeled with Hoechst dye. In hair samples from CH3 mice a high number of nuclei could be detected in hairs with at least two or more cell rows in the medulla, e.g. guard, auchene or awl hairs, whereas no nuclei were labeled in zigzag hairs that contain a single row of medulla cells (Fig. 12H and J).

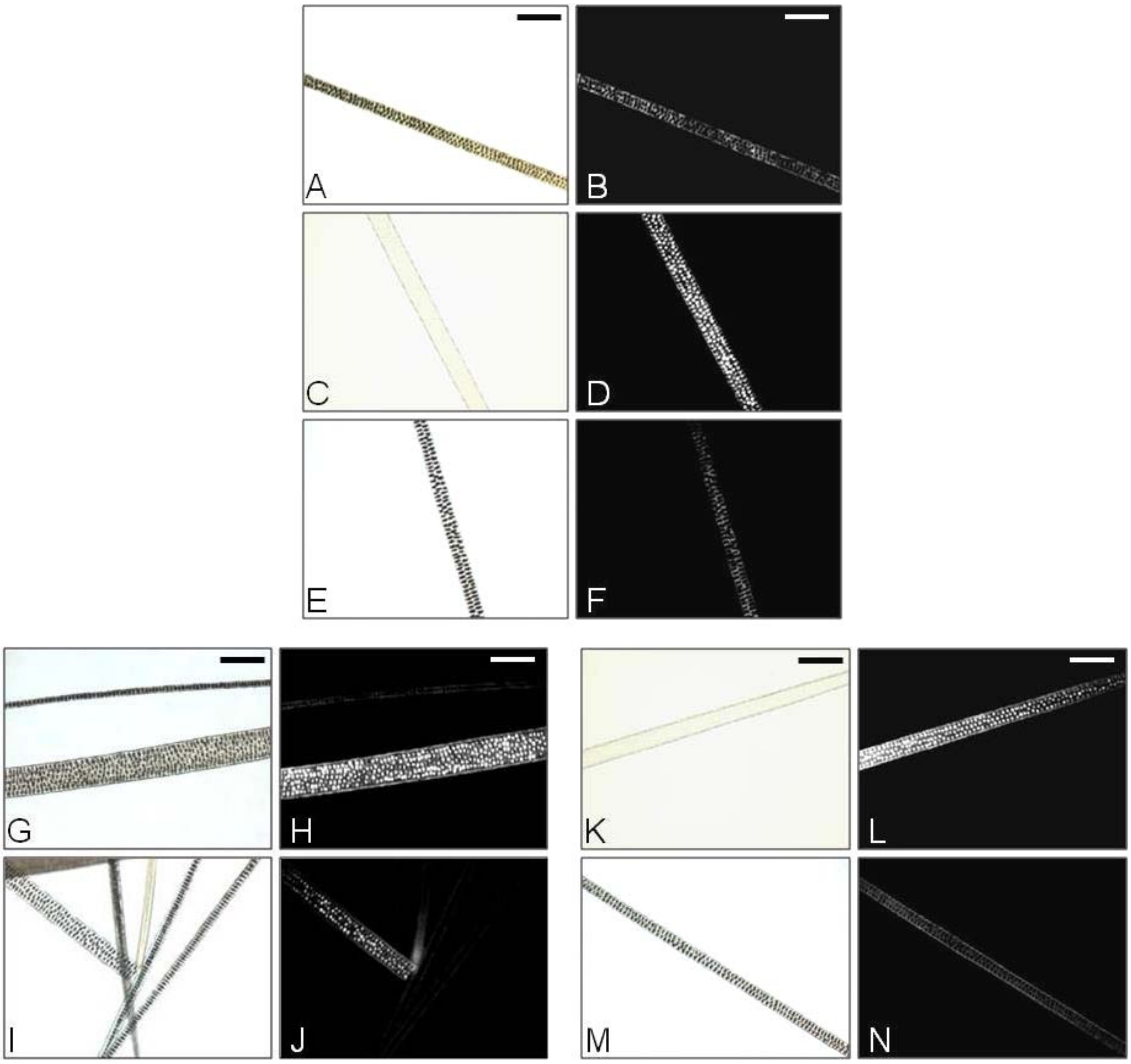

Figure 12: Hoechst-positive nuclei detected in various wild-type mouse strains. Hair from the wild-type strains 129 (A, B), BalbC (C, D), C57Bl6 (E, F), CH3 (G-J), FVB (K, L) and PWD (M, N) are shown. Photos were obtained under bright field (left) and UV light (right). Note that the intensity of the fluorescence signal was amplified by an automatic algorithm according to the total brightness of each individual image. Consequently, signals of different images cannot be compared to each other. Bars = 100 µm.

3.3.2 Detection of Hoechst-labeled nuclear DNA in vibrissae from BalbC and FVB mice

Subsequently, vibrissae from these wild-type strains were processed in the same way. Results differed slightly from the ones previously obtained in hair, forasmuch as vibrissae from not only 129 (Fig. 13B), C57Bl6 (Fig. 13F) and PWD (Fig. 13L) mice but also from CH3 (Fig. 13H) mice did not contain detectable nuclei. On the opposite, in vibrissae from BalbC

(Fig. 13D) and FVB mice (Fig. 13J) nuclei could be stained, thereby matching the results produced in hair from the back of the mice. Interestingly, no nuclei were retained in the thick cortex but exclusively in the medulla.

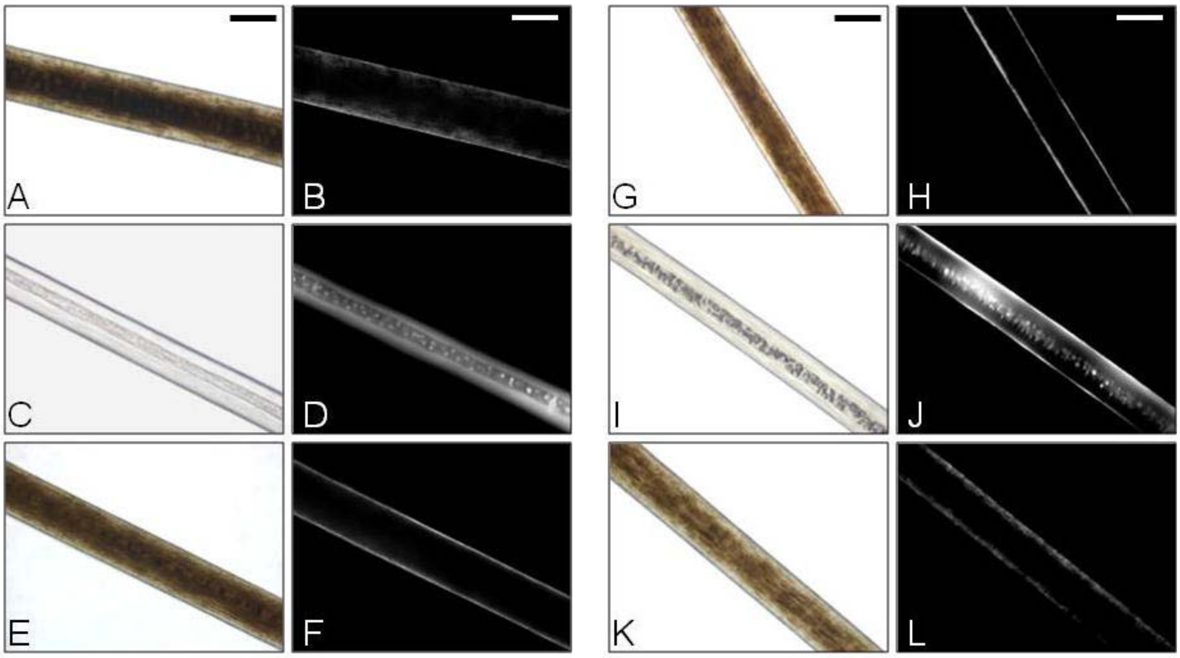

Figure 13: Hoechst-staining of nuclear DNA in vibrissae from different wild-type mouse strains. Vibrissae from the wild-type strains 129 (A, B), BalbC (C, D), C57Bl6 (E, F), CH3 (G, H), FVB (I, J) and PWD (K, L) are shown. Photos were obtained under bright field (left) and UV light (right). Note that the intensity of the fluorescence signal was amplified by an automatic algorithm according to the total brightness of each individual image. Consequently, signals of different images cannot be compared to each other. Bars = 100 μm.

3.3.3 Degree of DNA fragmentation in BalbC hair was higher than in DNase1L2 deficient hair

Next we compared the amounts of DNA in hair from wild-type mice of different genetic background and in hair from the DNase1L2 knockout mouse. For this purpose, white BalbC hair, which appeared to contain the most stainable nuclei of all mouse strains investigated, was mixed with dark hair from a DNase1L2-deficient mouse and labeled with Hoechst dye in the same tube. The different degrees of pigmentation allowed convenient distinction of hair types when the mixed hair samples were inspected under the microscope. Nuclei were stained in hair from both the DNase1L2 knockout mouse and the BalbC mouse (Fig. 14). However, when directly comparing the two hair samples on the same glass slide, it became evident that nuclear remnants in DNase1L2 deficient hair contained much more fluorescent dye than nuclear remnants in BalbC hair. Thus, in order to detect the weakly labeled nuclear remnants in BalbC hair, DNase1L2-deficient hair had to be greatly overexposed (Fig. 14C and F). This striking difference in labeling under identical conditions led to the conclusion that even though stainable nuclei could be detected in various wild-type mouse strains, DNA in these nuclei seemed to be degraded to a much higher extent than in hair of DNase1L2-deficient mice of the strain 129.

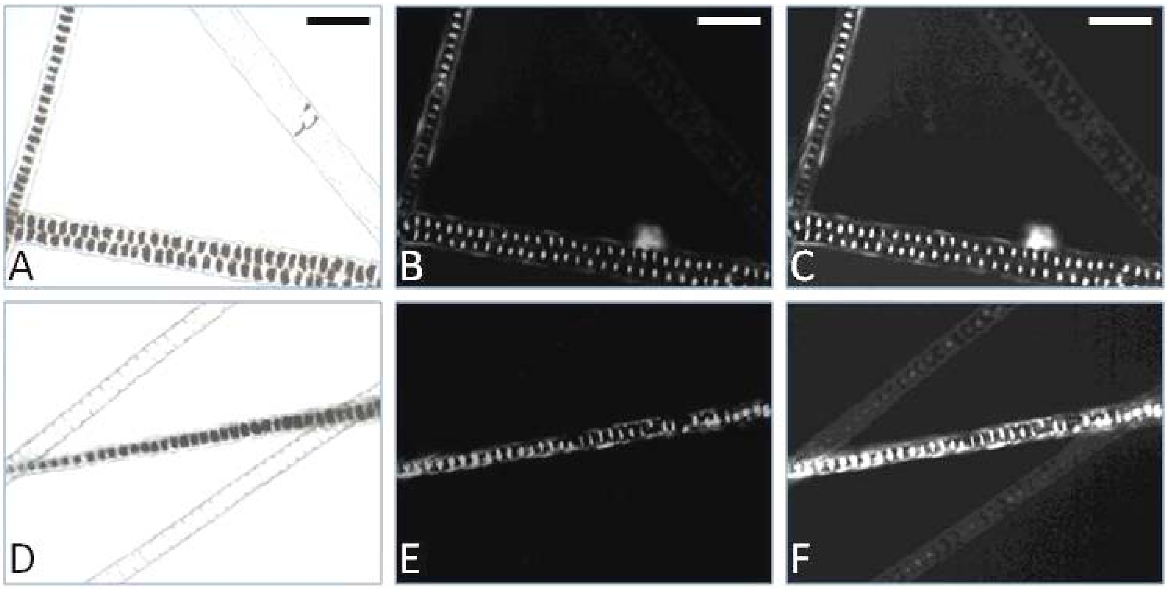

Figure 14: Fluorescent labeling of nuclei in hair from BalbC and DNase1L2 deficient mice. BalbC hairs (white) were mixed with hair from a DNase1L2 deficient (black) mouse, labeled and examined under the microscope. Samples were photographed under bright field (left) and UV light (middle, right). For better visibility of Hoechst-positive nuclei in BalbC hairs, samples were overexposed (C, F). Bars = 100 µm.

3.3.4 Quantitation of nuclear DNA in hair extracts obtained from different wild-type mouse strains and a DNase1L2 knockout mouse

Quantitative real-time PCR was performed with DNA extracts from 10 mg of hairs from each of the six mouse strains and from DNase1L2-deficient mice. Altogether, quantification of extracted DNA supported previous results obtained from Hoechst staining. Comparing hair from the wild-type mice (Fig. 15A), again, PWD hair contained the smallest amount of DNA, closely followed by 129 and C57Bl6 hair. DNA levels in hair from BalbC and FVB were higher, but surprisingly significantly lower than the DNA content found in CH3 hair. This could suggest that the degree of DNA fragmentation in CH3 hair is lower than for example in BalbC hair. Another explanation could be provided by the fact that in the fur of CH3 mice only thicker hairs are nucleated, possibly resulting in a higher amount of nuclei than altogether present in all hair types from other mice. It could also mean that, compared to other mice, the fur of CH3 mice consists to a higher extent of multiply medullated and thus nucleated hair types.

DNase1L2- deficient hair contained around 50- to 300-fold higher DNA levels than hair from any strain of wild-type mice (Fig. 15B). This confirmed the hypothesis that stainable nuclei in hair from wild-type mouse strains have suffered from a higher degree of fragmentation than nuclei in hair lacking DNase1L2.

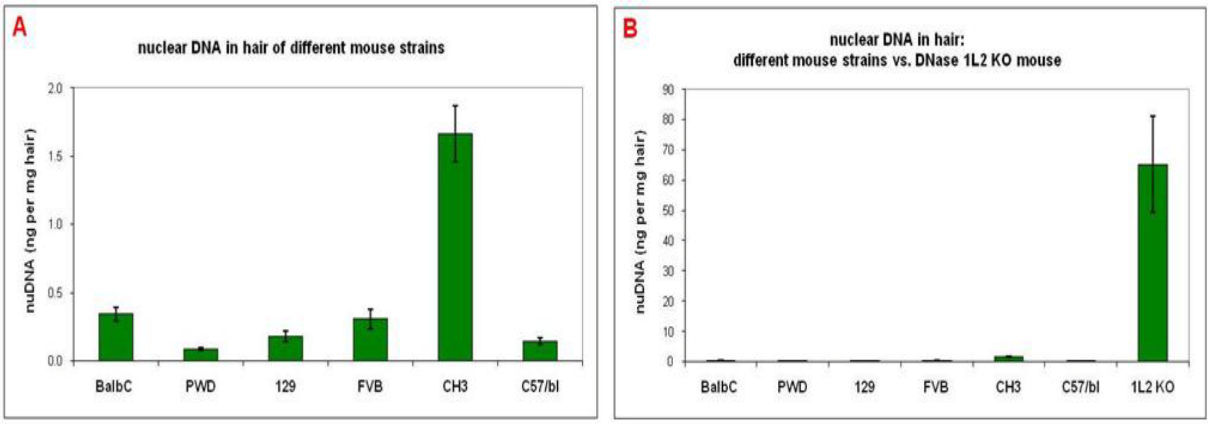

Figure 15: Real-time PCR was performed with nuclear DNA extracted from DNase1L2 deficient hairs and from hair samples obtained from wild-type mouse. 3 hair samples from each mouse were analysed. (A) shows nuclear DNA levels detected in hair of the various strains. (B) demonstrates direct comparison to DNA amounts amplified from DNase1L2 deficient hair. 1L2 KO, DNase1L2 knockout mouse.

3.4 Establishment of a correlation between the number of Hoechst-positive nuclei and the DNA content in human hair samples

The second part of the thesis focused on the investigation of DNA in human hair samples. The techniques of *in situ* DNA labeling and of quantification of DNA extracted from hair were adapted from murine hair to human hair, which differ in thickness and structural organization. The forensic literature shows that the success rate of DNA genotyping of hair extracts varies considerably between individuals. We hypothesized that differences in PCR yield from hair may be caused by differences in the number of incompletely degraded nuclei and in the amount of residual DNA in hairs. Therefore, we tested whether the amount of extractable DNA correlates with the number of stainable nuclei in hair. To evaluate the potential application of such a correlation in forensic medicine, hair extracts were also subjected to STR typing.

3.4.1 Fluorescent labeling of DNA in human hair

When attempting to label DNA in human hair, samples were processed similarly to murine hair. However, prior to the actual experiments, the staining protocol was in the need of further optimization steps. For better permeabilization, the concentration of the ammonia solution had to be increased to a percentage of 10% instead of 1% used in murine hair; the permeabilization step itself was extended and thus performed over night. It was tested whether nuclei, if present at all, were detectable in the entire length of a hair shaft, performed by cutting long hairs into 2 cm pieces followed by staining with Hoechst 33258. Observation under the microscope revealed that retained nuclei were not restricted to the area closest to the hair bulb but were distributed homogeneously and still detectable at the tip of the hair shaft.

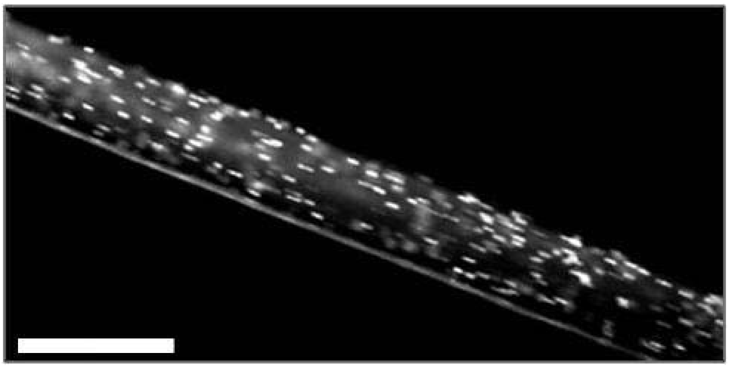

Figure 16: DNA labeling of human hair with Hoechst. For the illustration of the method, a hair from a human individual with extremely high numbers of retained nuclei is shown. Bar = 100 µm.

3.4.1.1 Scalp hairs showed high variation in the number of detectable nuclei

When labeling DNA within human scalp hairs with Hoechst, a high degree of fluctuation in the frequency of stained nuclei was immediately noticed. Hair samples from approximately 40% of tested donors contained no labeled nuclei at all (Fig. 17B), further 30% comprised a moderate number of retained nuclei (Fig. 17D, arrows) whereas in the last 30% of studied hair samples a high number of nuclei could be detected (Figs. 16 and 17F). The numbers ranged from 0.0 nuclei/mm to 75.3 nuclei/mm. The initial screening was followed by a quantitative analysis in combination with DNA extraction and PCR, as will be described below.

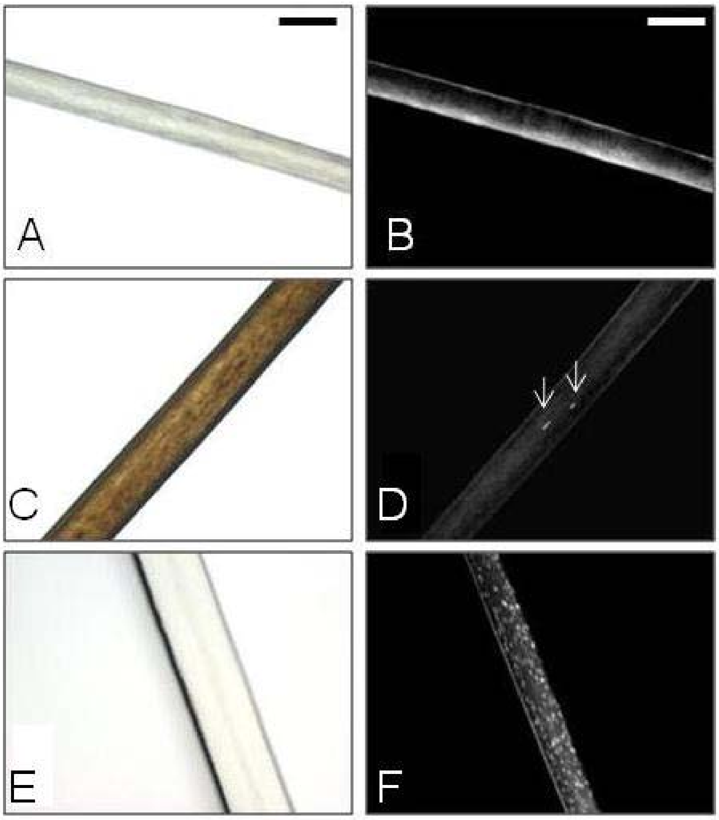

Figure 17: Hoechst-labeling of nuclear DNA in human hair containing no (B), few (D) or many (F) nuclei. Pictures were taken under bright field (left) and UV light (right). Arrows in (D) indicate Hoechst-positive nuclei. Bars = 100 µm.

3.4.1.2 *In situ* labeling of DNA in various types of body hair

Although the largest part of the study used human scalp hair, other hair types present on the human body were investigated as well, as they are also important for criminal investigations. Forensic hair samples are often derived from different parts of the body, such as pudendal, pectoral or facial (i.e. beard, lashes and eyebrows) hairs. Hair samples were collected from five individuals and subjected to DNA labeling with Hoechst. The previous screening of scalp hair had shown that three donors retained nuclei in some hair whereas the other two volunteers had no stainable DNA in scalp hair. In the course of this experiment arm hairs, axillary hairs, beard hairs, eyebrows, lashes and pubic hairs were studied.

In individuals where nuclei had already been detected during prior DNA labeling in scalp hair, chances were good to also find a relatively high number of stainable nuclei in pubic, axillary and beard hairs. In comparison to these hair types, nuclei in arm hairs, lashes and eyebrows were less abundant, although in some hairs a few nuclei could be detected. Usually, these nucleic remnants were detected close to the hair bulb and only rarely at the hair tip. On the opposite, in hair samples derived from donors in whose scalp hairs no stainable nuclei had been found, the probability of labeling retained DNA in other body hairs was low. However, in some hairs a few nuclei could be detected although expected otherwise due to the results obtained from scalp hairs. It should thus be noticed that a small range of variation was observed within both the same hair type and/or the same individual. Table 1 summarizes the whole experiment, presenting numbers of hairs from different body sites containing Hoechst-positive nuclear remnants.

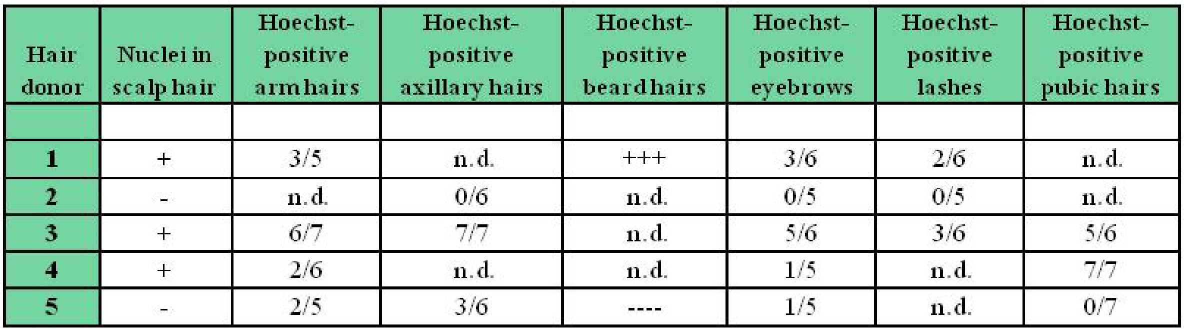

Hair donor	Nuclei in scalp hair	Hoechst-positive arm hairs	Hoechst-positive axillary hairs	Hoechst-positive beard hairs	Hoechst-positive eyebrows	Hoechst-positive lashes	Hoechst-positive pubic hairs
1	+	3/5	n.d.	+++	3/6	2/6	n.d.
2	-	n.d.	0/6	n.d.	0/5	0/5	n.d.
3	+	6/7	7/7	n.d.	5/6	3/6	5/6
4	+	2/6	n.d.	n.d.	1/5	n.d.	7/7
5	-	2/5	3/6	----	1/5	n.d.	0/7

Table 1: The frequency of Hoechst-positive nuclear remnants in body hair. 5 volunteers donated hairs derived from the arm and axle, as well as beard hairs, eyebrows, lashes and pubic hairs which were then stained for nuclear DNA. Numbers of Hoechst-stainable hairs out of all hairs examined are shown. While (+) and (–) stand for either presence or lack of detectable nuclei in scalp hair, the same is indicated by (+++) and (---) in shaved beard hairs, where no exact number of examined hairs could be counted. n.d., not determined.

When staining arm hair with Hoechst, a few nuclei were detectable in some hairs while no nuclei could be found in others (Fig. 18A and B). This was not only true for different individuals, but also for a hair sample derived from a person lacking nuclei in scalp hair (Fig. 18B). Axillary hair (Fig. 18C-E) showed comparable levels of retained nuclei as corresponding scalp hairs, although again hairs without nuclei were detected. In some hairs DNA was labeled in the hair bulb (Fig. 18C) serving as positive control for the efficiency of the staining protocol as the hair shaft remained unstained (Fig. 18D). When nuclei were present in the scalp hair, a relatively high amount of nuclear DNA could be labeled in beard hairs of the same individual (Fig. 18G). In beard hairs from another individual no nuclei could be found (Fig. 18F). The number of nuclei detected in eyebrows ranged from none or very few in some hairs (Fig. 18H and I) to many nuclei in most eyebrows.

While in lashes nuclear remnants could be stained only sporadically, irrespective of the scalp hair's profile (Fig. 18K), nuclei in pubic hairs showed similar distribution as nuclei in scalp hairs. Thus, some pubic hair samples either comprised a high number of retained nuclei (Fig. 18M) or no nuclei at all (Fig. 18L).

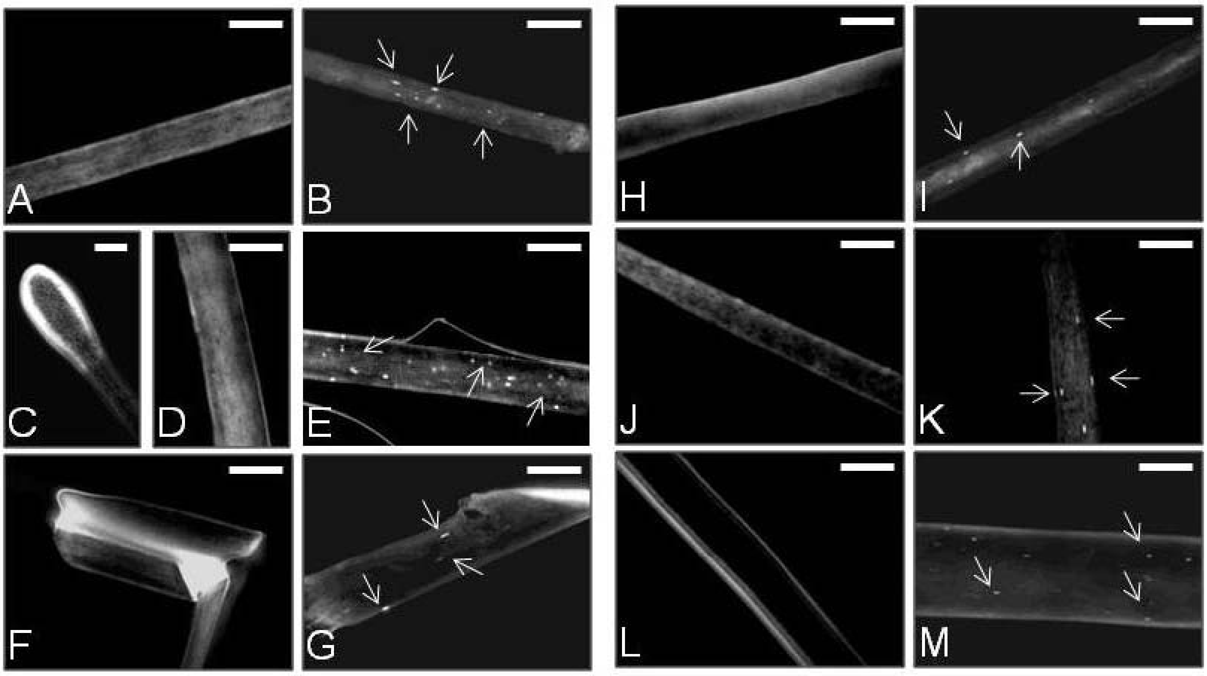

Figure 18: Fluorescent labeling of nuclei in various types of human body hair. 5 volunteers donated hairs derived from the arm (A, B) and axle (C-E), as well as beard hairs (F,G), eyebrows (H, I), lashes (J, K) and pubic hairs (L, M) which were then stained for nuclear DNA. Photos show hairs lacking (left) and hairs comprising Hoechst-positive nuclei (right). Bars = 100 µm.

3.4.2 Staining of DNase1L2 in a cross section of plucked hairs containing follicular tissue revealed single cells showing down-regulated expression of DNase1L2

In some human hair samples high numbers of Hoechst-positive nuclei were detected. Since our study conducted with murine hair samples had demonstrated that the lack of DNase1L2 was responsible for the retention of large amounts of nuclear DNA in hair, we wondered whether this was true for human hair as well.

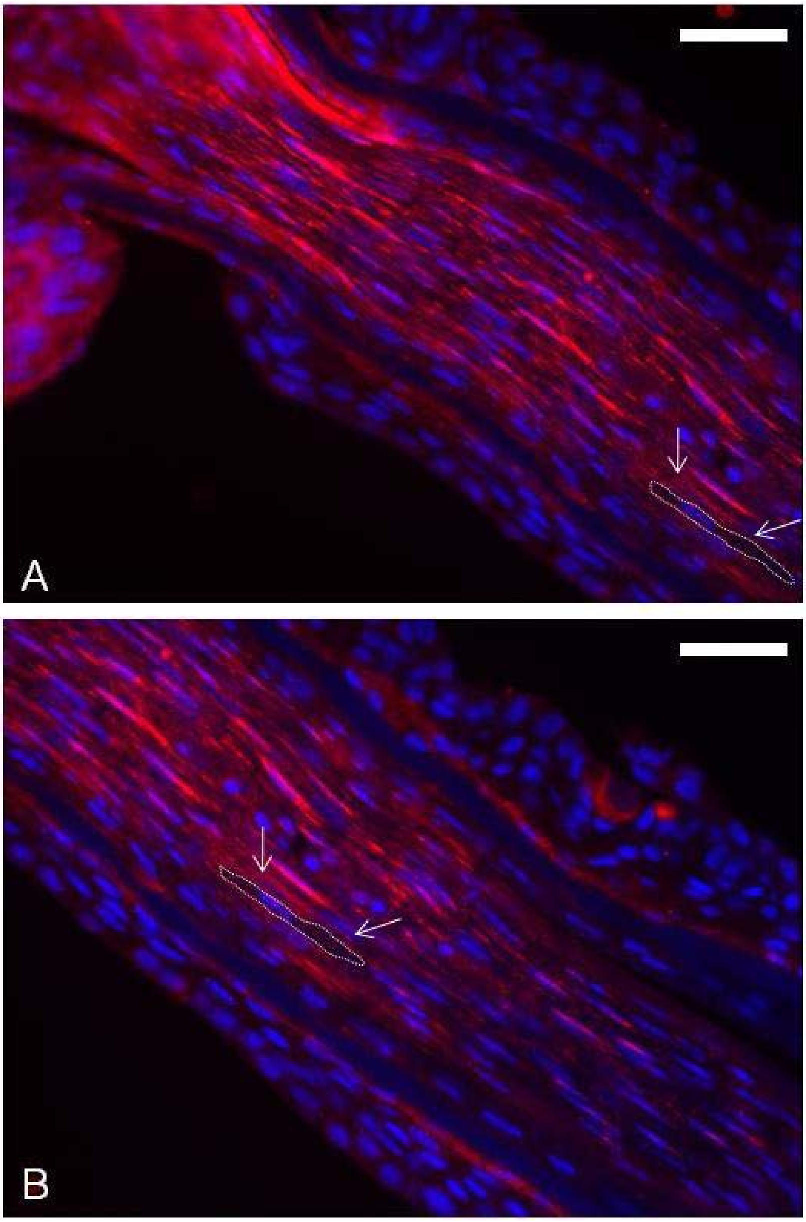

Figure 19: Immunohistochemical staining of DNase1L2 in a cross section of plucked hairs containing follicular tissue. A parallel bundle of plucked hairs was embedded in paraffin, cross sections were obtained and stained with Hoechst (nuclei, blue) and anti-DNase1L2-antibody (red). A cell lacking DNase1L2 is encircled (arrows), the same cell is marked in both panels. (A) shows the basal part of the hair, and (B) shows the adjacent part in the direction of growth. Please note that the immunolabeling for DNase1L2 appears to be blocked during progression of cell differentiation, possibly because of epitope masking. Bars = 40 µm.

It was hypothesized that in some of the cells of the hair matrix insufficient amounts of DNase1L2 were expressed so that nuclear DNA would not be completely degraded during conversion into corneocytes of the mature hair shaft. Therefore, approximately 20 hairs comprising the highest number of nuclei detected during our study were plucked from the donor's scalp and hairs containing follicular tissue were arranged into a parallel bundle. The sample was embedded in paraffin allowing for cross-sectioning and subsequent co-staining with Hoechst and immunolabeling with an anti-DNase1L2-antibody. As shown in Fig. 19, DNase1L2 was expressed in almost all cells of the upper hair matrix. However, some cells expressed lower levels of DNase1L2 than neighbouring cells. One cell almost devoid of DNase1L2 is marked in Fig. 19.

Since the percentage of corneocytes comprising stainable nuclei was low it was no surprise that only few DNase1L2 deficient cells were detected. If expression of the endonuclease was down-regulated in all follicular cells, hair shafts would comprise massive amounts of nuclear DNA as in hair of DNase1L2 knockout mice. The observed variability in the expression level of DNase1L2 may contribute to the appearance of DNA-positive nuclear remnants in hair.

3.4.3 Quantitation of nuclear and mitochondrial DNA levels in extracts from human keratinic tissue

Quantitative real-time PCR was used to amplify nuclear DNA extracted from both human finger nails and scalp hair. For amplification of nuclear DNA, primers were selected to anneal to a high-copy number transposable element from the Alu-Sb1 family. Mitochondrial DNA was amplified with mitochondrial DNA-specific primers. The investigation of the DNase1L2 knockout mouse had shown that DNase1L2 degrades nuclear but not mitochondrial DNA in hair whereas it degrades both nuclear and mitochondrial DNA in nails. If this is also true for humans, inter-individual variability in DNase1L2 activity may result in the amounts of residual nuclear and mitochondrial DNA in nails, whereas residual nuclear DNA should not correlate with residual mitochondrial DNA in hair. Moreover, quantitation of the extracted DNA was required to determine the appropriate amount of template for subsequent STR typing.

3.4.3.1 qPCR demonstrated strong correlation between the levels of nuclear and mitochondrial DNA detected in extracts from human finger nails

In order to investigate the mechanism involved in breakdown of both nuclear and mitochondrial DNA in human finger nails and to compare the hereby obtained results to those of experiments performed using murine nails, finger nails from 20 donors were collected and prepared for subsequent tests. Since so far no technique could be developed for visualizing nuclear DNA in human finger nails, the only possibility to determine DNA levels in nails was by performing quantitative real-time PCR.

Tissue adhering to nail samples was removed by ultrasonication and nails were lysed according to the standard protocol also used for hair samples. The DNA extract was then subjected to amplification of nuclear and mitochondrial DNA. A strong correlation (R^2 = 0.91) between nuclear and mitochondrial DNA levels in human nails was observed (Fig. 20). This further supported the hypothesis that degradation of nuclear and mitochondrial DNA is driven by the same enzyme, i.e. DNase1L2, in nail keratinocytes.

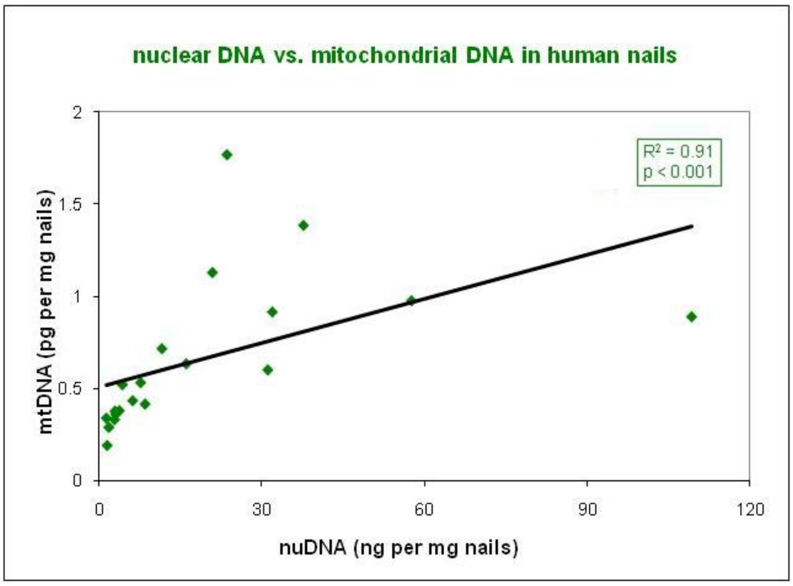

Figure 20: Correlation between nuclear and mitochondrial DNA extracted from human finger nails. Finger nails of 20 individuals were collected and used for DNA extraction and quantification by real-time PCR. Nuclear DNA was amplified with primers annealing to a high copy number repeat element. Spearman rank correlation (R^2) was determined. A strong correlation is shown, indicating a similar mechanism for breakdown of nuclear and mitochondrial DNA.

3.4.3.2 Quantitative real-time PCR was performed for lysates of pooled hair shafts

Following prior DNA labeling of nuclei, hair samples were prepared for quantitative real-time PCR, where the levels of both nuclear and mitochondrial DNA were determined. Unlike the usual situation encountered at sites of criminal investigations where only small amounts of forensic evidence are available, hairs derived from one individual were pooled in order to have sufficient material for a robust test of the correlation between the number of nuclei counted in hair and the DNA amplified from hair extracts.

3.4.3.2.1 The number of Hoechst-positive nuclei correlated with nuclear but not mitochondrial DNA extracted from human hair shafts

5 mg of hairs from 30 donors were lysed, followed by purification and quantitation of nuclear and mitochondrial DNA. It should be noted that individuals with dyed hair were excluded from this study.

The amount of amplified nuclear DNA correlated significantly ($R^2 = 0.65$) with the number of nuclei detectable by Hoechst labeling *in situ* (Fig. 21). A small study of hair from donors of European descent showed that the mass of 1 mg corresponds to 200 mm of hair. Based on this rough estimate, 30 stainable nuclei (as determined by counting over a given length of hair) yielded an amount of PCR product equal to the amount amplified from one intact nucleus of a living cell. Assuming that all amplified nuclear DNA was present in Hoechst-positive nuclei and that DNA was extracted and amplified with 100% efficiency, the data suggest that one stained nucleus on average contains 3% of the original DNA amount of an intact nucleus. In other words, this simplified model suggests that DNA is degraded by 100% in the vast majority of nuclei, whereas DNA breakdown occurs to only 97% in some nuclei. In reality, a distribution of degradation between 90 and 100% seems likely. If the efficiency of DNA extraction and PCR amplification was much lower than 100%, accordingly higher amounts of DNA may be present in the nuclear remnants and the degree of DNA degradation may be lower.

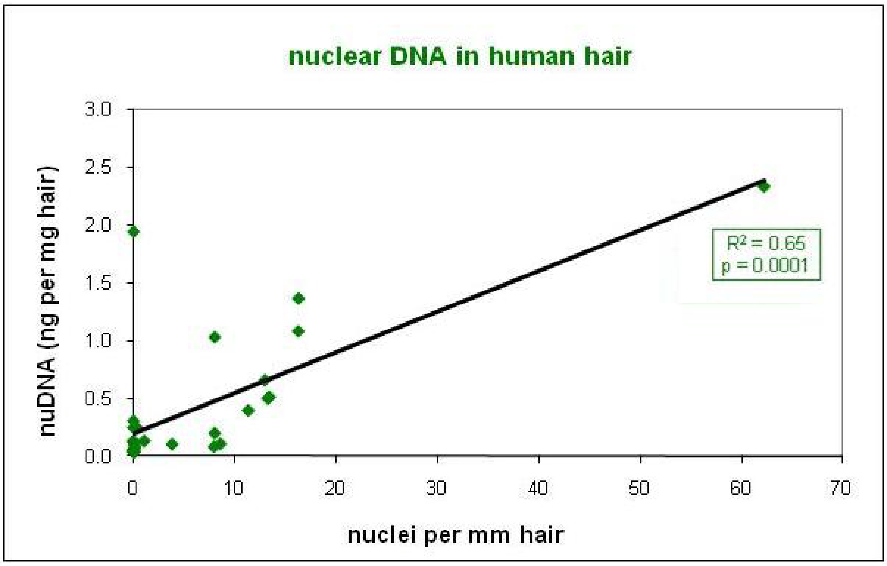

Figure 21: Correlation between the number of stainable nuclei in hair and extractable nuclear DNA. Hairs of different individuals were stained for DNA, and nuclei were counted under the microscope. A separate batch of hairs of the same individual was then used for DNA extraction and quantification by real-time PCR. Spearman rank correlation (R^2) was determined. A strong correlation between counted nuclei and the DNA content in hair is demonstrated.

No correlation (R^2 = 0.10) was observed between counted nuclei and the extracted amount of mitochondrial DNA (Fig. 22A). It was calculated that the mass of one plasmid containing the mitochondrial amplicon used for creating the standard curve needed for quantification of mitochondrial DNA was 4.37 x 10-^{18} g. Based on this calculation and the previous assumption that 1 mg hair corresponds to 200 mm of hair, it could be shown that the DNA amount from 3 million mitochondria was present in 1 mg hair, i.e. 1 mm of hair comprised the DNA amount equivalent to 15000 mitochondria.

Furthermore, no or only a weak correlation (R^2 = 0.27) was observed between the amounts of extractable nuclear and mitochondrial DNA (Fig. 22B). These findings suggest a mechanism for mitochondrial breakdown independent from that responsible for the degradation of nuclear DNA, as already seen in experiments performed with murine hair samples. Thus, unlike in nails, breakdown of mitochondrial and nuclear DNA seem to follow two different pathways in hair.

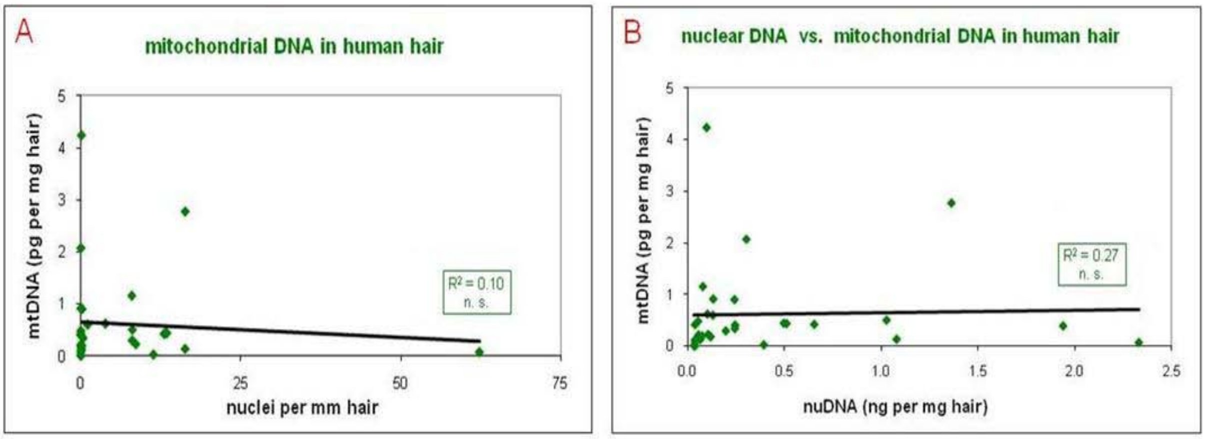

Figure 22: Lack of correlation between counted nuclei and amplified mitochondrial DNA (A) as well as between extractable nuDNA and extractable mtDNA (B). Hairs of different individuals were stained for DNA, and nuclei were counted under the microscope. A separate batch of hairs of the same individual was then used for DNA extraction and quantification by real-time PCR. Primers annealing to a high copy number Alu-element in the human genome was used for quantification of nuclear DNA while mitochondrion-specific primers were used to amplify mitochondrial DNA. Spearman rank correlation (R^2) was determined for both experiments. Graphs demonstrate that no correlations exist between amplified mitochondrial DNA and counted nuclei or the level of nuclear DNA, suggesting a different breakdown mechanism of mitochondria in hair.

3.4.3.2.2 Analysis of the impact of excluding outliers

When separately analysing each data point, two outliers were identified, thereby raising the question of how the correlation between counted nuclei and the amplified DNA amount would be influenced by elimination of these outliers. The first outlier was a deeply black hair sample of a donor of non-European descent from which, although comprising no Hoechst-positive nuclei, an extremely large amount of DNA could be amplified. The second sample consisted of a mixture of brown and white hair. Both samples contained many stainable nuclei, from which also a high PCR yield could be obtained. While the first sample may be seen as a “classical outlier”, the elevated number of labeled nuclear DNA in the second hair sample explains the high DNA content, which is the reason why this sample should be regarded as exceptional much rather than as outlier.

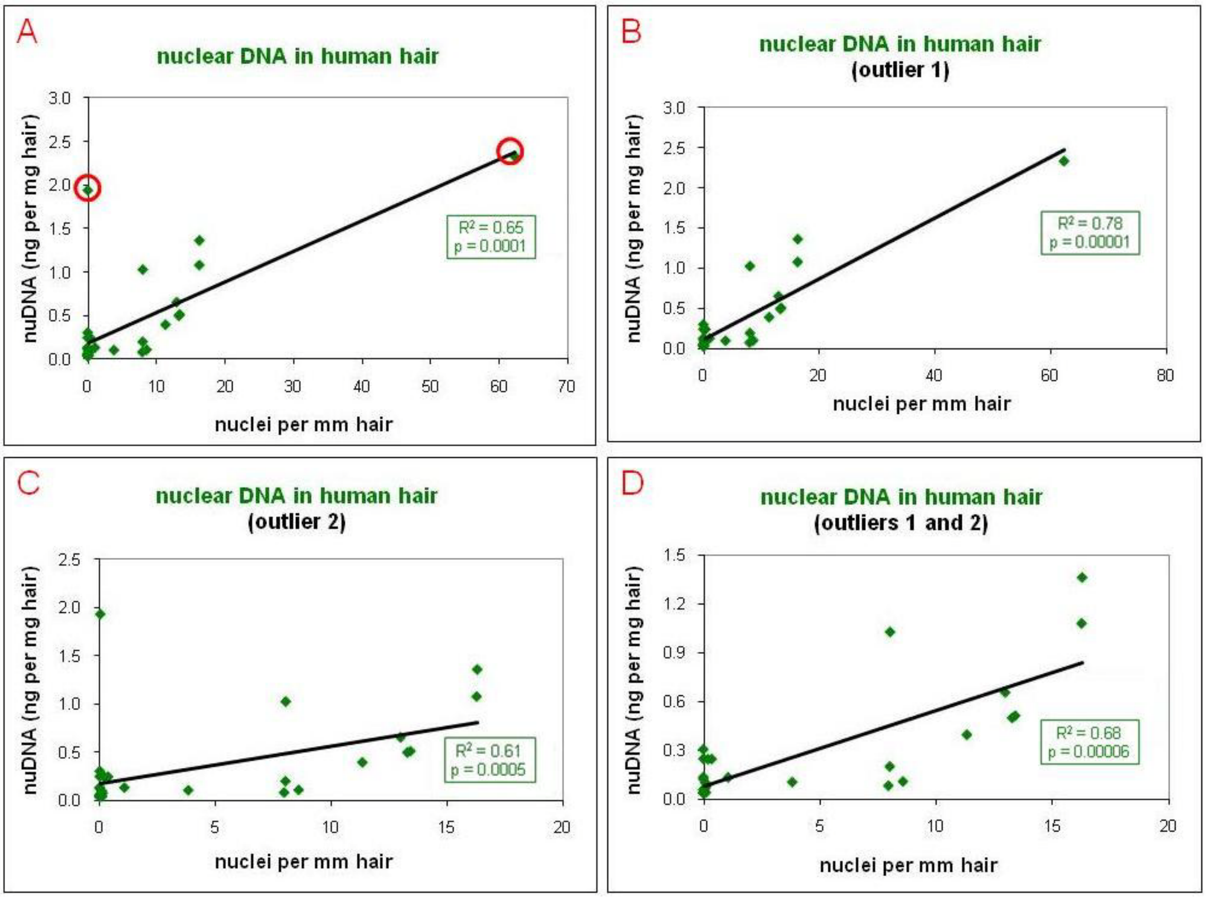

Figure 23: Exclusion of outliers leads to changes in the correlation between Hoechst-positive nuclei and the amount of amplified nuclear DNA. Two outliers (marked red, (A)) were excluded from the study resulting in changed coefficients of determination (R^2). (A) shows normal population, (B) depicts elimination of outlier 1, (C) presents exclusion of outlier 2 and (D) demonstrates exclusion of both data points. Spearman rank correlation (R^2) was determined for all possibilities.

To test the robustness of our conclusions, we investigated the consequences of eliminating either one or both of these samples from the input data (Fig. 23A). Fig. 23B shows exclusion of outlier 1, resulting in an significant raise of the coefficient of determination (R^2 = 0.78). This was expected because the discrepancy between the high PCR yield and the complete lack of nuclei no longer influenced the correlation. By eliminating only the second outstanding measurement (Fig. 23C), R^2 was reduced to some extent (R^2 = 0.61). If both outlying measurements were excluded (Fig. 23D), a relatively high correlation (R^2 = 0.68) between stainable nuclei and the amount of amplified DNA could be demonstrated, with the R^2 being slightly higher than that of the dataset including both outliers.

3.4.3.2.3 The number of stainable nuclei in human hair is independent from the donor's hair colour or age

Next we tested whether stainability of nuclear DNA *in situ* and PCR yield were associated with certain hair phenotypes, namely colour and age. When plotting the number of counted nuclei against PCR yield while separating the samples according to hair colours, the observation was made that strongly pigmented brown or black hair comprised higher numbers of nuclei than their less pigmented blond or reddish counterparts (Fig. 24A). In addition, Hoechst-positive nuclei were frequently found in samples containing white hair mixed with dark hair derived from the same individual. Similar results were obtained when plotting the hair colours themselves against the DNA amount extracted from hair samples (Fig. 24B). Our data allow only very preliminary conclusions since the number of studied samples was rather small with a relatively high percentage of dark hair.

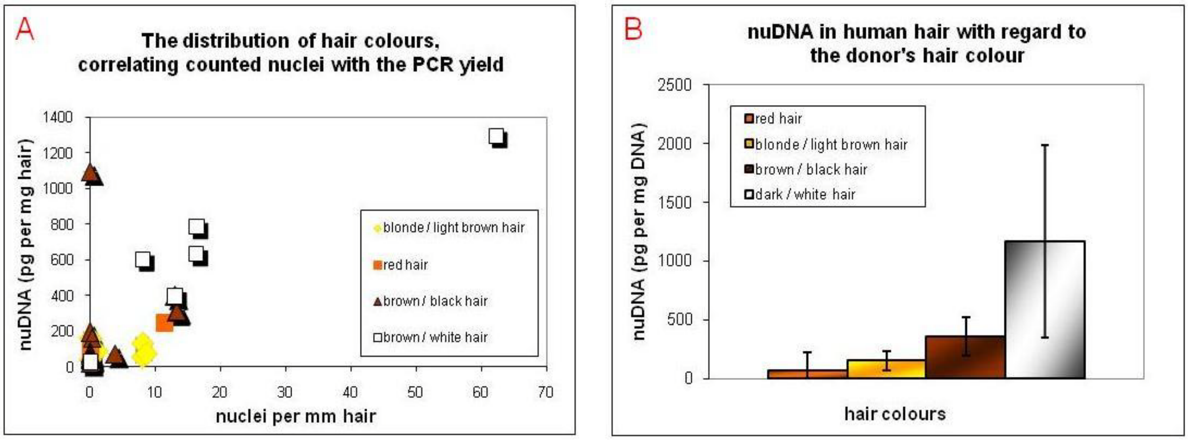

Figure 24: Coherence between the number of counted nuclei in hair and the donor's hair colour. Previously shown population (counted nuclei vs. amount of nuclear DNA) is divided into four hair colours, see legend (A). Average amounts of amplified nuclear DNA in hairs with different colours (B) are shown.

To estimate the potential influence of age on *in situ* labeling of DNA and PCR yield, hair samples were divided into three groups corresponding to the donor's age. While the first group comprised individuals aged between 1 and 10 years, the second consisted of volunteers at the age of 11 to 35, followed by the third and last group including donors between 35 and 60 years old. There was no obvious pattern except for the impression that in hair from older individuals higher numbers of Hoechst-positive nuclei were detected (Fig. 25A). Undoubtedly, this finding is influenced by the unequal distribution of the age groups within the samples and the corresponding fact that white hairs, in which stained nuclei are more easily detected (see below), are restricted to the highest age category. When the donor’s age was plotted against the nuclei detected in the corresponding hairs, no correlation (R^2 = 0.13) could be detected (Fig. 25B).

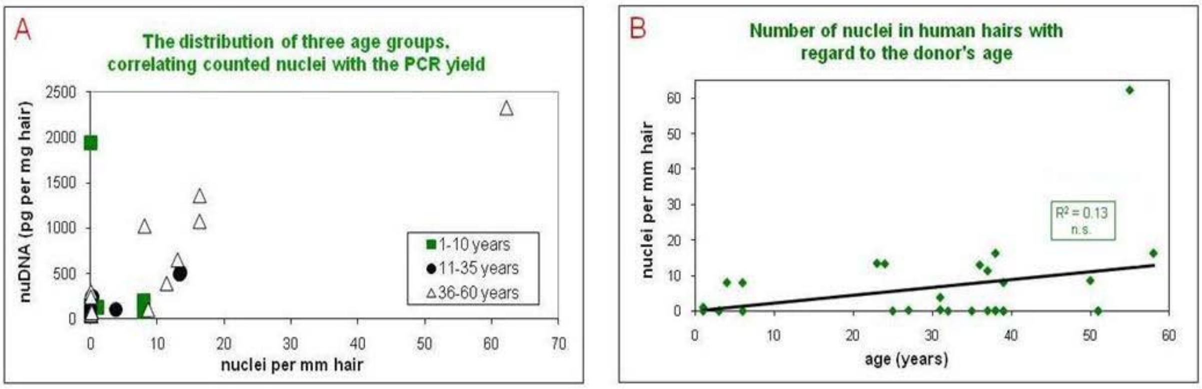

Figure 25: Number of counted nuclei in hair and the donor’s age. Previously shown population (number of counted nuclei vs. amount of nuclear DNA) is divided into three age groups, see legend (A). The number of nuclei detected in hairs was then plotted against the donor’s age; no correlation can be observed (B). Spearman rank correlation (R^2) was determined.

3.4.3.2.4 Natural hair pigmentation reduced detectability of nuclei but did not influence PCR efficiency

Although no correlation could be demonstrated between counted nuclei and either age of the donor or hair colour, differences in the number of stainable nuclei were observed when studying pigmented (i.e. dark) as well as pigmentless (i.e. white hairs) from the same individual. Thus, white and dark hairs were obtained from 8 volunteers and subsequently subjected to DNA labeling.

As seen in Fig. 26A, numbers of Hoechst-positive nuclei differed between these types of hair, resulting in more nuclei being detected in white hair than in dark hair. Therefore, the question was raised whether hair pigment only reduced the detectability of nuclei *in situ* or if it also affected the actual amount of retained nuclear DNA in hair, i.e. whether it was really the case that white hair comprised more DNA than their pigmented counterparts, as one might expect after careful examination of the Hoechst-labeled hair shafts. In order to answer this question, real-time PCR was performed with DNA purified from black and white hair samples.

As demonstrated in Fig. 26B, no difference existed between DNA amounts of either hair sample. This also suggested that natural pigment did not influence the efficiency of nuclear

DNA amplification. Furthermore, the specific, negative influence of the pigment of the detectability of DNA *in situ* might explain the previously mentioned phenomenon observed in the deeply black hair sample of outlier 1, where no nuclei could be detected by labeling of hair whereas the PCR yield was high.

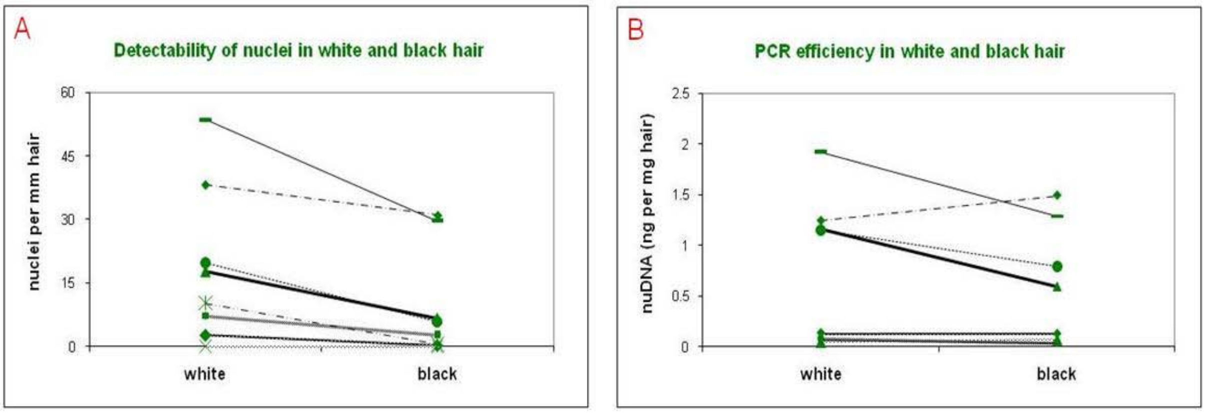

Figure 26: The influence of natural hair pigment on the detectability of nuclei *in situ* and the efficiency of nuclear DNA amplification. Black/brown and white hairs of 8 individuals were separated and stained for DNA; nuclei were counted under the microscope. Higher numbers of Hoechst-positive nuclei were detected in white hair (left), while detectability of nuclei is reduced in brown/black hair (right). Different hair batches from the same donors were then subjected to amplification of nuclear DNA by real-time PCR. PCR efficiency was not significantly affected (B). It should be noted that this study included a low sample number.

Thus, while presence of different types and quantities of melanin was responsible for reduction of the coefficient of determination, R^2, PCR yield was not affected. Accordingly, correlation between counted nuclei and amplified DNA was much better when only white hairs were investigated (Fig. 27A). This could be explained by the fact that in comparison to dark hair, white hair displayed the correct amount of comprised nuclei, thereby matching the results obtained during real-time PCR in a more accurate way. On the opposite, pigment does not strongly affect correlation between stainable nuclei and amplifiable mitochondrial DNA (Fig. 27B), which was virtually absent in any case.

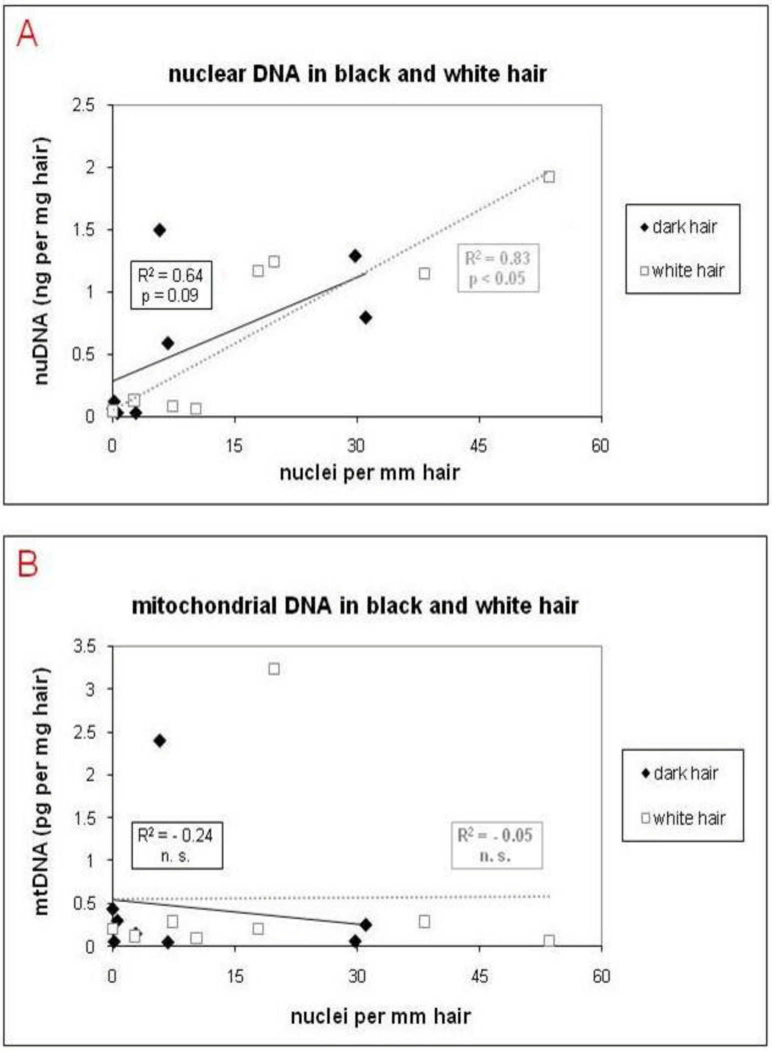

Figure 27: Influence of hair pigment on the coefficient of determination. Black/brown and white hairs of 8 individuals were analyzed for density of nuclei and for nuclear or mitochondrial DNA content. Spearman rank correlation (R^2) was determined. Presence of pigment (probably different types and quantities of melanin) reduces the coefficient of determination (R^2) for nuclear DNA (A) but does not strongly affect correlation for mitochondrial DNA (B), which does not exist.

3.4.3.2.5 *In vitro* dyeing and bleaching of hair affected both detectability and amplification of nuclear DNA

As mentioned above, chemically treated (dyed or bleached) hair had been excluded from the study described above. This decision was based on the initial suspicion that artificial pigment might interfere with PCR efficiency. Furthermore, melanin is able to inhibit DNA amplification by PCR under certain conditions. This effect is especially strong in the presence of H_2O_2, which is used in bleaching agents and permanent colorants. Melanin is destroyed by this oxidizing agent, loses its natural colour and becomes soluble in water. This results in the pigments being irreversibly linked to the DNA, making accurate amplification of the DNA template almost impossible. It was suggested that this phenomenon may be responsible for profiles being even more fragmentary than those obtained from untreated hairs (Müller et al., 2007). We therefore wanted to understand the mode in which chemical agents affected the behaviour of previously characterized hair during Hoechst-staining of nuclei and real-time PCR.

In a preliminary study, both dyed and bleached hairs were subjected to *in situ* DNA labeling and PCR quantification of DNA. When studying dyed hair, results obtained during DNA quantitation did not match the number of counted nuclei. Either an enormous number of structures resembling nuclei or no nuclei at all could be detected, while PCR levels varied greatly in both directions. In bleached hair no Hoechst-positive nuclei were found, whereas PCR yielded large amounts of DNA in the same hair sample.

To investigate the effect of chemical treatment in a controlled fashion, previously untreated hair samples from donors for which the amount of detectable nuclei and the DNA concentration in hair had already been determined, were subjected to *in vitro* dyeing and bleaching by commercially available agents. Microscopic examination of dyed hairs revealed that in most hairs the number of stainable nuclei was clearly reduced. In other hairs displaying no nuclei in previous staining, nucleus-like structures were detected. In contrast to natural pigment, the hair dye appears to decrease PCR efficiency when amplifying nuclear DNA. However, in some hair samples the application of the dye resulted in a higher DNA yield, possibly indicating contamination of the dye with DNA. Amplification of mitochondrial DNA from dyed hair showed even higher fluctuations.

Bleaching of hair followed by Hoechst-labeling resulted in brightly fluorescing hair concealing all possibly present nuclei. In addition to the reduction of the detectability of stainable nuclei, PCR yield from both nuclear and mitochondrial DNA was severely affected, again showing higher deviations in mitochondrial DNA. Thus, our methods are not applicable for accurate and reliable quantitation of DNA in dyed or bleached hair.

3.4.4 Direct quantitation of DNA levels in Hoechst-labeled hair samples

The number of stainable nuclei in hair could not be related to skin diseases, at least in the preliminary assessment by trained dermatologists at the Medical University of Vienna, or other parameters such as the donor’s age or natural hair colour. However, it appeared possible that our findings might have implications in forensic medicine. Specifically, we hypothesized that our findings may help to explain the high variation of the success rate of STR genotyping. However, as already mentioned, the pooling of multiple hair samples from each donor in previous experiments deviated from the setting typically encountered in forensic investigations. Since usually only single evidence hairs can be secured at sites of criminal investigations, it was of major importance for our study that both Hoechst-labeling and quantification of nuclear DNA could be applied to the very same hair.

In a proof-of-principle study, hairs from an individual with high levels of residual nuclear DNA were stained with Hoechst. In order to test possible PCR inhibitory properties of the mounting medium, some hairs were labeled with Hoechst without being mounted on glass slides. While other hairs were treated with Fluoprep (Biomerieux) allowing for detection of stainable nuclei under the microscope, a few hairs were left untreated before PCR. Hairs were washed with 0.1% PBS-T to remove adhering substances, followed by lysis of hair with extraction buffer. It was noted that lysis of Hoechst-stained hair took slightly longer than that of untreated hair.

Subsequent DNA amplification by real-time PCR revealed no differences in the detectable levels of nuclear or mitochondrial DNA among Hoechst-labeled or unlabeled hair samples described above. This demonstrated that quantitation of DNA extracted from Hoechst-labeled hair samples was possible.

3.4.4.1 Hoechst-labeling of nuclei and subsequent quantitation of DNA levels in single hairs from 40 donors

In the following study a set of single-hair samples from 40 donors was screened. One 2-cm piece of hair from each individual was labeled with Hoechst, allowing for accurate determination of the total absolute number of stainable nuclei. After counting of the detected nuclei, hairs were removed from the slides, washed with 0.1% PBS-T over night and subjected to DNA extraction and quantitation.

The data produced by real-time PCR showed again that the number of retained nuclei in hair is critical for the amplification yield of the PCR from nuclear DNA. Although the correlation ($R^2 = 0.57$) between the number of stainable nuclei and the amount of amplified DNA was not as strong as for pooled hairs, correlation can still be classified as good (Fig. 28A). As expected, no correlation ($R^2 = 0.11$) could be observed when plotting the number of counted nuclei against the amount of extracted mitochondrial DNA (Fig. 28B).

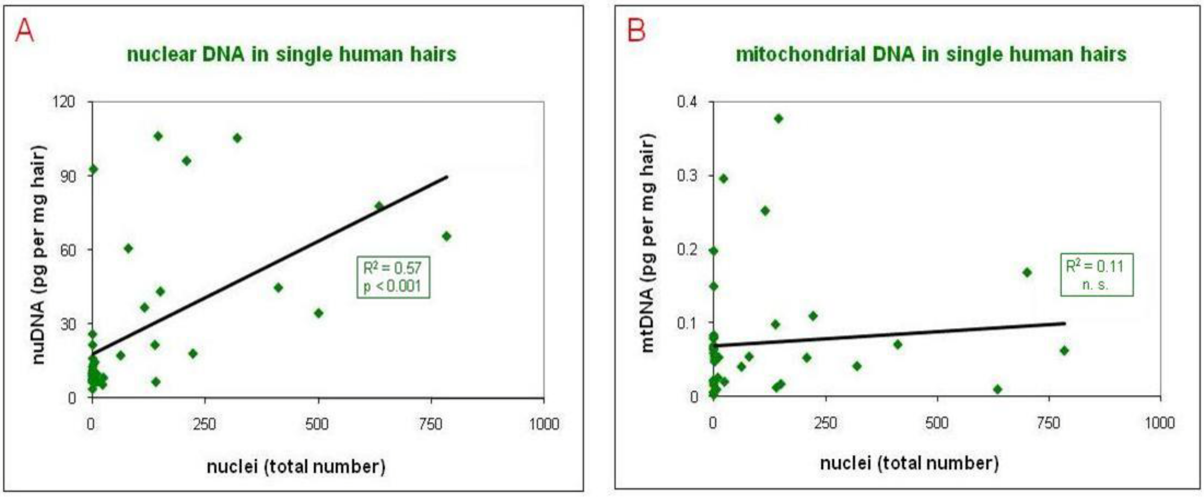

Figure 28: Correlation between the total number of counted nuclei and the amount of DNA extractable from single hairs. Nuclei in Hoechst-stained hair were counted under the microscope. Hairs were washed and directly used for DNA extraction and quantification by real-time PCR. Spearman rank correlation (R^2) was determined. (A) shows good correlation between the detected number of nuclei and the amount of amplified nuclear DNA. (B) demonstrates that no correlation can be observed between counted nuclei and levels of mitochondrial DNA in hairs.

3.4.4.2 The success of DNA genotyping in human hair correlated with the number of Hoechst-positive nuclei

In order to directly investigate the implication of our previous results on forensics, cooperation was established with Prof. Walther Parson at the Institute of Forensic Medicine in Innsbruck.

2-cm pieces of single hairs from 20 individuals were stained with Hoechst as described before. Out of these 20 samples 9 hairs comprising less than 0.1 nuclei per mm and 11 hairs containing more than 8 nuclei per mm were selected. These samples were then delivered to Innsbruck for DNA extraction and STR typing by miniSTR-multiplex PCR (Grubwieser et al., 2006). The STR results of each hair were then verified by STR typing of buccal scraping samples from the same donor.

Similar to previous experiments, a high correlation was observed between the total number of counted nuclei and the amount of amplified DNA (data not shown). In addition, both parameters also correlated (R^2 = 0.86) significantly with the number of positive, typeable STR loci (Fig. 29A). When looking specifically at hair samples comprising nuclei (Fig. 29B), correlation is slightly diminished (R^2 = 0.74) due to the few hairs, where no positive result could be obtained during DNA genotyping although nuclear remnants had been detected.

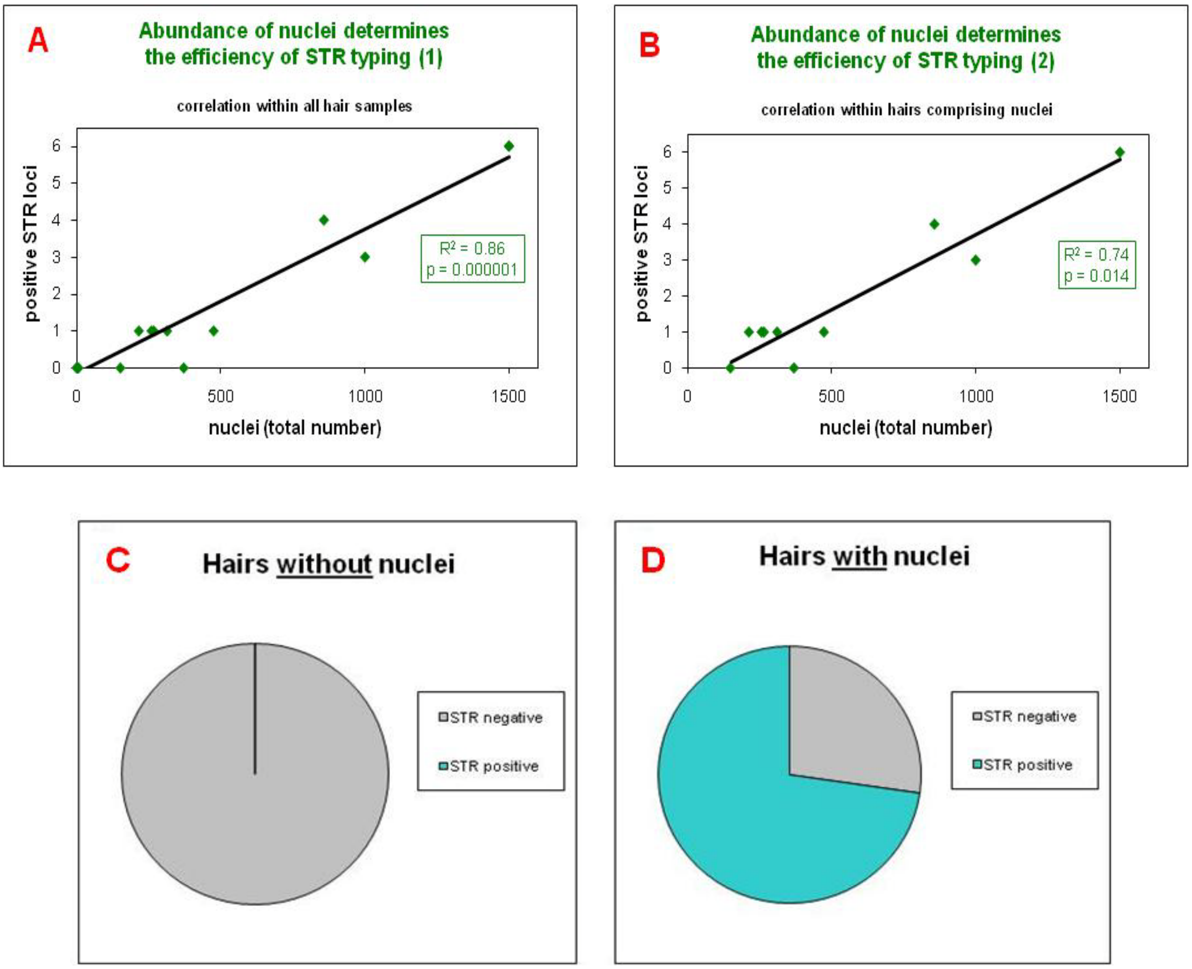

Figure 29: Correlation of the success of STR typing with the number of Hoechst-positive nuclei comprised in hair. STR loci D2S1338, D16S539, D18S51, TH01 and FGA and amelogenin on the Y-chromosome were amplified from 20 hair samples, subsequent to extraction and quantitation of DNA. Hair samples contained either < 0.1 nuclei/mm (n = 9) or > 8.0 nuclei/mm (n = 11). Spearman rank correlation (R^2) was determined. Correlation between counted nuclei and success of STR typing (i.e. the number of typeable STR loci) is shown for (A) all hair samples and for (B) hairs comprising nuclei. (C) and (D) demonstrate that all hairs lacking nuclei led to a negative STR result, while in almost 75% of hairs with nuclei STR loci could be typed.

But, most importantly, all hairs lacking nuclei were negative in STR typing (Fig. 29C), while almost 75% of hair containing nuclei led to a positive result (Fig. 29D). In most hairs where nuclear remnants could be detected, at least one out of six STR loci could be typed, in samples comprising higher numbers of stainable nuclei more or all loci could be amplified. These results support our hypothesis that inter-individual differences in the yield of DNA extracted from human hair samples are caused by varying amounts of incompletely degraded nuclear DNA in hair shafts. We suggest that our novel protocol for *in situ* labeling of DNA may be applied in future forensic investigations in order to predict the suitability of single hairs for STR genotyping.

4. DISCUSSION

4.1 *In situ* labeling and quantitation of DNA in hair

This thesis describes the establishment and application of a novel method for the visualization of nuclear DNA in hair, based on permeabilization of hair and labeling of nuclear remnants with DNA-binding dyes. In this study, the usefulness of *in situ* DNA labeling in hair was demonstrated in the investigation of DNA degradation in murine and human hairs. Importantly, this technique may be further optimized to be implemented in forensic medicine, serving as a tool for prediction of the likelihood of successful STR genotyping of single hairs.

So far, this method has shown a few weaknesses, as for example the whole procedure required long time to get the final results, i.e. three days. In order to become applicable in the forensic practice, time passing between the first washing step and the actual microscopy part has to be significantly diminished. This could be achieved by reducing the duration of incubation steps, such as permeabilization with ammonia or DNA labeling with Hoechst solution. In both cases, the solutions might be used in higher concentrations, although in the case of Hoechst dye this might lead to severe background staining.

A specific problem in the studies described here was the amplification of the fluorescence signal of Hoechst-positive nuclei by an automatic algorithm of the microscope. Since the output signals were adjusted according to the total brightness of each individual image, it was not generally possible to directly compare signals of different images, as observed during examination of hairs obtained from various wild-type mouse strains. Under these conditions, only the absence or presence of fluorescently labeled nuclei could be determined, whereas the degree of fragmentation of the nuclear DNA could not be assessed. To allow for comparison of fluorescence intensities of different images, automatic adjustments by the software must be turned off. However, if the DNA distribution in individual hairs with little DNA needs to be determined, strong signal amplification will be required.

Our DNA quantitation assay is based on previously published Alu-based quantitative real-time PCR systems (Nicklas et al., 2003b; Opel et al., 2008; Walker et al., 2003), using small amplicons which are preferable in analysis of highly fragmented DNA (Butler, 2007; Grubwieser et al., 2006) as found in hair. Since no inhibitory effects of Hoechst 33258 or the mounting medium could be observed, PCR was performable directly after labeling of hair samples with the fluorescent dye.

However, during amplification of DNA from murine hair samples of the same genotype, different absolute amounts of DNA were yielded in separate experiments. By contrast, the relative amounts, comparing different genotypes, was not strongly affected by this inter-experiment variation. Nevertheless, further optimization is necessary to improve the robustness of the analysis. It is advisable to develop a series of standards that should be used in every experiment. Studies to improve the quantitative reproducibility of the extraction and amplification procedure have been initiated at the Department of Dermatology, Medical University of Vienna.

The fact that many people use hair colorants is a challenge for detection and quantification of DNA in hair, since these dyes strongly influence both the detectability of nuclei *in situ* and the amplification of DNA by real-time PCR. Surprisingly, these colouring or bleaching agents did not only have inhibitory effects on real-time PCR, as previously suggested (Müller et al., 2007), but in some samples also seemed to elevate DNA amounts detected by this method. Here, we have not tested whether increased DNA originated from contamination or from blocking effects on inhibitors or completely different sources. Attempts should be made to also enable dyed or bleached hair to be reliably examined by these methods.

4.2 Mechanism of DNA degradation in hair and nails

Previous studies have suggested that the endonuclease DNase1L2 has a crucial role in some or all types of epidermal cornification (Fischer et al., 2007; Jäger et al., 2007). Targeted deletion of DNase1L2 in the mouse showed that the formation of the stratum corneum in the interfollicular epidermis did not depend on DNase1L2 whereas cornification of keratinocytes in the esophagus as well as in nails and hair required DNase1L2 for the complete removal of nuclear DNA. The absence of a phenotype in the epidermis of the DNase1L2 knockout mouse model indicates that keratinocyte cornification in the murine interfollicular epidermis proceeds in a DNase1L2-independent manner and that at least one different DNase must be involved in the complete degradation of nuclear DNA during stratum corneum formation. Identification and characterization of the responsible DNase(s) will be essential for the investigation of the function of DNA breakdown in the interfollicular epidermis.

Instead, this study provides key insights into the molecular regulation of a previously uncharacterized part of cornification, i.e. the breakdown of the nucleus in hair and nail keratinocytes. Detection of aberrantly retained nuclei in hair lacking DNase1L2 could demonstrate that DNase1L2 degrades nuclear DNA in terminally differentiated keratinocytes when they are converted to dead, but functional hair corneocytes, a phenomenon also found in nails. This finding was an essential step towards a better understanding of the mechanism involved in nuclear breakdown in the nail matrix and the hair shaft.

During *in situ* labeling of murine hair it was further noted that nuclei in the medulla showed higher affinity towards staining with Hoechst than nuclear remnants in the cortex. This phenomenon cannot be fully explained so far, but it seems likely that nuclear DNA in the medulla is less degraded than DNA in the cortex. This leads to the hypothesis that in hair, like in murine epidermis, a second, as-yet-unidentified, DNase plays a role in degradation of DNA in the absence of DNase1L2. DNA labeling patterns in examined hairs indicate that, if such an additional DNase actually exists, its levels of expression and/or activity are significantly lower in the medulla than in the cortex of hairs. An alternative scenario might be that DNA is simply more likely to be stained with Hoechst in medullated cells, due to unknown reasons.

The presence of Hoechst-positive nuclei in DNase1L2-deficient hair and the lack of such nuclei in wild-type hair did not result from better accessibility of the fluorescent dye towards the nuclear remnants. By mashing hairs of both DNase1L2 knockout and control mice, possible barriers (e.g. the hair’s cuticle) blocking the entry of the fluorescent dye were removed, thereby ensuring similar conditions for permeabilization. Detection of Hoechst-positive nuclear DNA in DNase1L2-deficient hair but not in wild-type hairs showed that ablation of this endonuclease did not simply affect protective layers on the surface of hairs but was indeed responsible for the retention of nuclear DNA in hair shafts.

This study further reveals so far undescribed differences between mitochondrial breakdown in hairs and nails. It could be shown that while degradation of mitochondrial DNA in nails at least partially depends on DNase1L2, a different pathway independent of this enzyme appears to exist in hair. Thus, the involvement of an additional, as-yet-unidentified DNase responsible for the removal of mitochondria during terminal differentiation of both murine and human hair keratinocytes seems likely.

In order to investigate the physiological purpose of degradation of nuclear DNA in hair an experiment, testing whether aberrantly retained DNA caused a phenotype under conditions of increased mechanical stress, was performed by my colleagues (Fischer et al., unpublished data). The study showed that DNase1L2-deficient hair was broken into significantly smaller fragments than wild-type hair. This finding suggested a function of DNA breakdown in establishing the mechanical properties of hair keratinocytes. It further indicates that degradation of nuclear DNA is not just an epiphenomenon of cornification but is of major importance for providing mechanical resilience of epidermal appendages.

The study conducted with human hair samples demonstrated the need for additional analysis of different parameters possibly correlating with the frequency of undegraded nuclei in hair shafts, such as the donor’s age or hair color. Preliminary results have been obtained during our investigations, but we recommend that similar studies be conducted involving larger sample numbers. The same applies to the examination of additional properties, namely thickness or fragility of human hair. Since in some hair shafts massive amounts of retained nuclear DNA can be detected while no nuclei persist in others, it is likely that these hairs show different degrees of resistance towards mechanical stress when evaluated in the style of the abovementioned fragmentation assay.

4.3 Inter-individual differences in DNA degradation in human hair

Since until now the extent to which degradation of nuclear DNA occurs during keratinisation of the human hair shaft has been elusive (Hellmann et al., 2001), this study provided a first demonstration of varying amounts of nuclear DNA being retained inside hair corneocytes from different individuals, similar to nuclei persisting in hairs from various wild-type mouse strains. By demonstrating highly different levels of incompletely degraded nuclei in hair shafts, our study reveals that not only the number and type of melanosomes cause variabilities in hair structure (Linch, 2009). It is still unclear what underlying causes are responsible for these distinct phenotypes detected in hair samples of different origin, since up to this point no polymorphism has been identified in the gene encoding DNase1L2. The basis for these fluctuations in residual DNA amounts in hair is unknown at present, both genetic and environmental factors may influence this trait.

However, this polymorphism in residual nuclear DNA in hair is able to explain a phenomenon observed in forensic medicine, namely highly varying success rates in typing of DNA extracted from single evidence hairs. Quantitation of nuclear DNA in the hair shaft prior to the actual STR analysis may be an initial indicator for the likelihood of success in obtaining a DNA profile (Linch et al., 2001). Until now, suitability of a hair for STR typing has usually been determined by the presence of soft tissue adhering to the hair shaft, such as hair root bulbs and follicular tissue containing nucleated cells (Linch et al., 2001). In general, hairs lacking a growing root or other tissue providing sources of nuclear DNA have been considered inappropriate for DNA genotyping (Roberts et al., 2007; Linch et al., 2001). It was reported that high quality profiles could be obtained from hairs where > 550 pg of nuclear DNA could be extracted, whereas only partial STR profiles were obtained in hairs containing < 60 pg of nuclear DNA (Opel et al., 2008). Although the vast majority of hairs (2-cm pieces) examined during our study contained 3-50 pg of nuclear DNA, hairs comprising between 100 and 250 pg of nuclear DNA could be observed as well. These amounts of DNA, corresponding to an approximate total number of 250 to 1500 counted nuclei per hair, led to partial or full DNA profiles. Thus, our results indicate that a subset of hair without adhering tissue, i.e. those with high numbers of DNA-containing nuclear remnants, should also be genotyped by STR.

As previously mentioned, the microscopic analysis should be a complementary approach for identification of a hair’s origin in addition to DNA analysis (Linch et al., 2001; Miller, 1987). Our protocol established for fluorescent labeling of nuclear remnants *in situ* provides a novel approach for pre-estimation of the success of subsequent STR typing. If hair shafts lack Hoechst-positive nuclei, hairs can still be subjected to microscopic analysis or typing of mitochondrial DNA. Typing of nuclear DNA strongly enhances the power of the evidence (Linch et al., 2001). Thus, assessing the probability for obtaining a DNA profile by fluorescent labeling of undegraded nuclei offers a valuable opportunity for determination of a hair’s suitability for STR analysis, the presence of stainable nuclear DNA in hair being a strong predictor for successful genotyping.

In summary, this project has provided new insights into the molecular mechanism of DNA degradation in hair formation and into a previously unknown polymorphism in human hair. The methods developed in this project may have applications in hair research, clinical dermatology and in forensics.

5. MATERIALS

5.1 Buffers

Lysis buffer – extraction of DNA from hair

50 mM Tris-HCl pH 8.0
100 mM NaCl
2.5 mM EDTA pH 8.0
2% w/v SDS
40 mM DTT
0,27 mg/ml Proteinase K

5.2 Kits

DNeasy Blood and Tissue Kit; Qiagen, Product Code: 69506
Light Cycler® Fast Start DNA Master SYBR Green I; Roche Applied Science, Product Code: 12239264001
Plasmix Miniprep Kit; Talent
QIAEX II Gel Extraction Kit; Qiagen, Product Code: 20021
TOPO TA Cloning® Kit (with pCR®2.1-TOPO® vector) with One Shot® TOP10 Electrocomp™ E. coli; Invitrogen, Product Code: K456001

5.3 Reagents and solutions

Agarose; GE Healthcare, Product Code 17-0554-02
BlondMe Developer (6% H_2O_2); Schwarzkopf
BlondMe Developer (9% H_2O_2); Schwarzkopf
DAPI VECTASHIELD® Mounting Medium with DAPI; Vector Labs, Product Code: H-1200
DL-Dithiothreitol (DTT); Sigma-Aldrich, Product Code: 43815-1G
DNA Molecular Weight Marker VI; Roche, Product Code: 11062590001
Domino Blondierpulver; Domino Haarkosmetik
1x DPBS; Invitrogen, Product Code: 14190
D-Squame stripping discs, 14mm; Cuderm, Dallas, TX

Ethanol 96%; Merck, Product Code: 1.00971.100
Fluoprep; Biomerieux, Product Code: 75521
Hoechst 33258 pentahydrate ; Invitrogen, Product Code: 1398
LightCycler® Capillaries (20 µl); Roche Applied Science, Product Code: 04929292001
Phosphate-buffered 4.5% formaldehyde
Poly Colour Black Brilliance; Schwarzkopf
Proteinase K > 600 mAU/ml, solution; Qiagen, Product Code : 19131
Red Hot® Taq DNA Polymerase; ABgene, Product Code: AB-0406/A
6x Sample Loading Dye; Fermentas, Product Code: R0611
Sodium dodecyl sulfate (SDS); USB, Product Code: 75819
5x Tris Borate-EDTA (TBE) Buffer; Sigma, Product Code: T6400
Tween 20; Sigma-Aldrich, Product Code: P1379

5.4 Primers

5.4.1 Primers for amplification of murine nuclear and mitochondrial DNA

M-L1-for: 5’-TGGTAGAGGACATCAAGAAGGAC-3’
M-L1-rev: 5’-TTCCTGTTTTTCTTTAAGGACTTGTAA-3’
M-mito-for: 5’-CCTCCGAATGATTATAACCTAGACTT-3’
M-mito-rev: 5’-AGGGTAACTTGGTCCGTTGA-3’

5.4.2 Primers for amplification of human nuclear and mitochondrial DNA

Alu-Sb1-for: 5’-GTCAGGAGATCGAGACCATCC-3’
Alu-Sb1-rev124: 5’-TCCTGCCTCAGCCTCCCAAG-3’
H-MITOfin-for: 5’-CTCAGATAGGGGTCCCTTGA-3’
H-MITOfin-rev: 5’-GCACTCTTGTGCGGGATATT-3’

5.4.3 Primers for sequencing of mitochondrial DNA in the pCR®2.1-TOPO® vector

M13 Rev (-29) (forward primer): 5’-CAGGAAACAGCTATGACC-3’
T7 promoter (reverse primer): 5’-CCCTATAGTGAGTCGTATTA-3’

5.4.4 Primers for the amplification of STR loci (miniSTR-multiplex PCR)

Amelo/forward: 5’-CCCTGGGCTCTGTAAAGAATAGTG-3’

Amelo/reverse: 5’-ATCAGAGCTTAAACTGGGAAGCTG-3’

D16S539mini/forward: 5’-ATACAGACAGACAGACAGGTG-3’

D16S539mini/reverse: 5’-GCATGTATCTATCATCCATCTCT-3’

D18S51mini/forward: 5’-TGAGTGACAAATTGAGACCTT TET-3’

D18S51mini/reverse: 5’-GTCTTACAATAACAGTTGCTACTATT-3’

D2mini/forward: 5’-CAGTGGATTTGGAAACAGAAATG-3’

D2mini/reverse: 5’-TCAGTAAGTTAAAGGATTGCAGG-3’

FGAmini/forward: 5’-GGCATATTTACAAGCTAGTTTCT-3’

FGAmini/reverse: 5’-ATTTGTCTGTAATTGCCAGC-3’

TH01mini/forward: 5’-CCTGTTCCTCCCTTATTTCCC-3’

TH01mini/reverse: 5’-GGGAACACAGACTCCATGGTG-3’

5.5 Equipment and Software

LightCycler® Carousel-Based System 1.2; Roche Applied Science

Meta Morph software version 4.5 (Universal Imaging Corporation)

Olympus AX70 microscope

Ultrasonicator: Laborpartner, Vienna

6. METHODS

6.1 DNase1L2 KO mouse

A DNase1L2-deficient mouse was generated in the course of the project “DNA breakdown in epidermal keratinocytes” which was funded by a grant from the Austrian Science fund to Leopold Eckhart (FWF: P20043). Gene targeting, selection of ES cells, blastocyst injections and initial breeding were performed by the Centre of Functional Genomics (CFG), Albany, NY and by the team of Prof. Erwin Wagner at the Research Institute of Molecular Pathology, Vienna, Austria. The project was coordinated by Dr. Heinz Fischer, Research Division of Skin Biology and Pathobiology, Department of Dermatology, Medical University of Vienna. In brief, the chromosomal region including *Dnase1l2* gene was cloned into a targeting vector. Exons 2-6 of the *Dnase1l2* gene were replaced by a neomycin resistance cassette and the vector was transfected into W4 ES cells of the mouse strain 129SvEv. ES clones were karyotyped and screened by Southern-blotting of *BstEII*- and SalI-digested genomic DNA using a radioactively labelled probe. The chromosomal regions flanking the Neo resistance cassette in the selected clones were amplified by long-range PCR and sequenced to confirm that the flanking genes, namely E4F1 and DCI, were free of mutations. Knockout mice in the mixed C57BL6 / 129 background and in the pure background of the strain 129 were generated.

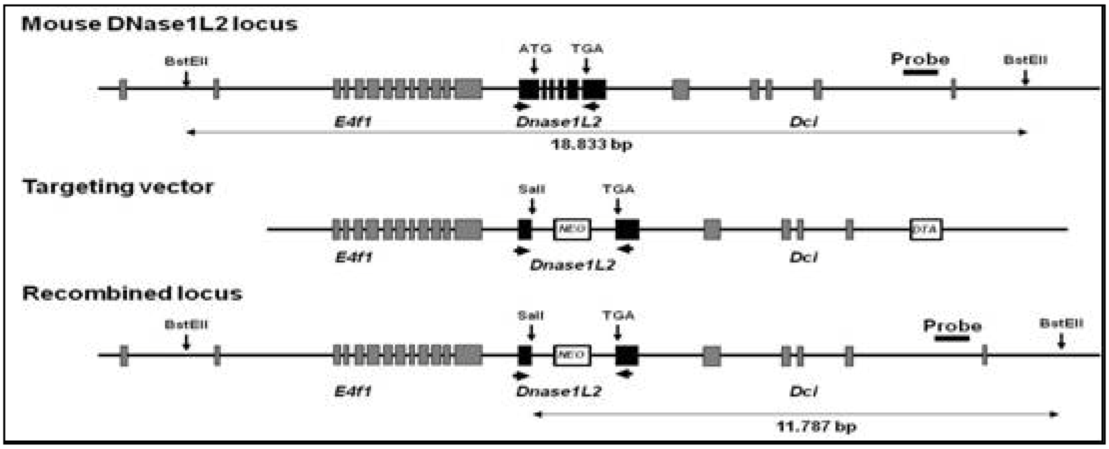
Mouse DNase1L2 locus
BstEII
ATG
TGA
Probe
BstEII
E4f1
Dnase1L2
Dci
18.833 bp
Targeting vector
SalI
TGA
NEO
DTA
E4f1
Dnase1L2
Dci
Recombined locus
BstEII
SalI
TGA
Probe
BstEII
NEO
E4f1
Dnase1L2
Dci
11.787 bp

Figure 30: Targeted deletion of the DNase1L2 gene in the mouse.

6.2 Murine hair samples

Murine hair samples were generated by shaving the mice' back hair. The samples were stored at -20°C. In order to separately analyse each of the four murine hair types, namely zigzag, guard, awl and auchene, attribution of hairs to each type was performed under the microscope according to (Schlake, 2007).

6.3 Human hair samples

Undyed hairs from 40 volunteers were obtained by cutting 1-3 cm from the tip of a hair strand, thereby excluding hairs containing the root bulb. All samples were coded and processed in an anonymous manner. According to the judgement of trained dermatologists, no pathological abnormalities were detected in any hair specimens. Hairs were stored at -20°C.

6.4 Fluorescent dye labeling of DNA *in situ*

Either a few 2-cm pieces of human hair or 2 mg of shaved mouse hair were transferred into a 0.5 ml tube. The hair was washed 3 times each by vigorous vortexing in 500 µl of 0.04% SDS, H_2O dd and 70% EtOH. Hairs were then dried over night at room temperature (RT) and subsequently permeabilized with 1% (mouse hair) or 10% (human hair) ammonia solution (pH 10.5) for 5 h at RT. After 3 times of washing with H_2O dd, hairs were incubated with DNA specific Hoechst 33258 (Invitrogen; 1:5000 in H_2O) over night at RT. Hairs were washed again with H_2O dd and mounted on glass slides using Fluoprep (Biomerieux). The slides were stored for about a day prior to photodocumentation to allow excess Hoechst to diffuse out of the hair.

6.5 DAPI-staining of pulverized hair

Mouse hair which had already been crushed into tiny pieces by means of liquid nitrogen and a mortar was directly applied to a microscope slide. These hair fragments were embedded in mounting medium containing DNA specific dye 4´,6-Diamidin-2-phenylindol (DAPI, VECTASHIELD, Vector laboratories). The slide was then stored in the dark for about 15 minutes, allowing the fluorescent dye to diffuse into the hair debris.

6.6 Immunohistochemical and immunofluorescent analysis of plucked scalp hairs

Approximately 20 hairs comprising high numbers of nuclei were plucked from the donor's scalp and hairs containing follicular tissue were arranged into a parallel bundle. Tissues were fixed in phosphate-buffered 4.5% formaldehyde for 24 h and embedded in paraffin. Sections of 4 µm were co-stained with Hoechst 33258 pentahydrate (10 mg in 1 ml H_2O; further dilution of 1:5000 in 1x DPBS) and anti-DNase1L2-antibody (1:400). Polyclonal antisera against DNase1L2 were produced by immunizing rabbits with purified recombinant DNase1L2 preparations produced in the yeast Pichia pastoris and affinity-purified against the antigen (Fischer et al., 2007). Immunofluorescence labeling was performed as described previously (Rendl et al., 2002).

6.7 Microscopy

The stainings were stored at RT and analyzed using an Olympus AX70 microscope and Meta Imaging Software (Metamorph).

6.8 Analysis of single hairs

Single hairs of 40 human hair samples were stained with Hoechst dye as described above. Visible nuclei were counted under the microscope, then the hair was removed from the slide and washed 3 times for 10 minutes with PBS 0.1% Tween. After washing, DNA was extracted from the hair according to the standard protocol (see below).

6.9 *In vitro* dyeing and bleaching of hairs

Human hair samples were dyed black with "Poly Colour Black Brillance" (Schwarzkopf) or treated with bleaching agents. The black hair dye was mixed with the supplied developing emulsion until a homogeneous mixture was obtained. Similarly, "Domino Blondierpulver" (Domino Haarkosmetik) was mixed with "BlondMe Developer (9% H_2O_2)" and "BlondMe Developer (6% H_2O_2)" (both from Schwarzkopf) to equal volumes, again forming a homogeneous mixture.

After washing of hair samples with 1 ml of 0.1% PBS-T for 10 min (750 rpm), hairs were transferred to fresh 1.5 ml tubes and incubated with either of the chemical agents. Incubation with the black dye was performed for 20 min whereas the hairs were subjected to the bleaching agent for 30 min. Hairs were then carefully removed from the tubes, transferred to fresh ones and washed with 1 ml of 0.1% PBS-T for 3 x 10 min (750 rpm). Afterwards hairs were processed according to standard protocols in order to label DNA with Hoechst or to lyse hairs with extraction buffer.

6.10 Lysis of hairs and nails

To remove stratum corneum squames or other cellular components adhering to the surfaces of the biological material, hair and nails were washed carefully prior to lysis. Tissue was weighed and transferred into 1.5 ml tubes. 1 ml of 0.1% PBS-T was added to human hair samples and 500 µl were added to murine hair, respectively.

Hairs were washed for 3x 10 minutes on a thermoblock (750 rpm) on room temperature. Between each washing step PBS-T was carefully removed with a small pipet tip and fresh PBS-T was added to the sample which was then vigorously vortexed to be placed onto the thermoblock again.

5 mg of human finger nails were cut into tiny pieces, followed by ultrasonication in 1 ml 2% SDS for 4x 30 seconds. The samples were cooled on ice between each step, and the washing buffer was changed between the 2nd and 3rd ultrasonication step. Eventually the samples were washed with fresh 1 ml 2% SDS followed by 3 times of washing with 96% ethanol. Then the nails were air-dried to enable accurate weighing which was essential for exact determination of the ratio of amplified DNA per mg of tissue. Ultrasonication was performed on a device from Laborpartner, Vienna, with maximum intensity (i.e. level 100) and medium pulsation (i.e. level 0.5). Due to their small sizes, murine nails could not be washed prior to lysis without risking to lose material. When processing tapestrips, washing was neither necessary nor possible.

Lysis buffer was generated in accordance with previous publications (Opel et al., 2008; Gilbert et al., 2004; Gilbert et al., 2007) with slight modifications (see chapter **5.1. Buffers**). A 50 ml stock of lysis buffer was prepared without DTT and proteinase K; these sensitive reagents were added just before actual lysis. For example, to 946.5 µl of this mix, 13.5 µl of proteinase K and 40 µl of DTT had to be added in order to obtain 1 ml of lysis buffer.

5 mg of human hair were lysed with 750 µl of lysis buffer, while 5 mg of murine hair were lysed in 500 µl of extraction buffer. 500 µl of buffer was added to 5 mg of human nails and 200 µl of buffer were added to 1 mg of murine nails. Tapestrips were transferred to 0.5 ml

tubes to which 500 µl lysis buffer were added. The samples were then incubated on 56°C (750 rpm); depending on the type of tissue the period of lysing varied from 30 minutes (mouse hair) over 60 minutes (tapestrips) to ten hours (human hair and nails). When lysis was still incomplete after some hours, extra proteinase K (up to 0.65 mg/ml) and DTT (up to 70 mM) was added to the digestion buffer.

6.11 DNA extraction from hairs and nails

DNA was purified with the Qiagen DNeasy Blood and Tissue Kit according to the protocol provided by the manufacturer with the following modifications. Instead of the lysis protocol of the kit, DNA-containing lysate was prepared as described above. After complete lysis, buffer AL and 96% EtOH were added to the same volume as the lysate. The mixture was loaded onto the column whereby a maximum of 750 µl were loaded at once, followed by centrifugation and loading of the next aliquot. After extensive washing the DNA was eluted with 2 aliquots of 100 µl buffer EB. The DNA extracts were stored at -20°C until PCR analysis.

6.12 Quantitative real-time PCR

qPCR was performed using the LightCycler® Carousel-Based System 1.2 and the Light Cycler® Fast Start DNA Master SYBR Green I (both Roche Applied Science) according to the manufacturer’s protocol. Mouse mitochondrial DNA was amplified with the primers M-mito-for and M-mito-rev while mouse nuclear DNA was amplified with the primers M-L1-for, and M-L1-rev (see chapter **5.4.1. Primers**). Human mtDNA was amplified with the primers H-MITOfin-for and H-MITOfin-rev. Human nuDNA was amplified with the primers Alu-Sb1-for and Alu-Sb1-rev124 that had been published previously (Opel et al., 2008; see chapter **5.4.2. Primers**). All PCRs consisted of a denaturation step at 95°C for 10 minutes and 55 cycles consisting of incubations at 95°C for 5 seconds, 65 °C for 5 seconds, and 72 °C for 15 seconds. Primer pair efficiencies were determined according to (Kadl et al., 2002).

6.13 Creation of standard curves for quantification of PCR yield

In order to accurately quantify DNA amounts amplified during real-time PCR, standard curves were generated using genomic DNA and plasmids containing cloned target sequences, i.e. mitochondrion-specific amplicons. The following includes considerations and calculations essential for determining the mass of nuDNA and plasmid templates which correspond to certain copy numbers of target nucleic acid sequences. Dilution series were prepared in the range of 3.000.000.000 to 300 copies (nuDNA) and 300.000 to 30 copies (plasmids containing mtDNA).

Standard curves were generated according to published protocol (Applied Biosystems: http://www3.appliedbiosystems.com/cms/groups/mcb_marketing/documents/generaldocuments/cms_042486.pdf; 14.5.2009).

6.13.1 Creation of a standard curve for the quantification of nuclear DNA

After determining the mass of DNA per haploid genome of interest (i.e. human genome = 3.3 pg, mouse genome = 3.25 pg), the mass of the genome was then divided by the copy number of the target gene per haploid genome (100.000 copies of LINE1- or Alu-elements). This led to the mass of DNA per copy of the gene of interest. As next step the mass of genomic DNA containing the desired copy numbers was calculated (here: from 300.000.000 to 300 copies in steps of 10) by multiplying the copy numbers of interest by the mass of the haploid genome. Afterwards the volume used for a single PCR reaction (= 1.5 µl) had to be taken into consideration in order to calculate the concentration of genomic DNA needed to achieve the required copy numbers in each PCR reaction. Serial dilutions were obtained from (human and murine) genomic DNA preparations in the calculated concentrations. The concentrations of the stock solutions were either 6.66 ng/µl, containing 300.000.000 copies of the human genome or 66.5 ng/µl, comprising 3.000.000.000 copies of the mouse genome.
(AppliedBiosystems:
http://www3.appliedbiosystems.com/cms/groups/mcb_marketing/documents/generaldocuments/cms_042486.pdf; 14.5.2009)

6.13.2 Creation of a standard curve with a plasmid DNA template

Since no preparation of purified mitochondrial DNA was available, plasmids containing murine and human mitochondrial DNA amplicons were generated. These could then be purified and used to create standard curves for the quantification of mtDNA.

6.13.2.1 Cloning of PCR products into the pCR2.1 TOPOR vector

For amplification of mitochondrion-specific DNA, following components were mixed in a 0.5 ml tube:

Synthesis Buffer 10x……….……5 µl
$MgCl_2$……………………….……3 µl
dNTPs…………………………….…1 µl
Primer (sense; 10 µM)……….....1.5 µl
Primer (antisense; 10 µM).....…...1.5 µl
Red Hot DNA Polymerase………0.2 µl (1µl = 5U)
H_2O…………...………………..36.8 µl
template.…………………………...1 µl
total:…………….. ……………....50 µl

Reactions were performed in a 50-µL reaction mixture containing 1 unit of Red-Hot Taq-Polymerase (Roche). 30 cycles were run at following temperature settings:

94°C.……………...3’
94°C.……………30’’
55°C.……………30’’
72°C.……………30’’
72°C.……………...7’
4°C………………∞

6.13.2.2 Agarose gel electrophoresis

Afterwards a 1.5% agarose gel was made by boiling 1.5 g of agarose in 100 mL 1x TBE buffer (prepared with 5x Tris Borate-EDTA (TBE) Buffer; Sigma). 4.5 µl of ethidium bromide (10 mM) were added to the gel before letting it cool down in the gel chamber. In the meantime 20 µl of PCR product were mixed with 4 µl of 6x Sample Loading Dye (Fermentas). DNA Molecular Weight Marker VI (Roche) was used as a reference marker. After loading the samples into the slots the gel was run for about 40 minutes at 85 Volt.

6.13.2.3 DNA extraction from agarose gels

The separated DNA fragments were made visible under UV light so the proper DNA band could be excised with a clean, sharp scalpel. The gel slice was then transferred to a tube, afterwards the extraction was performed using the QIAEX II Agarose Gel Extraction Kit (Qiagen) as suggested by the manufacturer.

6.13.2.4 DNA sequencing

20 µl of purified PCR products (min. 50-100 ng/µl) were transferred into 1.5 ml tubes. The samples were further processed by Eurofins MWG Operon, Germany. Primers used for sequencing were either enclosed to the samples or provided by the sequencing company. In order to sequence PCR products cloned into the MCS of pCR2.1 TOPO^R vector, forward primer "M13 Rev (-29)" and reverse primer "T7 promoter" were used (see chapter **5.4.3 Primers**).

6.13.2.5 Transformation

3 µl of each PCR product were mixed with 1 µl H_2O, 1 µl salt solution and 1 µl pCR2.1 TOPO^R vector (Invitrogen). The reagents were gently mixed and incubated on room temperature for 20 minutes. In the meantime for each reaction a vial of One Shot® E. coli (75 µl) was thawed on ice, before 2 µl of cloning reaction mix were added to each tube. The mixture was incubated on ice for 30 minutes, afterwards heat-shock was performed on 42°C for 30 seconds without shaking. 250 µl of SOC medium (room temperature) were immediately added to the mix which was then incubated on 37°C for 1 hour (400 rpm). 50 µl from each transformation mix were spread onto LB-amp plates which were incubated at 37°C over night.

6.13.2.6 Direct PCR from bacterial colonies

Some of the growing colonies were gently picked with a pipet tip and dipped into following PCR mix:

Synthesis Buffer 10x………..……2.5 µl
$MgCl_2$…………………………..……1.5 µl
dNTPs……………………………..….0.5 µl
Primer (sense; 10 µM)……….........0.5 µl
Primer (antisense; 10 µM).....….......0.5 µl
Red Hot DNA Polymerase………...0.1 µl (1µl = 5U)
H_2O…………...…………………..18.4 µl
total:…………….. ……………........25 µl

Reactions were performed in a 25-µL reaction mixture containing 1 unit of Red-Hot Taq-Polymerase (Roche). 30 cycles were run at following temperature settings:

Temperature settings (30 cycles):
95°C.……………...5’
95°C.……………30’’
55°C.……………30’’
72°C.……………...1’
72°C.……………...8’
4°C………………∞

6.13.2.7 Preparation of plasmid-DNA

A colony was inoculated and grown in 3 ml of appropriate selection medium at 37°C over night, then 1.2-1.5 ml of bacterial cells were pelleted by centrifugation (1 min, 10000 rpm, RT). The following steps were performed with the Plasmix Kit (Talent) according to the manufacturer’s instructions.

6.13.2.8 Preparation of a standard curve with plasmids containing mitochondrial DNA

These plasmids containing murine and human mitochondrial PCR amplicons were now used to create a standard curve necessary for determination of the amount of mtDNA detected during real-time PCR. At first the mass of a single plasmid molecule had to be calculated, using the size of the entire plasmid containing the insert (plasmid + human mitochondrial amplicon = 3931 bp = 4.37×10^{-18}g; plasmid + mouse mitochondrial amplicon = 4026 bp = 4.41×10^{-18}g). Afterwards the mass of plasmid equaling the copy numbers of interest was calculated (here: from 3.000.000.000 to 30 copies, in steps of 10) by multiplying the copy numbers of interest by the mass of a single plasmid. In the next step the proper concentrations of plasmid DNA needed to achieve the desired copy numbers were calculated by dividing the total mass needed by the volume to be pipetted into each PCR reaction. Eventually a serial dilution of the plasmid DNA was prepared in the calculated concentrations. As cloned sequences are highly concentrated in purified plasmid DNA stocks, a series of serial dilutions had to be performed to achieve an appropriate working stock of plasmid DNA for quantitative PCR applications. The concentration of the stock solution was either 8.73 ng/µl, containing 3.000.000.000 copies of the human mitochondrial amplicon or 8.8 ng/µl, comprising 3.000.000.000 copies of the mouse mitochondrial amplicon.

(Applied Biosystems:
http://www3.appliedbiosystems.com/cms/groups/mcb_marketing/documents/generaldocuments/cms_042486.pdf; Stand: 14.5.2009)

6.14 STR typing

STR typing was carried out at the Institute of Legal Medicine in Innsbruck as published in (Grubwieser et al., 2006). A miniSTR-multiplex PCR, used to amplify highly degraded DNA as found in human hair, was performed. 5 STR loci, namely D2S1338, D16S539, D18S51, TH01 and FGA, as well as amelogenin on the Y-chromosome were amplified from both hair samples and buccal scrapes, subsequent to extraction and quantitation of DNA. Total volumes for one reaction were either 25 or 50 µl, comprising 10 or 20 µl DNA, respectively. PCR mixes contained 1x PCR buffer II, 1.5 mM $MgCl_2$, 0.2 mM dNTP (each), 250 mg BSA (Sigma) and 1 U AmpliTaq Gold polymerase (Applied Biosystems).

Primers were added in following concentrations, namely 80 nM primers D16S539mini, 100 nM primers TH01mini and Amelo, 160 nM primers D2mini, 200 nM primers D18S51mini and 300 nM primers FGAmini (see chapter **5.4.4. Primers**). PCR was carried out on a Gene

Amp PCR System 9600, performing 30 cycles following an initial denaturation step at 95°C for 11 min. Each cycle included denaturation at 94°C for 1 min, annealing at 56°C for 1 min and elongation at 72°C for another min. PCR was completed by final incubation of the samples at 60°C for 45 min. To 1 µl aliquots of the amplification products 20 µl of deionized formamide and 1 µl of internal lane standard (Genescan-500 TAMRA, AB) were added. Subsequently, samples were denaturated at 95°C for 2 min and snap-cooled on ice, before being subjected to electrophoresis on an ABI PRISM 3100 Genetic Analyzer using POP 6 and default conditions. Analysis of data was performed using GeneScan Analysis (versions 2.1 and 3.7) and Genotyper (version 3.6) software (both AB).

6.15 Statistical analyses

Student's t-test was calculated using Microsoft Excel 2003. Two-tailed t-tests of type 2, which is used for two samples with equal variance, or type 3, for samples with non-equal variance, were applied where appropriate. Probabilities $p < 0.05$ were accepted as significant.

Correlation analyses were performed using the SPSS software, version 16.0 (SPSS Inc., Chicago, IL). Spearman rank correlation is a non-parametric test designed to measure the degree of association between two variables without making any assumptions about their distribution. More precisely, bivariate Spearman's correlation coefficient was used to analyze variables that are not normally distributed. In addition to the correlation analysis, the coefficient was further tested using a two-tailed significance test. Based on the significance value, hypotheses were accepted ($p < 0.05$) or rejected ($p > 0.05$).

7. REFERENCES

1. Alibardi L, Toni M, Valle LD. Hard cornification in reptilian epidermis in comparison to cornification in mammalian epidermis. Exp Dermatol. 2007

2. Alonso L, Fuchs E. The hair cycle. J Cell Sci. 2006

3. Birngruber C, Ramsthaler F, Verhoff MA. The color(s) of human hair—forensic hair analysis with SpectraCube. Forensic Sci Int. 2009

4. Bolognia J, Jorizzo J, & Rapini R. Dermatology (Vol. 1). Toronto, Mosby, 2003

5. Butler, JM. Forensic DNA Typing: Biology, Technology, and Genetics of STR Markers (2nd Edition). Elsevier Academic Press, New York, 2005.

6. Butler JM. Short tandem repeat typing technologies used in human identity testing. Biotechniques. 2007

7. Campbell VW, Jackson DA. The effect of divalent cations on the mode of action of DNaseI. The initial reaction products produced from covalently closed circular DNA. J Biol Chem. 1980

8. Candi E, Schmidt R, Melino G. The cornified envelope: a model of cell death in the skin. Nat Rev Mol Cell Biol. 2005

9. Danforth nomenclature, 1925

10. Davidson P, Hardy MH. The development of mouse vibrissae in vivo and in vitro. J Anat. 1952

11. Fadeel B, Orrenius S, Zhivotovsky B. Apoptosis in human disease: a new skin for the old ceremony? Biochem Biophys Res Commun. 1999

12. Fischer H, Eckhart L, Mildner M, Jaeger K, Buchberger M, Ghannadan M, Tschachler E. DNase1L2 degrades nuclear DNA during corneocyte formation. J Invest Dermatol. 2007

13. Gilbert MT, Wilson AS, Bunce M, Hansen AJ, Willerslev E, Shapiro B, Higham F, Richards MP, O'Connell TC, Tobin DJ, Janaway RC, Cooper A. Ancient mitochondrial DNA from hair. Curr Biol. 2004

14. Gilbert MT, Tomsho LP, Rendulic S, Packard M, Drautz DI, Sher A, Tikhonov A, Dalén L, Kuznetsova T, Kosintsev P, Campos PF, Higham T, Collins MJ, Wilson AS, Shidlovskiy F, Buigues B, Ericson PG, Germonpré M, Götherström A, Iacumin P, Nikolaev V, Nowak-Kemp M, Willerslev E, Knight JR, Irzyk GP, Perbost CS, Fredrikson KM, Harkins TT, Sheridan S, Miller W, Schuster SC. Whole-genome shotgun sequencing of mitochondria from ancient hair shafts. Science. 2007

15. Grubwieser P, Mühlmann R, Berger B, Niederstätter H, Pavlic M, Parson W. A new "miniSTR-multiplex" displaying reduced amplicon lengths for the analysis of degraded DNA. Int J Legal Med. 2006

16. Haake AR, Holbrook K. Development and structure of skin. In: Wolff K, Goldsmith LA, Katz SI, Gilchrest BA, Paller A, Leffell DJ, editors. Fitzpatrick's Dermatology in General Medicine. 5th ed. New York: McGraw Hill; 2007

17. Hellmann A, Rohleder U, Schmitter H, Wittig M. STR typing of human telogen hairs-a new approach. Int J Legal Med. 2001

18. Hengartner MO. The biochemistry of apoptosis. Nature. 2000

19. Jäger K, Fischer H, Tschachler E, Eckhart L. Terminal differentiation of nail matrix keratinocytes involves up-regulation of DNase1L2 but is independent of caspase-14 expression. Differentiation. 2007

20. Jones SJ, Worrall AF, Connolly BA. Site-directed mutagenesis of the catalytic residues of bovine pancreatic deoxyribonuclease I. J Mol Biol. 1996

21. Kawane K, Nagata S. Nucleases in programmed cell death. Methods Enzymol. 2008

22. Kerr JF, Wyllie AH, Currie AR. Apoptosis: a basic biological phenomenon with wide-ranging implications in tissue kinetics. Br J Cancer. 1972

23. Krenke BE, Tereba A, Anderson SJ, Buel E, Culhane S, Finis CJ, et al. Validation of a 16-locus fluorescent multiplex system. J Forensic Sci 2002

24. Kroemer G, Galluzzi L, Vandenabeele P, Abrams J, Alnemri ES, Baehrecke EH, El-Deiry WS, Blagosklonny MV, Golstein P, Green DR, Hengartner M, Knight RA, Kumar S, Lipton SA, Malorni W, Nuñez G, Peter ME, Tschopp J, Yuan J, Piacentini M, Zhivotovsky B, Melino G; Nomenclature Committee on Cell Death 2009. Classification of cell death: recommendations of the Nomenclature Committee on Cell Death 2009. Cell Death Differ. 2009

25. LaFountain MJ, Schwartz MB, Svete PA, Walkinshaw MA, Buel E.TWGDAM validation of the AmpF*l*STR Profiler Plus and AmpF*l*STR COfiler STR multiplex systems using capillary electrophoresis. J Forensic Sci 2001

26. Laskowski, M, Sr.: Venom Exonuclease, The Enzymes, 3rd Ed. Vol. 4,P. Boyer, Academic Press, NY, 1971

27. Linch CA, Whiting DA, Holland MM. Human hair histogenesis for the mitochondrial DNA forensic scientist. J Forensic Sci. 2001

28. Linch CA. The ultrastructure of tissue attached to telogen hair roots. J Forensic Sci. 2008

29. Linch CA. Degeneration of nuclei and mitochondria in human hairs. J Forensic Sci. 2009

30. Lippens S, Denecker G, Ovaere P, Vandenabeele P, Declercq W. Death penalty for keratinocytes: apoptosis versus cornification. Cell Death Differ. 2005

31. Lippens S, Hoste E, Vandenabeele P, Agostinis P, Declercq W. Cell death in the skin. Apoptosis. 2009

32. Miller LS. Procedural Bias in Forensic Science Examinations of Human Hair. Law and Human Behavior, Vol. 11, No. 2. (1987), pp. 157-163.

33. Moll R, Divo M, Langbein L. The human keratins: biology and pathology. Histochem Cell Biol. 2008

34. Moretti TR, Baumstark AL, Defenbaugh DA, Keys KM, Smerick JB, Budowle B. Validation of short tandem repeats (STRs) for forensic usage: performance testing of fluorescent multiplex STR systems and analysis of authentic and simulated forensic samples. J Forensic Sci 2001

35. Müller K, Klein R, Miltner E, Wiegand P. Improved STR typing of telogen hair root and hair shaft DNA. Electrophoresis 2007

36. Nagata S. Apoptotic DNA fragmentation. Exp Cell Res. 2000

37. Nagata S, Nagase H, Kawane K, Mukae N, Fukuyama H. Degradation of chromosomal DNA during apoptosis. Cell Death Differ. 2003

38. Nagata S. DNA degradation in development and programmed cell death. Annu Rev Immunol. 2005

39. Nicklas JA, Buel E. Quantification of DNA in forensic samples. Anal Bioanal Chem. 2003 (a)

40. Nicklas JA, Buel E. Development of an Alu-based, real-time PCR method for quantitation of human DNA in forensic samples. J Forensic Sci. 2003 (b)

41. Niederstätter H, Köchl S, Grubwieser P, Pavlic M, Steinlechner M, Parson W. A modular real-time PCR concept for determining the quantity and quality of human nuclear and mitochondrial DNA. Forensic Sci Int Genet. 2007

42. Nishimoto S, Kawane K, Watanabe-Fukunaga R, Fukuyama H, Ohsawa Y, Uchiyama Y, Hashida N, Ohguro N, Tano Y, Morimoto T, Fukuda Y, Nagata S. Nuclear cataract caused by a lack of DNA degradation in the mouse eye lens. Nature. 2003

43. Omary MB, Coulombe PA, McLean WH. Intermediate filament proteins and their associated diseases. N Engl J Med. 2004

44. Opel KL, Fleishaker EL, Nicklas JA, Buel E, McCord BR. Evaluation and quantification of nuclear DNA from human telogen hairs. J Forensic Sci.2008

45. Paus R, Cotsarelis G. The biology of hair follicles. N Engl J Med. 1999

46. Polakowska RR, Piacentini M, Bartlett R, Goldsmith LA, Haake AR. Apoptosis in human skin development: morphogenesis, periderm, and stem cells. Dev Dyn. 1994

47. Popescu C, Höcker H. Chapter 4. Cytomechanics of hair basics of the mechanical stability. Int Rev Cell Mol Biol. 2009

48. Price PA. The essential role of Ca2+ in the activity of bovine pancreatic deoxyribonuclease. J Biol Chem. 1975

49. Roberts KA, Calloway C. Mitochondrial DNA amplification success rate as a function of hair morphology. J Forensic Sci. 2007

50. Samejima K, Earnshaw WC. Trashing the genome: the role of nucleases during apoptosis. Nat Rev Mol Cell Biol. 2005

51. Schlake T. Determination of hair structure and shape. Semin Cell Dev Biol. 2007 Apr;18(2): 267-73. Epub 2007

52. Shiokawa D, Tanuma S. Characterization of human DNase I family endonucleases and activation of DNase gamma during apoptosis. Biochemistry. 2001

53. Ullu E, Tschudi C. Alu sequences are processed 7SL RNA genes. Nature. 1984

54. Walker JA, Kilroy GE, Xing J, Shewale J, Sinha SK, Batzer MA. Human DNA quantitation using Alu element-based polymerase chain reaction. Anal Biochem. 2003

55. Wyllie AH, Kerr JF, Currie AR. Cell death: the significance of apoptosis. Int Rev Cytol. 1980

56. http://www.texascollaborative.org/hildasustaita/hairstructure.gif (08.08.2010)

57. Real-time PCR methods (Roche Applied Science): http://www.roche-applied-science.com/PROD_INF/MANUALS/pcr_man/chapter_7.pdf; (10.08.2010)

58. Applied Biosystems: http://www3.appliedbiosystems.com/cms/groups/mcb_marketing/documents/generaldocuments/cms_042486.pdf; (14.5.2009)

8. APPENDIX

8.1 List of figures

Figure 1: The structure of the hair bulb (http://www.texascollaborative.org/hildasustaita/hairstructure.gif)..12

Figure 2: Hoechst staining of nuclear DNA comprised in murine hair……………………………..….…...28

Figure 3: Fluorescent labeling of DNA in hair from 129 mice deficient in DNase1L2……………………….29

Figure 4: Murine hair debris embedded in mounting medium containing DAPI…………………………...30

Figure 5: Hoechst-labeling of nuclear DNA in all hair types of the murine fur. ………………..…………….31

Figure 6: Fluorescent staining of nuclear DNA comprised in vibrissae.…………………………..……......32

Figure 7: Real-time PCR performed with nuclear and mitochondrial DNA extracted from hair samples obtained from wild-type and DNase1L2-deficient mice…………………….……………..33

Figure 8: Real-time PCR performed with nuclear and mitochondrial DNA extracted from murine nails...….34

Figure 9: Real-time PCR performed with nuclear and mitochondrial DNA extracted from tapestrips containing murine stratum corneum…………………………………………………...….…35

Figure 10: Hoechst labeling of wild-type and DNase1 deficient hair………………………………....……37

Figure 11: Fluorescent labeling of nuclear DNA in normal and DNase1L3 deficient hair………………...…38

Figure 12: Hoechst-positive nuclei detected in various wild-type mouse strains…………………………..…39

Figure 13: Hoechst-staining of nuclear DNA in vibrissae from different wild-type mouse strains…………..40

Figure 14: Fluorescent labeling of nuclei in hair from BalbC and DNase1L2 deficient mice………………...41

Figure 15: Real-time PCR performed with nuclear DNA extracted from DNase1L2 deficient hairs and from hair samples obtained from wild-type mouse……………………………...……….…42

Figure 16: DNA labeling of human hair with Hoechst...43

Figure 17: Hoechst-labeling of nuclear DNA in human hair containing no, a few, or a high number of nuclei……………………………………………………...…………......................44

Figure 18: Fluorescent labeling of nuclei in various types of human body hair..46

Figure 19: Immunohistochemical staining of DNase1L2 in a cross section of plucked hairs containing follicular tissue...47

Figure 20: Correlation between nuclear and mitochondrial DNA extracted from human finger nails……..…49

Figure 21: Correlation between the number of stainable nuclei in hair and extractable nuclear DNA.............51

Figure 22: Lack of correlation between counted nuclei and amplified mitochondrial DNA as well as between extractable nuDNA and extractable mtDNA...52

Figure 23: Exclusion of outliers leads to changes in the correlation between Hoechst-positive nuclei and the amount of amplified nuclear DNA..53

Figure 24: Coherence between the number of counted nuclei in hair and the donor’s hair colour...................54

Figure 25: Coherence between the number of counted nuclei in hair and the donor’s age..............................55

Figure 26: The influence of natural hair pigment on the detectability of nuclei *in situ* and the efficiency of nuclear DNA amplification...56

Figure 27: Influence of hair pigment on the coefficient of determination...57

Figure 28: Correlation between the total number of counted nuclei and the amount of DNA extractable from single hairs...60

Figure 29: Correlation of the success of STR typing with the number of Hoechst-positive nuclei comprised in hair...61

Figure 30: Targeted deletion of the DNase1L2 gene in the mouse...73

8.2 List of tables

Table 1: The frequency of Hoechst-positive nuclear remnants in body hair...45

8.3 List of abbreviations

amp	ampicilline
bp	base pairs
BSA	bovine serum albumine
CAD	caspase activated DNase
Ct	cycle treshold
DAPI	4´,6-Diamidin-2-phenylindol
dd	double-distilled
DNase	deoxyribonuclease
dNTP	deoxyribonucleotide triphosphate
DPBS	Dulbecco’s phosphate buffered saline
DTT	1,4-Dithiothreitol
EDTA	ethylenediaminetetraacetic acid
ES	embryonic stem cell
EtOH	ethanol
H_2O_2	hydrogen peroxide
IRS	inner root sheath
kb	kilo bases
KO	knockout
LB	lysogeny broth
LINE-1	long interspersed nuclear element 1
MCS	multiple cloning site
mRNA	messenger RNA
mtDNA	mitochondrial DNA
MUW	Medizinische Universität Wien
n.d.	not determined

NLS	nuclear localization signal
n.s.	not significant
nuDNA	nuclear DNA
-OH	-hydroxyl
ORS	outer root sheath
-P	-phosphate
0.1% PBS-T	phosphate buffered saline with 0.1% Tween-20
PCD	programmed cell death
PCR	polymerase chain reaction
qrt-PCR	quantitative real time polymerase chain reaction
rpm	revolutions per minute
RT	room temperature
SDS	sodium dodecyl sulfate
SOC	Super Optimal Broth (Catabolite repression)
SSR	simple sequence repeat
STR	short tandem repeat
TS	tapestrip
UV	ultra violet
w/v	weight per volume
WT	wild-type

8.4 Curriculum Vitae

Sandra Szabó

Date of Birth: 07.05.1986, Oberwart
Citizenship: Austria

EDUCATION

Dec. 2008 – Dec. 2009:	Diploma Thesis "New methods for detection and quantification of DNA in hair and their implementation in forensic medicine" at the Research Division of Skin Biology and Pathobiology, Medical University of Vienna. Supervisors: Dr. Leopold Eckhart and Dr. Marcela Hermann
March – June 2007:	CEEPUS-scholarship for an exchange semester at the Department of Pharmacy and Biomedicine in Zagreb, Croatia
since 2004:	studies of Molecular Biology at the University of Vienna
1996 – 2004:	Bundesgymnasium Oberschützen
1992 – 1996:	Volksschule Wiesfleck

RESEARCH AND TRAINING

September / October 2009:	Visiting Assistant in Research at the Department of Ecology and Evolutionary Biology, Yale University, USA; Dr. Günter Wagner
October 2008:	Internship at the Max F. Perutz Laboratories Vienna; Dr. Gernot Walko
July 2008:	Internship at the St. Anna Children's Cancer Research Institute; Dr. Heinrich Kovar
April / May 2008:	Internship at the Department of Dermatology, Research Division of Skin Biology and Pathobiology, Medical University of Vienna; Dr. Leopold Eckhart
February 2008:	Internship at the Max F. Perutz Laboratories Vienna; Dr. Marcela Hermann
March - June 2007:	Internship at the Department of Pharmacy and Biomedicine in Zagreb, Croatia; Dr. Dubravka Juretic

PUBLICATIONS:

Identification of reptilian genes encoding hair keratin-like proteins suggests a new scenario for the evolutionary origin of hair. Eckhart L, Valle LD, Jaeger K, Ballaun C, Szabo S, Nardi A, Buchberger M, Hermann M, Alibardi L, Tschachler E. Proc Natl Acad Sci USA. 2008